Elucidating the role of the two-component systems QseBC and PmrAB in mediating resistance to positively charged antibiotics

By

Melanie Noelle Hurst

Dissertation

Submitted to the Faculty of the

Graduate School of Vanderbilt University

in partial fulfillment of the requirements

for the degree of

DOCTOR OF PHILOSOPHY

in

Microbe-host Interactions

May 31, 2022

Nashville, Tennessee

Approved by:

John Karijolich, Ph.D.

Mariana Byndloss, D.V.M, Ph.D.

Maria, Hadjifrangiskou, Ph.D.

Eric Skaar, Ph.D., M.P.H

Antonis Rokas, Ph.D.

For Pappaw

ACKNOWLEDGEMENTS

I would like to thank my advisor, Dr. Hadjifrangiskou for her mentorship, guidance, and patience during my training as a scientist. I would like to thank my committee for their mentorship and direction throughout my thesis completion. I would like to thank the Trent lab for their collaboration and contribution. I would also like to thank the members of the Hadjifrangiskou lab, past and present for their continued support. I would like to acknowledge my funding sources: T32 and F31 which supported me during my training. Finally, I would like to thank, Dr. Maureen Seitz. Without her expert care and support, this thesis would have not been possible.

TABLE OF CONTENTS

FIGURES

LIST OF TABLES

ABBREVIATIONS

AST -Antibiotic Susceptibility Testing

EHEC – Enterohemorrhagic *Escherichia coli*

GFP – Green Fluorescent Protein

LB – Lysogeny Broth

LPS – Lipopolysaccharide

MIC – Minimum Inhibitory Concentration

PMB – Polymyxin B

PmrAB – Polymyxin Resistance A/B

qPCR – Quantitative Polymerase Chain Reaction

QseBC – Quorum Sensing B/C

SNP – Single Nucleotide Polymorphism

TCS – Two Component System

UTI – Urinary Tract Infection

UPEC – Uropathogenic *Escherichia coli*

YESCA – Yeast Extract Casamino Acids

CHAPTER I

INTRODUCTION

This thesis will address how uropathogenic bacteria mount resistance to positively charged antibiotics. I will first introduce heteroresistance, a type of antibiotic resistance in which only a subpopulation of a group of bacteria mount resistance to an antibiotic. I will then describe heteroresistance in uropathogenic *Escherichia coli* (UPEC) driven by the two-component systems, PmrAB and QseBC. I then assign a role for the response regulator QseB, as a controller of metabolism during LPS the modification of lipid A. Finally, I show that another two-component system, KguRS is implicated during response to positively charged antibiotics.

ANTIBIOTIC USE, THE RISE OF ANTIBIOTIC RESISTANCE AND BACTERIAL GAMBLES

Portion of this introduction is in preparation for submission as a mini-review to the journal "Antimicrobial Agents and Chemotherapy". Co-authors for this manuscript are Hamilton D. Green, Dr. Jonathan E. Schmitz and Dr. Maria Hadjifrangiskou

Antibiotic Use through history and the rise of antibiotic resistance

The use of antibiotic preparations predates modern medicine. Human skeletal remains from ancient Sudanese Nubia (350-550 CE) and in the late Roman period of Egypt have been shown to contain tetracycline (Bassett et al., 1980, Nelson et al., 2010). These ancient people likely consumed grain that had been contaminated with *Streptomyces* species that were producing tetracycline. In ancient Egypt it was known that many species of mold grown on bread had antimicrobial properties. In the middle ages, mold was used in China and Greece to treat a variety of ailments. Later in 1871, Pasteur observed that some bacteria had the ability to inhibit other bacteria (Durand et al., 2019). However, it would not be until later that humans began to isolate antimicrobials and use them clinically. In 1909, Paul Ehrlich discovered arsphenamine which was later commercialized as Salvarsan. This antibiotic was active against the causative agent of syphilis, *Treponema pallidum*, although it was fairly toxic. In 1929, Alexander Fleming discovered penicillin. He described a method to isolate *Bacillus influenzae* from penicillium mold broth (Fleming, 2001). Not long after, at Bayer, chemists Josef Klarer and Fritz Mietzsch synthesized the first sulfa drug (sulfonamidochrysoidine). It was discovered to be antibacterial by Gerhard Domagk in 1935. Sulfonamidochrysoidine was commercialized as Prontosil and was widely used to treat *Neisseria* and *Streptococcus* infections. As sulfonamides were already used in the dye industry, it was not a

patentable antibiotic and many companies produced it. Soon thereafter, a method for the mass production and commercialization of penicillin was coined by Ernst Chain and Howard Florey (Chain et al., 1993). This ushered in a new golden age of antibiotics.

Antibiotic discovery was pioneered by the use of the Waksman platform (Lewis, 2020). This platform utilized actinomycetes or antimicrobial producing bacteria for their ability to inhibit growth of a test pathogen on a petri dish (Schatz et al., 2005). Following this method, nearly 20 classes of antibiotics were discovered, including the β-lactams, aminoglycosides, tetracyclines, chloramphenicol, and macrolides. This era of discovery came to an abrupt end in the 1970's. The platform was rediscovering the same antibiotics classes. A switch to whole cell screening methods against *Mycobacterium tuberculosis* discovered three new antibiotics: isoniazid, pyrazinamide, and ethambutol (Lewis, 2020). From there antibiotic discovery took a synthetic approach. The first advances converted narrow spectrum antibiotics against Gram positive bacteria to broad spectrum analogues (i.e, penicillin to ampicillin). A synthetic methodology continued and employed the use of proteomics, genomics, and use of crystal structures to guide high throughput screens. Unfortunately, this did not increase the discovery of new antibiotics. Despite some novel antibiotics recently becoming commercialized, the last antibiotic class, daptomycin, was discovered in 1986 (Tally and DeBruin, 2000). Any new antibiotics since have been improvements on old antibiotic classes (Durand et al., 2019).

The introduction of antibiotics was soon followed by emergence of antimicrobial resistance. Notably, the ability to mount antibiotic resistance is ancient; resistance genes to β-lactams and tetracyclines and have been found in permafrost samples dating back 30,000 years ago (D'Costa et al., 2011)! This is not surprising as many antibiotics are derived from natural sources, and interspecies co-evolution occurred long before humans isolated these compounds. Bacteria can gain resistance through

the acquisition of mobile genetic elements, mutation, or encoded chromosomal genes. Soon after the introduction of sulfonamides, *Neisseria gonorrhoeae* isolates gained resistance. Penicillin use was quickly favored over sulfonamides, but resistance also quickly emerged against it as well (Figure 1).

Despite the threat of resistance, antibiotics quickly become a magic bullet for the treatment of many ailments and substantially thwarted morbidity and mortality due to infectious disease over the decades (Zaman 2017). However, increased use, or misuse of antibiotics has been accelerating resistance (Goosens, 2005). In addition to their use in the clinic, antibiotics are also utilized in agriculture where they minimize infection and increase livestock quality. Poor stewardship in the clinic and in agricultural industry has led to an increase in antibiotic resistance over time. Isolates have emerged that are multi- or pan-drug resistant. Recent reports show that 63,000 Americans die every year from hospital acquired infections (Aminov, 2011), and 25,000 Europeans die from multi-drug resistant infections (Freire-Moran et al., 2011).

The World Health Organization warns that if antibiotic resistance increases unchecked, there will be more frequent infections and death from small injuries. This underscores the need to understand antibiotic resistance mechanisms to curb future resistance.

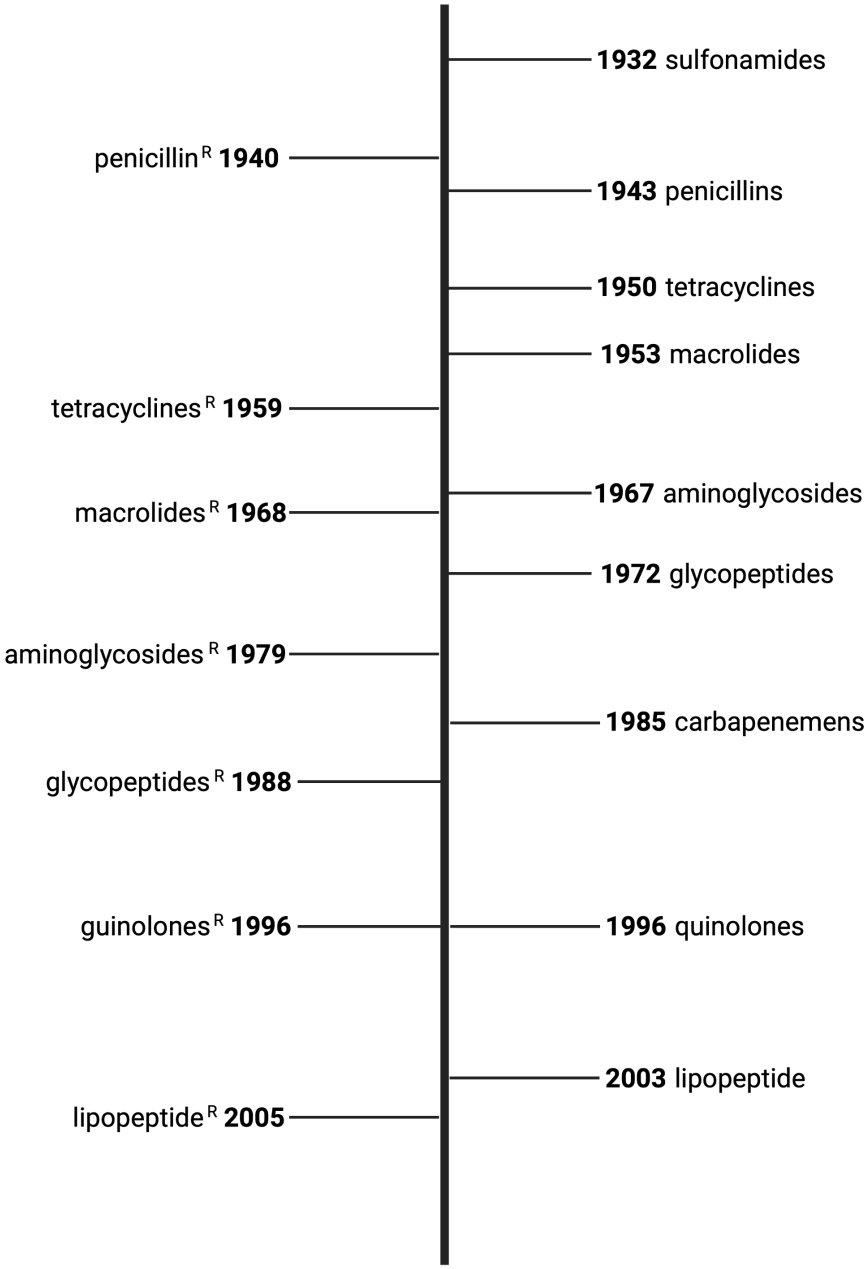

Figure 1: Timeline of antibiotic discovery and corresponding resistance emergence.
A timeline of the discovery of antibiotic classes and then later emergence of resistance. Note, penicillin resistance was discovered before penicillin was used clinically. Figure adapted from (Ventola 2015). Created with Biorender.com

Heteroresistance in clinical isolates

The study of antibiotic resistant bacterial isolates has largely focused on the movement of acquired mobile genetic elements. Other phenomena of resistance, have gone largely understudied. One such phenomenon is heteroresistance, first described in the literature for the Gram-negative *Hemophilus influenza* in 1947 (ALEXANDER, 1948) and later, in 1963 for Gram-positive bacteria (SUTHERLAND and ROLINSON, 1964).

Clinical isolates are typically tested for their overall susceptibility to a given antibiotic. Isolates are deemed susceptible or resistant based on pre-established guidelines for each species of bacteria (CLSI guidelines for the US (**CLSI**, 2018), EUCAST for Europe (EUCAST, 2022)). However, bacteria within the same population may vary in their response to antibiotic stress and be classified as "heteroresistant". Heteroresistance can be defined simply as a population-wide variation in resistance to antibiotics. However, the exact definition and ways to study heteroresistance vary widely. Below, I provide what is currently used in the field to define different types of heteroresistance (**Figure 2**).

Types of heteroresistance

Polyclonal heteroresistance – Polyclonal heteroresistance is the result of a mixed infection (Andersson et al., 2019). Reports of these types of infections have been limited to *Mycobacterium tuberculosis* and *Heliobacter pylori* (Rinder et al., 2001) although this thesis dissertation will provide evidence of heteroresistance in uropathogenic *Escherichia coli*. In *M. tuberculosis* and *H. pylori,* mixed populations are detected in patient samples such as stool, sputum, or in stomach biopsy samples without a single-cell colony purification step. (Rinder et al., 2001, Mascellino et al., 2017, Brennan et al., 2021).

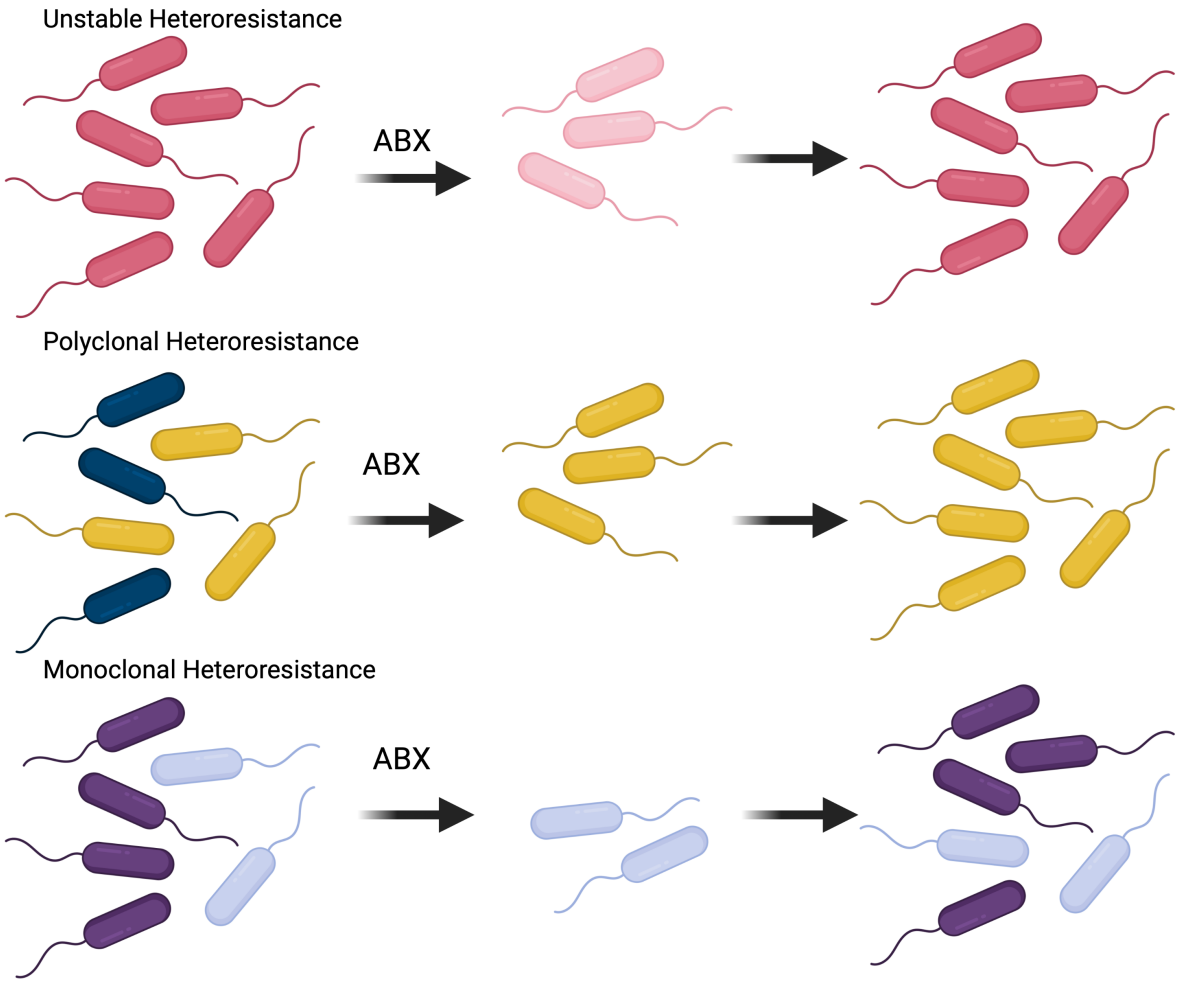

Figure 2: Model of the main types of heteroresistance
Each type of heteroresistance is depicted by a group of bacteria prior to treatment to antibiotics. In the case of unstable heteroresistance, a clonal population is exposed to antibiotics. This creates a selective pressure for a genetic change, such as gene amplification, that allows a subpopulation to survive. After the removal of antibiotics the population reverts back to the original genetic background of the founding population. In polyclonal heteroresistance, two genetically distinct subpopulations comprise a total population. One of these populations is resistant to the antibiotic of choice. After exposure to the antibiotic, the resistant subpopulation survives. In monoclonal heteroresistance, two distinct populations are present. A subpopulation that has stochastic genetic changes allows it to survive an antibiotic assault. The surviving population structure is then constituted of both the resistant subpopulation and the susceptible subpopulation as prior to antibiotic assault. Created with Biorender.com

Mixed infections occur when two different strains of the same species of bacteria initiate infection at two different times. The entire population is then comprised of two genetically distinct strains of the same species one of which is antibiotic resistant while the other is not. One study (Zheng et al., 2015) found that mixed infections might be the main type of heteroresistance in *M. tuberculosis*. In *H. pylori* similar observations have been made (Kim et al., 2003).

Mixed infections may lead to worse disease outcomes and may be responsible for failure of treatment (Alebouyeh et al., 2015, Kim et al., 2003). This is in part because heteroresistance may not be detected by traditional methods, which involve plating the pathogen for isolation and randomly choosing a single colony for antibiotic susceptibility testing (**CLSI**, 2018). Antibiotic susceptibility testing on a pure single colony would result in one of the two phenotypes giving either a susceptible or resistant reading depending upon which population the clone was derived from (Andersson et al., 2019). In these cases, molecular methods are better for detecting heteroresistance and focus on mutations in genes known to be implicated in resistance (Rinder et al., 2001, Brennan et al., 2021).

Monoclonal heteroresistance – Emergence of resistance to only a portion of the population can also occur via the acquisition of chromosomal mutations (Figure 2). This typically occurs when a population of bacteria infects and is *then* subjected to antibiotic treatment. The selective pressure of the antibiotic drives rare spontaneous resistant mutants to form. These mutants then increase in numbers in the presence of the antibiotic use, giving rise to a heteroresistant population comprised of the original susceptible parent and the evolved resistant clone.

A common mechanism of monoclonal heteroresistance is gene amplification. Gene amplifications are among the most common types of mutation. They occur with a frequency between > 10^{2} and around 10^{-4} depending upon the genomic region (Anderson and Roth, 1981). Gene amplifications

as a cause of antibiotic resistance were first described in plasmids (SUGINO and HIROTA, 1962) and then in chromosomal β-lactamase genes of *E. coli* (Normark et al., 1977). Resistance conferred by gene amplification is often due to over-production of target molecules, efflux pumps, or antibiotic modifying enzymes (Sandegren and Andersson, 2009, Hjort et al., 2016). Gene duplications are inherently unstable and will be lost if not continuously selected (Pettersson et al., 2009). In *Salmonella enterica* serovar *Typhimurium,* gene duplication events were shown to occur and disappear across the genome. In these studies, the frequency of any given cell growing in culture harboring a duplication was 10% (Anderson and Roth, 1981).

In addition to gene duplication events, point mutations, insertion sequences, and small deletions may also be drivers of monoclonal resistance. For example, two-component systems can be effectively turned off or on by a single point mutation (Ram and Goulian, 2013, Dewachter et al., 2019). Like with mixed infections, traditional clinical laboratory techniques may not be adequate in detecting monoclonal heteroresistance if antibiotic susceptibility testing is performed on a pure single colony.

Unstable, or Reversible Heteroresistance - Unstable or reversible heteroresistance describes a situation in which a clonal population displays distinct responses to antibiotic treatment, with some members of the population displaying resistance to the drug, because it stochastically has specific genes expressed, or specific proteins present that confer an advantage in the presence of the antibiotic. Testing of a pure clone in this case would always display heterogeneity, because of the inherent ability of the culture to produce two distinct, yet reversible phenotypes. Because this type of heteroresistance is oftentimes the result of differential gene expression or differential protein abundance or enzyme activity in clonal cells and is thus reversible. For example, a portion of the population can survive in the presence of an antibiotic because it has a specific set of genes turned on, compared to its clonal cells, in which

mRNA for these genes is not stochastically present. If the antibiotic is removed and cells are passaged, then the population reverts to the susceptible profile. This type of heteroresistance is the least characterized and the most difficult to investigate or identify in the context of diagnosis in the clinical lab. ***This thesis dissertation addresses this gap in the field.***

Heteroresistance in the clinic

In the clinical laboratory, pathogen identification is almost always followed by antibiotic susceptibility testing (AST), in which a *single* colony is selected from the diagnostic plate for subsequent propagation and AST (**CLSI**, 2018). This process cannot detect a mixed infection, or polyclonal heteroresistance, as it performs downstream testing on a single clone. In the case of reversible/unstable hetero-resistance, downstream AST may yield inconclusive results from the same single colony. Both scenarios pose challenges in selecting the appropriate antibiotic regimen for patient treatment.

Three factors complicate proper analysis of heteroresistant isolates in the clinical lab: the level of resistance; the frequency-; and the stability of resistant subpopulations. ***Level of resistance –*** Resistant subpopulations may grow close to the minimum inhibitory concentration (MIC) on an AST selective agar plate, or grow at two, four or eight times the MIC in broth (Barin et al., 2013, da Silva et al., 2018, Oikonomou et al., 2011, Hermes et al., 2013). Some suggest that in order to classify an isolate as heteroresistant, the resistant subpopulation should grow above the clinical breakpoints for the antibiotic being used (Hermes et al., 2013). ***Frequency –*** Depending on the detection method used, resistant subpopulations may comprise less than one percent of the isolate. This poses challenges in determining the potential of this resistant subpopulation to dominate an infection. ***Stability –*** Finally, stability of the subpopulation is of concern. As described above, subpopulations can be stable – if they acquired mutations – or unstable, if resistance is the result of altered gene expression profiles. Unstable

subpopulations revert back to a susceptible population after isolation or small number of passages (Plipat et al., 2005, Hjort et al., 2016). Stable subpopulations do not revert and instead have genetic changes that are permanent. Reviews on the field have called on the standardization of heteroresistance papers to make it clearer and easier to compare studies and to help create reliable guidelines for the clinical laboratory.

The methods required to detect heteroresistance are often not performed in the clinical microbiology lab. Although some heteroresistant subpopulations may be detected using diffusion assays like disc diffusion or E-test trips, the gold standard for detection is a population analysis profile. This method requires agar microdilution and is too time-consuming and labor-intensive for a clinical microbiology lab to undertake (van Hal et al., 2011, Satola et al., 2011, El-Halfawy and Valvano, 2013). Additionally, AST may even call for the user to ignore emergent subpopulations in determining the minimum inhibitory concentration, as it is evidenced in the EUCAST guidelines for fosfomycin AST (EUCAST, 2022). As a result, heteroresistance may affect clinical outcomes including the failed response of the patient to the antibiotic regimen.

Recent studies have revealed heteroresistance in several pathogens worldwide against a variety of antibiotics including those of last resort, such as carbapenems and polymyxins (El-Halfawy and Valvano, 2013). A study by Nicoloff *et al* tested a panel of clinical isolates against 28 antibiotics. They found a high prevalence of heteroresistance in the tested isolates, despite these same isolates defined as sensitive by clinical microbiology standards. The study determined that resistance was gained through gene amplifications and often reverted back to a susceptible phenotype when grown in the absence of antibiotics (Nicoloff et al., 2019, Lázár and Kishony, 2019). Research has also linked heteroresistance in *S. aureus* to vancomycin to treatment failure (Hiramatsu et al., 1997). However, others have found that

vancomycin is still effective in treating these strains due to a relatively low difference in minimum inhibitory concentration between the heteroresistant and susceptible strains (Khatib et al., 2011). Work by the Weiss group found heteroresistance in *Enterobacter cloacae* to colistin, an antibiotic of last use. Notably, when they tested in a murine model of infection, the authors demonstrated that heteroresistance impacts treatment outcomes with colistin. Mice infected with heteroresistant strains of *E. cloacae* failed antibiotic therapy, compared to those infected with a susceptible strain (Band et al., 2016). Therefore, while several studies are now pointing towards heteroresistance posing a threat in treatment regimens, there is a lack of true epidemiological and clinical data on the impact of heteroresistance. This is confounded by the lack of reliable methods to quickly identify heteroresistance in the clinical lab and gauge its role in infection.

Heterogeneity as a fitness mechanism

Bacteria encounter a variety of changing environments and therefore must respond quickly and adapt. One such way that bacteria may be able to survive in a constantly changing world is through phenotypic or genotypic heterogeneity, where subpopulations with distinct characteristics arise within a single-species population of bacteria. An excellent example is the occurrence of “peppermint” colonies of E. coli (Figure 3), where within-strain heterogeneity arises in the ability of the cells to take up the dye Congo red. Variation within a population may be driven by stochasticity in molecular processes such as gene expression (Elowitz et al., 2002) or partitioning of cellular material after cellular division (Huh and Paulsson, 2011, Ackermann, 2015). Studies have shown that essential genes in *Escherichia coli* and *Saccharomyces cerevisiae* are often more tightly regulated and have less noise in their expression when compared to non-essential genes (Newman et al., 2006, Lehner, 2008). Conversely, regulatory networks

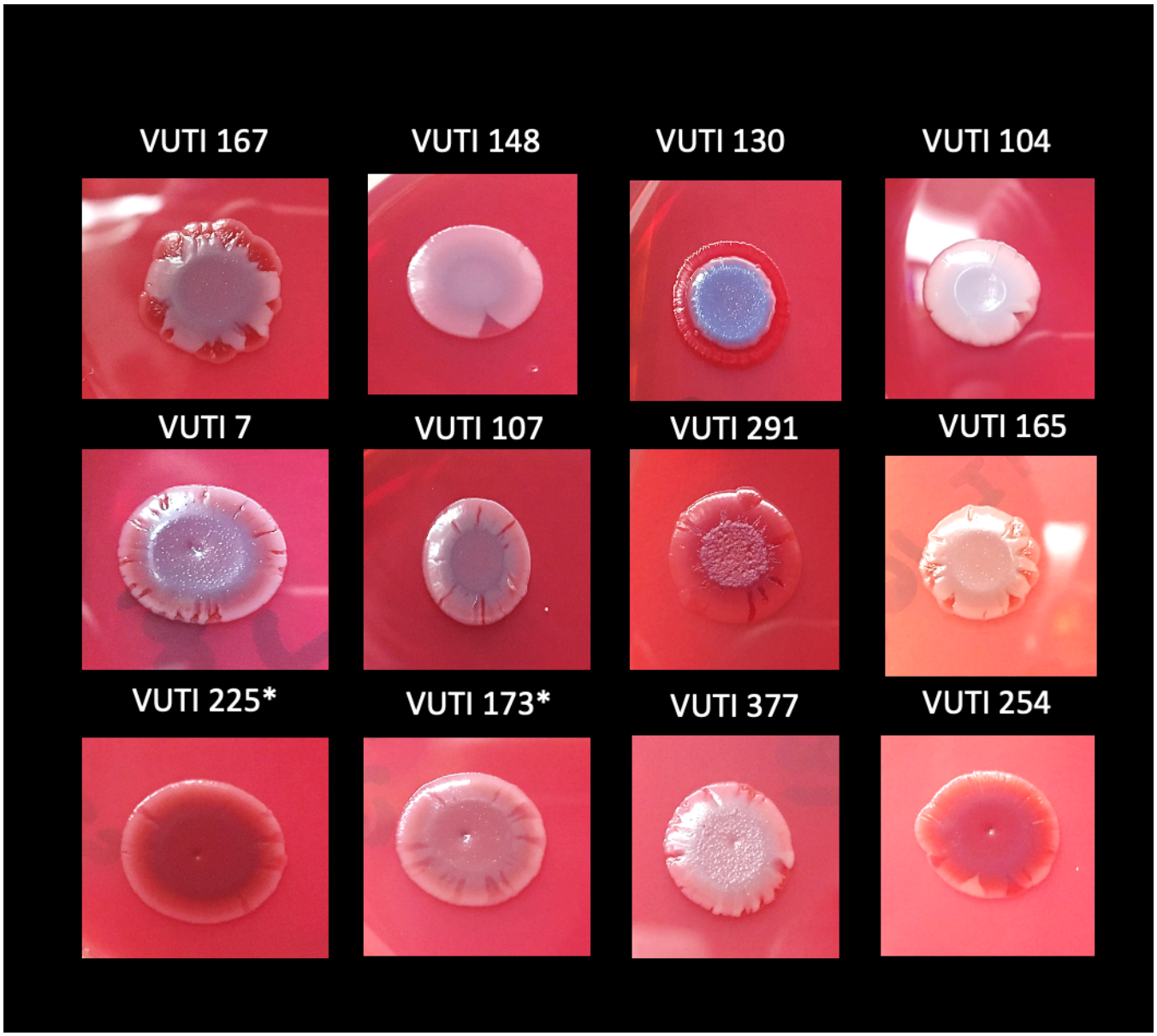

Figure 3: UPEC isolates display peppermint phenotype
A display of several colony biofilms of UPEC isolates showing a heterogenous display of Congo red uptake on YESCA agar plates supplemented with Congo Red referred to as ”peppermint” isolates.

may amplify gene expression and boost variation in gene expression (Smits et al., 2006). Populations may also display heterogeneity through their interactions with the environment and other cells (Reuven and Eldar, 2011). For example, a diffusible signal that comes into contact with a receptor of any given cell may lead to variable responses within the population. Cells may have different receptor numbers or locations and therefore have varying interpretations and thresholds for a response, leading to heterogeneity.

Heterogeneity within a population may allow an otherwise genetically identical population to "hedge its bets" against changing environments or to create tolerance against stress or antimicrobial agents (Wakamoto et al., 2013, Balaban et al., 2004, Arnoldini et al., 2014). Typically, cells sense their environment through signal transduction systems that rely on signal activation that then leads to a response by the cell, usually through gene expression. However, environments may have a multitude of signals or may change so quickly, that cells are unable to respond fast enough. In these situations, a subpopulation of cells with a given system already activated may have a fitness advantage and survive a specific threat (Wolf et al., 2005, Thattai and van Oudenaarden, 2004). Heteroresistance – introduced in this Chapter - is a form of population heterogeneity.

Two-component systems and heterogeneity

One mechanism of heterogeneity within bacteria is differential gene expression. Differential gene expression, as discussed above, can be the result of different responses to an environmental signal due to different abundance or activation of relevant receptors on the bacterial cell surface. One such example of signaling pathways are two-component systems (TCS). TCS are typically comprised of a membrane-embedded sensor histidine kinase and a response regulator, which both contain conserved

regulatory domains. Upon receipt of a signal, the histidine kinase auto-phosphorylates at a conserved histidine residue in the cytoplasmic Histidine dimerization domain (Bourret et al., 1989, Stock et al., 1989, Stock et al., 2000). The phosphoryl group is then transferred to a conserved aspartate residue on the N-terminal "receiver domain" of its cognate response regulator. Once activated, response regulators go on to elicit a response in the cell (Bourret et al., 1989, Stock et al., 1989, Stock et al., 2000). This response is often a change in gene expression as many response regulators are DNA binding proteins that act as transcriptional regulators (Mizuno, 1997, Stock et al., 2000). Histidine kinases are typically comprised of one or more sensing domains, a histidine/dimerization kinase domain, and a catalytic ATP-binding domain. The catalytic domain hydrolyzes ATP which allows the kinase to auto-phosphorylate. Response regulators are typically comprised of two-domains: the receiver domain that contains the conserved aspartate residue that undergoes phosphorylation, and an output domain that is typically but not always, a helix-turn-helix or winged-helix DNA binding domain. Histidine kinases are often bi-directional and can act as either phosphatases or reverse phosphotransferases and dephosphorylate cognate response regulators (Goulian, 2010). This activity is important for both resetting the signaling cascade after activation and preventing response regulators from being phosphorylated by other proteins in the cell.

Because TCS react to specific signals and elicit a response, it may be advantageous to a population of bacteria to have a subpopulation with any given TCS already activated in order to survive an environmental stress. Heterogeneity may be especially observed in situations where multiple TCS are involved and sense the same signal. This allows for a variety of responses and cellular states (Jung et al., 2019, Plener et al., 2015). TCS often undergo mutations, or gene amplification after a bacterial population is exposed to antibiotics (Jung et al., 2019).

Importance of this thesis dissertation

In the presented dissertation I provide a body of work that demonstrates the presence of heteroresistance in uropathogenic *Escherichia coli*, the primary cause of urinary tract infections (UTI). In chapter II, I present evidence of both monoclonal heteroresistance in UPEC clinical isolates and reversible heteroresistance that is conserved across multiple *E. coli* pathotypes. In Chapter III, I present work that demonstrates how a regulatory system comprised of the PmrAB and QseBC two-component systems (TCS) control reversible resistance to positively charged antibiotics, by orchestrating shifts in central metabolism and modifications on lipid A of the LPS. In Chapter IV I identify the implication of a third TCS, KguRS, in sensing oxoglutarate levels and contributing to the antibiotic response by UPEC. Finally, in Chapter V, I discuss avenues in which this research can be expanded to further elucidate mechanistic details of heteroresistance in UPEC and to guide efforts for better evaluation of antibiotic resistance in the clinical setting.

CHAPTER II

UROPATHOGENIC *ESCHERICHIA COLI* DISPLAYS HETERORESISTANCE TO THE LAST-RESORT ANTIBIOTIC POLYMYXIN B

Portion of this work is in preparation for submission to the Journal of Bacteriology. Additional authors on this manuscript are: Rachel Mersfelder, Michelle Wiebe and Dr. Maria Hadjifrangiskou

Introduction

Uropathogenic *E. coli* (UPEC) are a pathotype of *E. coli* that cause 70 – 90% of all urinary tract infections (UTIs) in humans (Foxman, 2014). UTIs disproportionately afflict women, in which UPEC are thought to exit from the gut, cross the perineum and vagina, and enter the urethra. There, bacteria can adhere to and invade the bladder, causing cystitis. Bacteria constantly travel from the bladder to the kidneys and back, and occasionally can enter the bloodstream, leading to urosepsis (Al-Hasan et al., 2010). Each of these host domains poses different challenges for UPEC, ranging from changes in oxygen tension, pH, type of nutrients available and the type of innate immune response initiated (Subashchandrabose and Mobley, 2015). As such, UPEC strains use several stress response mechanisms to overcome the imposed stress, many of which are controlled by two-component systems (Breland et al., 2017a).

Interestingly, several studies have documented heterogeneous phenotypes that may benefit infection: One extensively characterized example is in the heterogeneous expression of fimbriae (Khandige and Møller-Jensen, 2016). Surface fimbriae are secreted proteins that participate in adhesion

to and invasion of host cells (Mulvey et al., 1998) and are often categorized as UPEC virulence factors (Connell et al., 1996). However, their elaboration may lead to enhanced immune recognition or come at a fitness cost. Many fimbriae, like type 1 pili and P pili are controlled by phase variation (Schwan, 2011, Hernday et al., 2002). In the case of type 1 pili, only a fraction of the UPEC population expresses type 1 pili during a murine model of infection (Stærk et al., 2016, Floyd et al., 2016). Others have demonstrated that population composition is driven by environment (Bayliss, 2009, Khandige and Møller-Jensen, 2016).

UPEC also demonstrates heterogeneity in its expression and usage of quinol oxidases within biofilm communities (Beebout et al., 2019). Biofilms are three-dimensional structures comprised of secreted extracellular materials and bacteria. Across the biofilm many chemical gradients are established, such as oxygen or nutrients. In the case of respiration in the biofilm, we have previously shown distinct spatial organization of the three UPEC quinol oxidases, cytochrome *bo, bd, and bd2* (Beeboutt 2019). Likewise, heterogeneity is observed in the expression of quinol oxidases in vivo and their deletion results in distinct alterations in pathogenic behavior (Beebout et al., 2019). In this case, UPEC display heterogeneity in cytochrome expression within the biofilm depending upon their location and the availability of oxygen.

Studies in MG1655 have shown that two-component systems are a source of heterogeneity (Jung et al., 2019). This combined with work to demonstrate that UPEC displays heterogeneity in other systems has led me to hypothesize that two-component systems may themselves be expressed heterogeneously in UPEC. This work demonstrates how the two-component systems, PmrAB and QseBC are heterogeneously expressed in uropathogenic *E. coli*, allowing the bacteria to become heteroresistant to

polymyxin B. Moreover, this work reveals the presence of heteroresistance to polymyxin B in clinical isolates of UPEC

Methods

Strains and constructs

Experiments were performed in the characterized cystitis strain UTI89 and isogenic mutant created previously, UTI89Δ*qseC* (Kostakioti et al., 2009). Strains VUTI 149, 163, 184, and 247 were isolated from the urine of patients at Vanderbilt University Medical Center and are banked at microVU (https://www.vumc.org/microvu/home). The transcriptional reporter plasmid pP*qse*::GFP was previously constructed (Kostakioti et al., 2009).

Colony biofilm setup and section preparation

Strains were propagated overnight shaking at 37°C in lysogeny broth (LB) (Fisher). Biofilms were seeded using 10 μL of the overnight culture, which was spotted onto 1.2X yeast extract/casamino acids (YESCA) agar and incubated at room temperature for up to 11 days. At day 11, biofilms were flash frozen in O.C.T. compound (Electron Microscopy Sciences) and cryosectioned as previously described (Vlamakis et al., 2013, Beebout et al., 2019).

Confocal microscopy

Biofilms that were cryosectioned and placed onto microscopy slide (see Colony biofilm setup and section preparation) were stained with TO-PRO-3 iodide (ThermoFisher Scientific), a DNA stain, to visualize all bacteria. The slides were washed with PBS and mounted with ProLong Gold and

(ThermoFisher Scientific) a glass coverslip. Images were acquired using a Zeiss LSM710 Inverted confocal microscope. Post image acquisition image processing was performed in Zen (Zeiss). Resulting figures were created using Photoshop (Adobe).

In vitro evolution experiments

For clinical isolates VUTI 149, 163, and 247 an *in vitro* evolution experiment was performed. Strains were grown overnight at 37°C, with shaking. The next day, strains were sub-cultured 1:1000 in fresh Mueller Hinton broth with the addition of a sublethal concentration of polymyxin, at 0.75X the MIC. Samples were sub-cultured 1:1000 in fresh Muller Hinton broth and polymyxin every 24 hours for 5 total passages. The MIC was determined for each passage using a modified broth microdilution method that substituted charged (polystyrene) plates for those without a charge (polypropylene) (Hancock, 1999).

Isolation of heteroresistant subpopulations from clinical isolates

E. coli was isolated from patient urine samples and banked by MicroVU in 25% glycerol freezer stocks. Strains were grown at 37°C overnight with shaking in lysogeny broth (Fisher). Strains were then diluted to OD_{600} = 0.5 in PBS, and adjusted to a 0.5 McFarland standard. Samples were then streaked out on prepared Mueller Hinton agar plates (BD) to create a lawn, using a cotton applicator (Puritan). A single polymyxin E-test strip (Biomerieux) was placed onto the lawn. Plates were incubated at 37°C for 16 hours. From samples in which two populations were phenotypically present on the plate after incubation: VUTI149, 163, 184 and 247, each population (sensitive and resistant) was isolated and grown overnight at 37°C in lysogeny broth and stored in 25% glycerol at -80°C.

Sequencing of *in vitro* evolved UPEC strains

Genomic DNA from the parent, as well as the second and fifth passage of VUTI63 and 247 were isolated (Qiagen) and sequenced (GeneWiz). Briefly, libraries were prepared using the NEBNext UltraT DNA Library Prep Kit for Illumina. The genomic DNA was fragmented by acoustic shearing with a Covaris LE220 instrument. Fragmented DNA was end repaired and adenylated. Adapters were ligated after adenylation of the 3' ends followed by enrichment by limited cycle PCR. DNA library was validated using a D100 ScreenTape on the Agilent 4200 TapeStation and was quantified using Qubit 2.0 Fluorometer. The DNA library was also quantified by real time PCR, clustered on a flowcell and loaded on the Illumina Miseq instrument. Resulting reads were assembled using the Genome Assembly tool using SPAdes hosted on the Patric Databse. Genomes were then annotated using the Escherichia group as reference using the Annotation tool hosted by Patric. To determine variation between the passages and parental strain, the reads of the resistant subpopulation were compared to the assembled genome of the sensitive parental population using the Variation Analysis tool hosted on Patric's database.

Transcriptional profiling by qPCR

Bacteria were grown overnight at 37°C, with shaking in LB. N-minimal media (Guckes et al., 2013a) were inoculated with strains of interest at starting optical density at a wavelength of 600 nm (OD_{600}) of 0.05. Strains were grown to mid-logarithmic growth phase (OD_{600} = 0.5). At this time, 4-milliliters of culture was withdrawn for processing. All samples were centrifuged at 4000 x g for 10 minutes upon collection. The supernatant was decanted and the fraction containing the cell pellet was flash frozen in dry ice – ethanol and stored at -80°C until RNA extraction.

RNA from cell pellets was extracted using the RNeasy kit (Sigma Aldrich) and quantified using Agilent Technology (Agilent). A total of 3 micrograms (μg) of RNA was DNAse treated using the DNAfree kit (Ambion) as we previously described (Hadjifrangiskou et al., 2011). A total of 1μg of DNAse-treated RNA was subjected to reverse-transcription using SuperScript III Reverse Transcriptase (Invitrogen/ThermoFisher Scientific) and following the manufacturer's protocol.

The cDNA was then diluted and loaded with TaqMan mastermix onto a 96 well plate. Probes and primers targeting *qseB* and *gyrB* (housekeeping gene) were added. qPCR was performed on a StepOne Plus (Applied Biosystems) according to manufacturer's protocol. Resulting amplifications were analyzed using the change in C_T method.

Results

Heterogeneity in *qseBC* expression is observed in UPEC

QseBC is a TCS implicated in UPEC pathogenesis (Kostakioti et al., 2009, Hadjifrangiskou et al., 2011). Early characterization of the system in enterohemorrhagic *E. coli* (EHEC) proposed that QseC is an "adrenergic receptor" that senses norepinephrine, epinephrine, and the elusive autoinducer-3 (Clarke et al., 2006). However, several studies have since demonstrated a lack of QseC sensing of these three ligands (Guckes et al., 2017, Merighi et al., 2009, Guckes et al., 2013a). Deletion of *qseC* attenuates virulence in EHEC (Hughes et al., 2009) and (Kostakioti et al., 2009, Hadjifrangiskou et al., 2011). Interestingly, deletion of the whole system or *qseB* (the cognate response regulator) alone does not cause attenuation in virulence (Kostakioti 2009), which was the first indication that QseB must interact with an additional sensor histidine kinase that catalyzes its activation in the absence of QseC (Kostakioti et al., 2009). Subsequent suppressor mutagenesis studies in a UPEC strain lacking *qseC* identified the

Polymyxin B resistance (Pmr) sensor PmrB as a QseB interacting partner (Guckes et al., 2013a). The PmrAB TCS has been well characterized for its involvement in mediating resistance to polymyxins. It does this through activation of PmrA, a transcription factor, which upregulates LPS modifying enzymes that ultimately change the overall charge of the outer membrane. This decreases the attractiveness of positively charged antibiotics like the polymyxins. Deletion of *pmrA* or *qseB* in UPEC leads to a significant decrease in polymyxin resistance in UPEC, while deletion of both response regulators (Δ*qseB*Δ*pmrA*) or the PmrB sensor (Δ*pmrB*) leads to strain that is exquisitely susceptible to polymyxins (Guckes et al., 2017).

We hypothesized that signaling by PmrAB-QseBC is heterogeneously expressed in UPEC populations. To begin to address this hypothesis, we first evaluated the stochastic expression of the *qseB* locus in UPEC strain UTI89, in the absence of antibiotics or other stresses that may induce the *qseBC* system (Guckes 2013). Given that activated QseB regulates its own transcription (Guckes et al., 2017), we utilized a previously created *qseBC* promoter construct fused to GFP, to assess the basal activity of the *qseBC* promoter within a UPEC community. We chose to perform these analyses on UPEC biofilms, since UPEC forms biofilms at different niches during infection (Brannon et al., 2020). Biofilms of wild-type UTI89 and its isogenic mutant UTI89Δ*qseC* were evaluated for these studies. The biofilms were cryo-sectioned onto microscopy slides, as previously described (Beebout et al., 2019). Confocal Laser Scanning Microscopy (CLSM) was performed, using TO-PRO-3 iodine to stain DNA and visualize all bacteria (Figure 4A, blue). In the wild-type biofilm, green puncta are visible throughout the biofilm (Figure 4A, green). This is consistent with heterogenous expression of *qseBC*. In the UTI89Δ*qseC* biofilm – which serves as a control, nearly all visualized bacteria are green (Figure 4B), because loss of QseC,

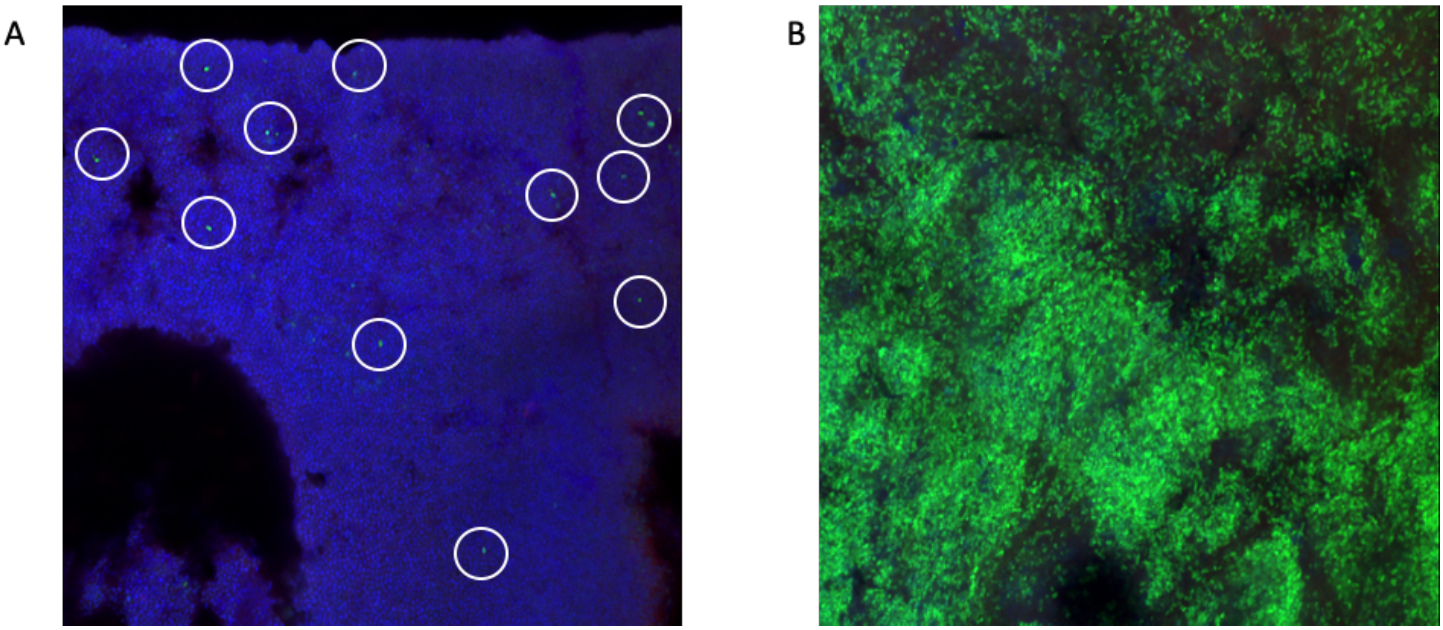

Figure 4: The *qse* operon is heterogeneously expressed within a UPEC biofilm
A) Confocal microscopy image of a UTI89/P*qse*::GFP cryosectioned biofilm. The biofilm was stained with TOPRO 3 to show all cells. Green puncta are circled in white. This shows some cells have *qse* activity in the absence of signal and represent a subpopulation. B) Confocal microscopy image of a UTI89Δ*qseC*/P*qse*::GFP acts as a control. This biofilm shows almost homogeneous green cells, demonstrating activation of *qse*. This is due to excessive action of QseB by PmrB, leading to increased activity at the *qse* promoter.

leads to aberrant activation of QseB, and high levels of activity at the *qse* operon (Kostakioti et al., 2009). This observation indicates the presence of subpopulations that have the QseBC TCS activated within the UPEC biofilm community. This raises the possibility that if such subpopulations also exist in clinical strains, they may lead to heteroresistance to polymyxin B. We next tested this possibility.

Identification of clinical strains that display hetero-resistance to polymyxin B

We assessed a group of strains isolated from urine collected from patients at Vanderbilt University Medical Center and banked with MicroVU for their susceptibility to polymyxin B using the E-test strip disc diffusion method. This allowed us to test a large volume of strains and quickly identify potential heteroresistant colonies in the zone of inhibition. We tested 390 isolates and discovered four strains with prominent heteroresistant subpopulations present in the zone of inhibition (Figure 5). We isolated the resistant subpopulations from the parental population and reassessed for polymyxin B susceptibility. We found that the resistant subpopulations were stably resistant to polymyxin B. To determine genetic mutations associated with the resistant subpopulations we performed whole genome sequencing on two of the resistant subpopulations: VUTI 163 PMB^R and VUTI 247 PMB^R and parental strains: VUTI 163 and VUTI 247. We then compared these populations back to the sensitive strains using the Variation Analysis tool hosted on Patric's database. Both resistant subpopulations mapped back to the parental strain with small nucleotide polymorphism (SNP) differences suggesting monoclonal heteroresistance. In VUTI 163 PMB^R there were changes in *sucB*, *eno,* and the intergenic regions of rRNAs. In VUTI 247 PMB^R there were changes in *murl, cpsG,* and upstream of *gadX*. Interestingly, there were no changes found in genes that are typically associated with resistance to polymyxins, such as *pmrCAB*. Instead, both isolates harbor mutations in genes related to metabolism and the acid stress response (Figure 5).

A

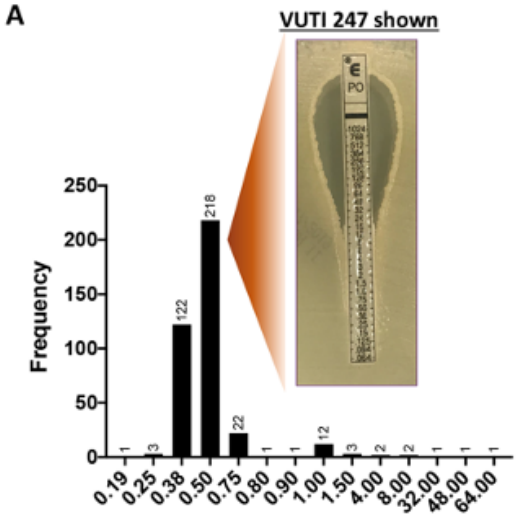

B

Isolate Name	VUTI-149	VUTI-163	VUTI-184	VUTI-247
Patient Gender (Age Range)	F (61-70)	F (36-50)	M (36-50)	F (51-60)
Disease State	Cystitis	Cystitis	Cystitis	Routine Visit urine collection
Co-morbidities?	N/A	N/A	N/A	Diabetes
Clinical lab Antimicrobial Susceptibility Profile	Sulfamethoxazole Beta-lactams Chloramphenicol	Sensitive to all tested using MIC	Sensitive to all tested using MIC	Levofloxacin
Mutations in PMB^R subpopulations by population analysis	Not yet sequenced	Missense mutation in *sucB* (993CGGT>TCTA →SerLeu331SerPro)	Not yet sequenced	Missense mutation gcc→gac in *murI* promoter Multiple mutations in *cpsG-wcaJ* (colanic acid biosynthesis) Missense mutation ggc→gcT upstream of *gadX*

Figure 5: Heteroresistant isolates were discovered in a bank of UPEC isolates

A) Histogram of MICs from tested UTI isolates B) Table showing patient, antibiotic resistance, and sequencing information from heteroresistant isolates.

Recent studies in *Klebsiella pneumoniae* and *Acinetobacter baumanni* have reported the emergence of *in vivo* resistance during a course of treatment with colistin (Cannatelli et al., 2014, Lesho et al., 2013, Gerson et al., 2019). Various mutations were identified but the majority were often found in the *pmrCAB* operon. This led us to ask if UPEC isolates can develop resistance to polymyxin B, in an *in vitro* evolution experiment and whether these mutations would affect *qseBC* induction.

We chose four urinary *E. coli* isolates banked at Vanderbilt University Medical Center (Figure 6A) Each strain was passaged at 0.75X their MIC for polymyxin B, for a total of five passages. The change in MIC for each isolate was determined after each passage. As the number of passages increased so did the MIC for each isolate (Figure 6B).

Isolates demonstrate varying amounts of *qseB* transcript as they are passaged

Parallel to MIC measurements, we quantified the amount of *qseB* transcript in VUTI149, VUTI184, and VUTI247 parental isolates, and their corresponding second and fifth *in vitro* evolution passaged strains. The transcript abundance of the passaged "evolved" strains was compared to the respective parental strain. The relative fold change of *qseB* transcript compared to the parental isolates varied (Figure 6C). In VUTI 149, the relative fold change increased from passage 2 to passage 5. In VUTI 163, the relative fold change decreased from passage 2 to 5. In VUTI 184, neither strain had relative fold changes that were significantly different from the parental strain. In VUTI 247 the relative fold change was not significantly different between the two passages but elevated relative to the parental strain (Figure 6C).

To determine the genetic changes in the evolved resistant isolates, we performed whole genome sequencing on the parental isolate, second passage, and fifth passage

A

Isolate	Polymyxin B MIC (µg/mL)
VUTI 149	0.5
VUTI 163	0.5
VUTI 184	1.0
VUTI 247	1.0

B

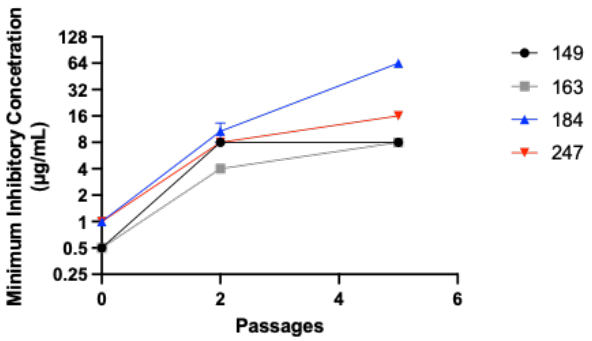

C

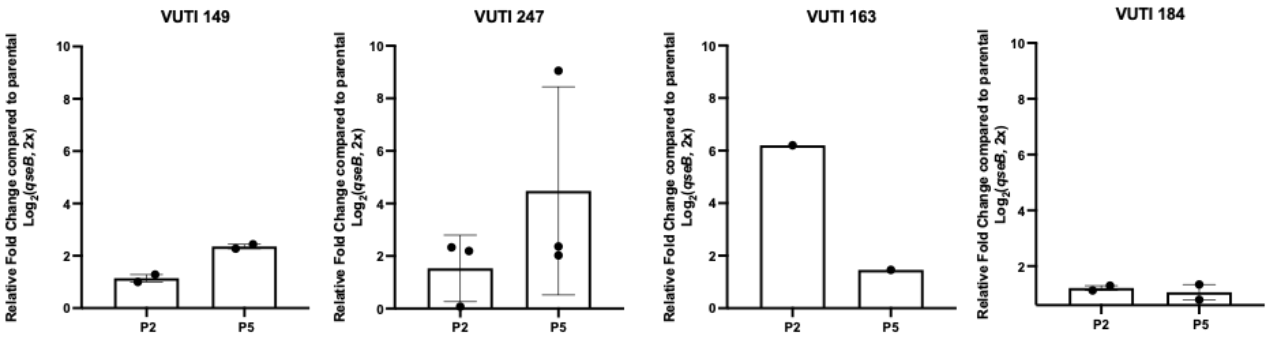

Figure 6: *In vitro* evolution experiment reveals an increase in resistance to polymyxin B
A) Initial minimum inhibitory concentration (MIC) of each isolate prior to *in vitro* evolution experiment. B) Graph depicts changes in MIC at passage 2 and 5. C) Isolates at passage 2 and 5 were assessed for activation of *qse* promoter by measuring *qseB* transcript levels.

of VUTI 163 and 247, the two strains that demonstrated no increase in qseB transcription. To compare changes between the passages and the parental strain, the Variation Analysis tool on Patric's database was used. In VUTI 163, comparisons between passage 2 and the parental strain revealed changes in *gadA*, type 6 secretion genes, phage genes, and amine metabolism. In this same isolate, comparisons between passage 5 and the parental strain showed changes in *gadA*, *gadX*, and *wzxC* (Table 1). Similarly, in VUTI 247, comparisons between passage 2 and the parental strain showed changes in *gadA* and *pmrA*. In the same isolate, comparisons between passage 5 and the parental strain revealed mutations in *gadA, pmrA,* phage genes, and type 6 secretion genes (Table 1). These results point towards mutations in *gad* genes as potentially associated with increased in polymyxin resistance, given that polymyxin resistant subpopulations with *gad* mutations were isolated from clinical isolates and through *in vitro* evolution experiments.

Collectively this work demonstrates the presence of both reversible and stable heteroresistance in uropathogenic *E. coli*.

Discussion

Heteroresistance is often defined as a portion of a population displaying resistance to an antibiotic during antibiotic susceptibility testing (AST). Heteroresistance is often not detected or ignored during typical AST performed by a clinical microbiology laboratory (EUCAST). Yet, heteroresistant strains that cause infections may lead to worse disease outcomes (REF). Here, we describe the heterogeneous activation of chromosomally encoded systems that allow UPEC to survive polymyxin B, a last-resort

Resistant Passage	VUTI-163	VUTI-247
P2	*gadA* *T6SS genes* *Phage genes* *Amine metabolism*	*gadA* *pmrA*
P5	*gadA* *gadX* LPS modifier *wzxC*	*gadA* *pmrA* *Phage genes* *Type 6 secretion genes*

Table 1: Sequencing results of passaged strains: Table showing sequencing results from passages of evolved daughters compared to original parental strain

antibiotic. We also demonstrate findings of polymyxin B heteroresistant clinical UPEC isolates and an *in vitro* evolution experiment to drive polymyxin B resistance.

Several lines of evidence suggest that two-component systems may be a source of heterogeneity within a population. Because they are utilized by bacteria to sense and respond to changing environments, they are lucrative targets to heterogeneously express. It is advantageous to have part of the population primed and ready to survive an environment that it may encounter. We demonstrate that within a colony biofilm, UPEC heterogeneously activates the *qse* operon. This is not surprising as UPEC forms biofilms during infection and the QseBC has been shown to be important during infection.

Because QseBC and PmrAB are conserved two-component systems in *E. coli* we searched a bank of UPEC clinical isolates for heteroresistance to polymyxin B. We found four isolates with two populations: a stable resistant subpopulation and a sensitive population. Interestingly, sequencing revealed SNPs in and upstream of metabolism genes instead of in *qseBC, pmrCAB,* or LPS modification genes. However, a limitation of the Variation Analysis tool utilized is that it does not account for gene amplifications which are a common driver of heteroresistance. Yet, previous work has shown that QseC is implicated in central metabolism and these mutations in metabolism genes (*gadX* and *sucB)* may be necessary to drive resistance to polymyxin B (see Chapter 3).

Because of case reports in *Klebsiella pneumoniae* and *Acinetobacter baumanni* demonstrating that polymyxin B resistance can be gained in the course of treatment, we tested the ability of the sensitive clinical UPEC isolates to gain resistance in a *in vitro* evolution experiment. We passaged the strains at a sublethal MIC for five days and found that all strains rapidly gained resistance to polymyxin B. Interestingly, when sequenced passaged strains had SNPs in metabolism genes (ga*dX* and *gadA*), and *pmrA*. This further suggests a role for metabolism in polymyxin B resistance. These data also

demonstrate that bacteria can quickly utilize existing chromosomal systems to mount resistance to antibiotics; which may influence how last-resort antibiotics, like polymyxin B are used clinically.

Work in Chapter 3 will elucidate a novel role for the response regulator, QseB. This chapter provided evidence that PmrAB is a driver of heteroresistance. Yet, *gadA* and *gadX* mutations were observed, suggesting a role for metabolism or acid resistance in response to polymyxin B. In Chapter 3, I will elucidate these mechanisms, and demonstrate a role for *gad* during a challenge with positively charged antibiotics.

CHAPTER III

TRANSIENT RESISTANCE TO POSITIVELY CHARGED ANTIBIOTICS IN UROPATHOGENIC ESCHERICHIA COLI IS ASSOCIATED WITH METABOLIC SHIFTS CONTROLLED BY THE QSEB RESPONSE REGULATOR

At the time of this dissertation defense, portion of this work was in review at PNAS

Additional authors on this manuscript are: Connor J. Beebout, Alexis Hollingsworth, Dr. Kirsten R. Guckes, Alexandria Purcell, Tomas A. Burmuez, Diamond Williams, Seth A. Reasoner, Dr. M. Stephen Trent, and Dr. Maria Hadjifrangiskou

Introduction

Antibiotic resistance is a global pandemic and includes high rates of antibiotic treatment failure. One in every ten antibiotic prescription fails even when the clinical laboratory's antimicrobial susceptibility panel predicts susceptibility to a given drug. (Collaborators, 2022, Johnson et al., 2012, de Jong et al., 2019, Karve et al., 2018, Band and Weiss, 2019). The molecular underpinnings behind such treatment failures remain largely undefined. This work elucidates a previously uncharacterized mechanism in *Escherichia coli* that fuels transient resistance to positively charged antibiotics, such as the "last-line" antibiotic polymyxin B.

Enterobacteriaceae are common human pathogens, accounting for urinary tract infections, bloodstream infections and pneumonias (Paterson, 2000). Among the antibiotics currently used to treat infections caused by multi-drug resistant Enterobacteriaceae, are aminoglycosides and polymyxins, which are polycationic in nature and therefore contact the bacterial cell envelope by binding to negatively charged moieties on the lipopolysaccharide (LPS) (Taber et al., 1987, Teuber and Bader, 1976).

This interaction leads to increased permeability and penetration of the aminoglycoside or polymyxin into the periplasm. A mechanism used by bacteria to repel cationic antibiotics is to make the bacterial cell envelope less negatively charged (Teuber and Bader, 1976). Altering the net charge of the envelope can be accomplished through different mechanisms, including dephosphorylation of the lipid A component of LPS (Figure 7A), or addition of positively charged groups – such as phosphoethanolamine and aminoarabinose – directly to the lipid A group during synthesis (Lee et al., 2004). In *E. coli*, the majority

of LPS modifications occur during LPS biogenesis (Figure 7A) at the periplasmic leaflet of the inner membrane (Simpson and Trent, 2019) and consume several products of central metabolism. For example, the ArnB transaminase catalyzes a reversible reaction of undecaprenyl-4-keto-pyranose to undecaprenyl 4-amino-4-deoxy-L-arabinose by consuming glutamate and producing oxoglutarate in the process. Intriguingly, early work by the Raetz group indicated that the ArnB-mediated addition of amino-arabinose is energetically unfavorable and requires excess glutamate, as determined through an *in vitro* radiometric enzymatic assay.(Breazeale et al., 2003). Given the central role of glutamate in *E. coli* physiological functions (Kumar and Shimizu, 2010, Yan, 2007, Bennett et al., 2009), this raises a fundamental question of how *E. coli* manages the metabolic burden associated with LPS modification.

A significant body of work revealed PmrA as the transcriptional activator of genes required for modifying the nascent LPS (Gunn et al., 1998, Gunn et al., 2000, Lee et al., 2004, Vaara et al., 1981, Zhou et al., 2001). However, little is known about what controls the metabolic shifts that occur to accommodate LPS modification. Here we demonstrate that the QseB transcription factor fills in the role of metabolic controller, during *E. coli*'s response to positively charged antibiotics. Transcriptional analysis of mutants deleted for either *qseB*, or *pmrA* and *qseB*, reveal that both transcription factors influence

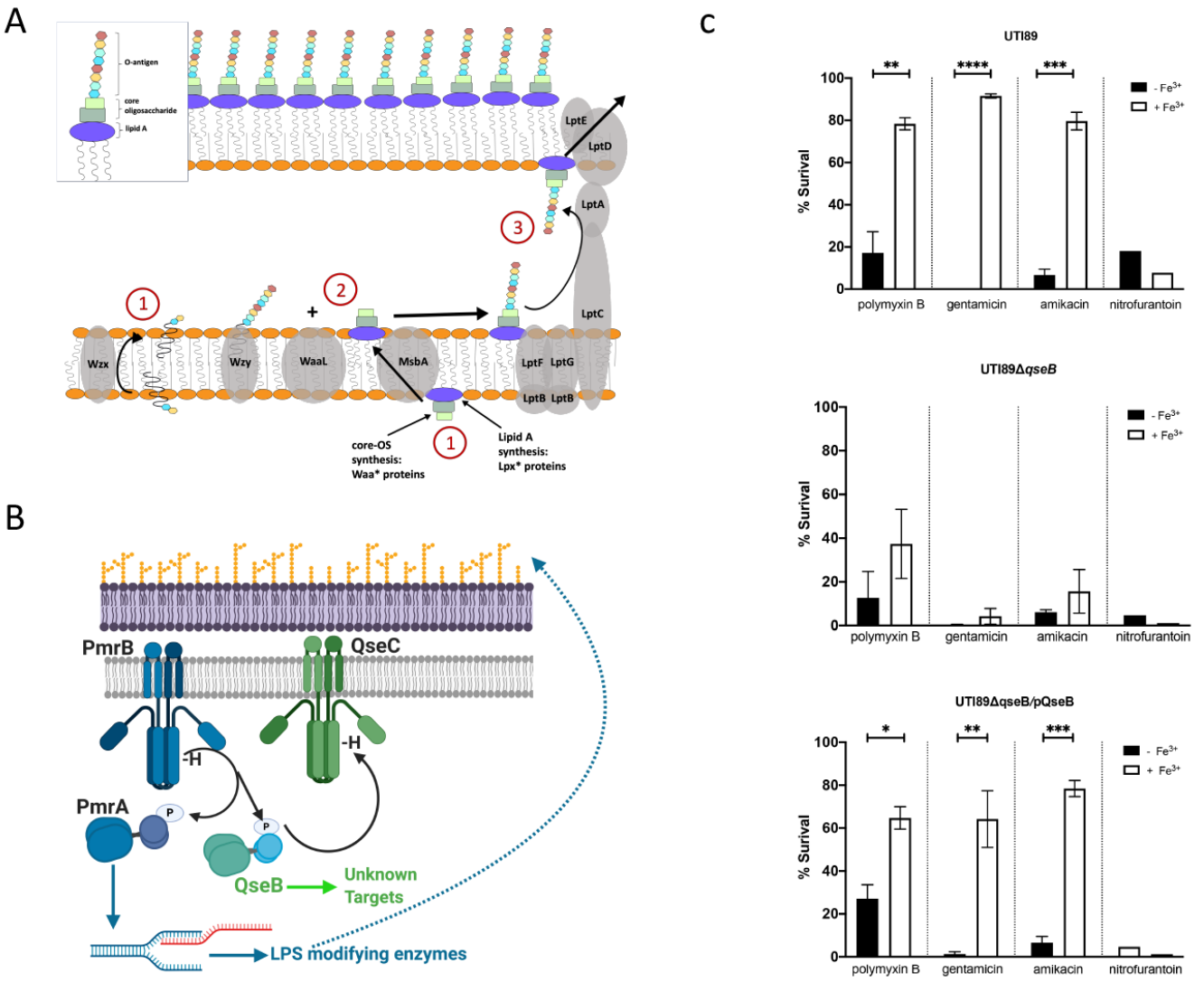

Figure 7: The PmrAB-QseBC two-component systems confer resistance to positively charge antibiotics

A) Cartoon depicts -ina simplified manner -the steps in lipopolysaccharide (LPS) biosynthesis inEscherichiacoli.(B) Cartoon depicts the mechanism of activation of the two-component systems PmrAB (blue) and QseBC (green). PmrBis a membrane bound histidine kinase that is activated by ferric iron. Upon activation it auto-phosphorylates and then transfers the phosphoryl group onto its cognate response regulator PmrA and the non-cognate QseB. PmrA acts as a transcription factor, regulating the transcription of LPS modifying genes. QseB is also transcription factor, the targets of which during antibiotic response were unknown prior to this study. (C) Graphs depict results of polymyxin B, gentamicin, and amikacin survival assays for each strain. Cells were allowed to reach mid logarithmic growth phase in the presence or absence of ferric iron and normalized. Cells were then exposed to antibiotic or to diluent alone (sterile water), for one hour. At this time cells were serially diluted and plated to determine colony forming units per milliliter (ml). To determine percent survival, cells

exposed to antibiotic were compared to isogenic untreated controls (mean ± SEM, n = 3 biological repeats). To determine statistical significance, an unpaired t-test was performed between the untreated strain and the same strain treated with ferric iron. **, $p < 0.01$; ***, $p < 0.001$ ****, $p < 0.0001$.

the expression of LPS modifying genes. However, deletion of *qseB* most profoundly affects metabolism genes centered on glutamate biosynthesis and 2-oxoglutarate-glutamate homeostasis. Accordingly, deletion of *qseB* alters glutamate levels in the cell, coincident with increased antibiotic susceptibility in the *qseB* deletion mutant. Deletion of representative QseB-regulated metabolism genes influence corresponding metabolite levels during antibiotic challenge and display a susceptibility profile that phenocopies the *qseB* deletion mutant. Exogenous addition of oxoglutarate, but not glutamate rescues the *qseB* deletion phenotype, suggesting that the cell relies on *de novo* replenishment of glutamate during the antibiotic response. Finally, analysis of LPS modification in strains lacking different permutations of *pmr* and *qse* genes demonstrates – for the first time – that QseB contributes to modification of the LPS.

Methods

Biological Resources: Bacterial Strains, Plasmids, and Growth Conditions

Bacterial strains, plasmids and primers used in this study are listed in Table 2. Overnight growth was always performed in liquid culture in Lysogeny Broth (Fisher) at 37°C with shaking, with appropriate antibiotics, as noted in the results. Details pertaining to growth conditions for each assay used in the study can be found in the relevant sections below.

RNA Isolation

RNA from cell pellets was extracted using the RNeasy kit (Sigma Aldrich) and quantified using Agilent Technology (Agilent). A total of 3 micrograms (μg) of RNA was DNAse treated using the DNAfree kit (Ambion) as we previously described (Hadjifrangiskou et al., 2011). A total of 1μg of DNAse-treated

	SOURCE	IDENTIFIER
Bacterial Strains		
MG1655	Lab stock	N/A
CFT073	Lab stock	N/A
EDL933	ATCC	700927
86-24	Lab stock	N/A
ETEC 393	Rúgeles *et al* 2010	N/A
ETEC 386	Rúgeles *et al* 2010	N/A
UTI89	Lab stock	N/A
UTI89Δ*qseB*	Kostakioti *et al*	N/A
UTI89Δ*ilvC*	This study	N/A
UTI89Δ*panD*	This study	N/A
pTrc99A	Lab stock	N/A
pQseB-pTrcc99A	Kostakioti *et al*	N/A
Oligonucleotides		
GATGCGCGTGAAGGCCTGATTG	Guckes *et al* 2013	*gyrB*_qPCR_L
CACGGGCACGGGCAGCATC	Guckes *et al* 2013	*gyrB*_qPCR_R
CCTTATGATGCGGTGATCCTG G	Guckes *et al* 2013	*qseB*_qPCR_For
TCCCAGACGCAGCCCTTCTA	Guckes *et al* 2013	*qseB*_qPCR_Rev
6FAMTGCGCGAATGGCGA	Guckes *et al* 2013	*qseB*_qPCR_probe
VICACGAACTGCTGGCGGA	Guckes *et al* 2013	*gyrB*_qPCR_probe
CGAAGATGCTGCCCATG	This study	*yfbE*_qPCR_For
GCTGGCGGGCAAGATT	This study	*yfbE*_qPCR_Rev
6FAMAGGGCGACATATTGGCGCAAAAGG TACTGCT	This study	*yfbE*_qPCR_probe
TACATTGAAGGTGATGGAATCGGTGTAG ATGTAACCCCAGCCATGCTGAAGTGTAG GCTGGAGCTGCTTC	This study	*icdA*_knockout_For
GGCATTGATTGCGCCTTCCATACCTTTAA CAATCAGGTCAGCCGCTTCAGCATATGA ATATCCTCCTTAG	This study	*icdA*_knockout_Rev
CGCTCGAAGGAGAGGTGAAT	This study	*icdA*_knockout_test_For
GCCCGTTTCAATATTTAACACATG	This study	*icdA* _knockout_test_Rev
ATCGCCCGTCTCAAAGGTATTAATGAAGA TCTCTCGTTAGAAGAAGTTGCGTGTAGG CTGGAGCTGCTTC	This study	*panD*_knockout_For
TAGTCTGACCTCTTCTACTGCATGATTAG CACTTTTCGTCAGGATTAAACCATATGAA TATCCTCCTTAG	This study	*panD*_knockout_Rev
GCTATGACCGCCAGAAACATG	This study	*panD*_knockout_test_For
GCGGTGAAATATCCCTGCGT	This study	*panD*_knockout_test_Rev

Table 2: List of strains, constructs, primers, and probes used in Chapter 3.

RNA was subjected to reverse-transcription using SuperScript III Reverse Transcriptase (Invitrogen/ThermoFisher Scientific) and following the manufacturer's protocol.

RNA Sequencing and Analysis

Strains were grown in N-minimal media at 37 °C with shaking, and samples were obtained as described for the transcriptional surge experiments. RNA was extracted and DNAse-treated as desc in the RNA isolation section. DNA-free RNA quality and abundance were analyzed using a Qubit fluorimeter and Agilent Bioanalyzer. RNA with an integrity score higher than 7 was utilized for library preparation at the Vanderbilt Technologies for Advance Genomics (VANTAGE) core. Specifically, mRNA enrichment was achieved using the Ribo-Zero Kit (Illumina) and libraries were constructed using the Illumina Tru-seq stranded mRNA sample prep kit. Sequencing was performed at Single Read 50 HT bp on an Illumina Hi Seq2500. Samples from three biological repeats were treated and analyzed. Gene expression changes in a given strain as a function of time (15 minutes post stimulation versus unstimulated; 60 minutes post stimulation versus unstimulated) were determined using Rockhopper software hosted on PATRIC database.

chIP-on-chip

To determine promoters bound by QseB, the strain UTI89Δ*qseB* was complemented with a construct expressing a Myc-His-tagged QseB under an arabinose-inducible promoter (Kostakioti et al., 2009, Guckes et al., 2013b, Guckes et al., 2017). As a control for non-specific pull-downs, an isogenic strain harboring the pBAD-MycHis A empty vector was used. Cultures were grown in Lysogeny Broth in the presence of 0.02μM arabinose to ensure constant expression of QseB, at concentrations similar to

those we previously published as sufficient for QseBC complementation (Kostakioti et al., 2009). Formaldehyde was added to 1% final concentration, following the methodology as described by Mooney et al., (Mooney et al., 2009). Upon addition of formaldehyde, shaking was continued for 5 min before quenching with glycine. Cells were harvested, washed with PBS, and stored at -80 °C prior to analyses. Cells were sonicated and digested with nuclease and RNase A before immunoprecipitation. Immunoprecipitation was performed using an anti-Myc antibody (ThermoFisher, (Guckes et al., 2013b)) on six separate reactions, three for the experimental and three for the control strain. The ChIP DNA sample was amplified by ligation-mediated PCR to yield >4 μg of DNA, pooled with two other independent samples, labeled with Cy3 and Cy5 fluorescent dyes (one for the ChIP sample and one for a control input sample) and hybridized to UTI89-specific Affymetrix chips (Hadjifrangiskou et al., 2011).

Polymyxin B Survival Assays

To assess susceptibility of strains to polymyxin B, strains were grown in N-minimal media in the absence (unstimulated) and presence (stimulated) of ferric iron (at a final concentration of 100μM) as described for the transcriptional surge experiments and in Figure 7. When bacteria reached an OD_{600} of 0.5, they were normalized to an OD_{600} of 0.5 in 5ml of 1X phosphate buffered saline (PBS) and split into two groups: A) Nothing added – "Total CFU's control"; B) PMB added at a final concentration of (2.5 μg/mL) – "– PMB treated". The "stimulated (+Ferric iron) samples also received ferric iron at a final concentration 100μM. Samples were incubated for 60 minutes at 37 °C after which samples were serially diluted and plated on nutrient agar plates (Lysogeny Broth agar) to determine colony forming units per milliliter (CFU/mL). Percent survival as a function of ferric iron pre-stimulation was determined by using the formula

$$\frac{((\boldsymbol{PMB} + \boldsymbol{Fe^{3+}})\frac{\boldsymbol{CFU}}{\boldsymbol{mL}}) - (\boldsymbol{PMB}\frac{\boldsymbol{CFU}}{\boldsymbol{mL}})}{\left(\boldsymbol{Fe^{3+}}\frac{\boldsymbol{CFU}}{\boldsymbol{mL}}\right) - (\boldsymbol{unstimulated}\ \frac{\boldsymbol{CFU}}{\boldsymbol{mL}})}\ \boldsymbol{X\ 100} = \%\ \boldsymbol{survival}$$

For polymyxin B (PMB) survival assays performed concurrently with metabolite measurements (see relevant section below), samples were taken across time (at induction (t=0), 15, 60, and 180 minutes post ferric iron additions). For PMB survival assays performed concurrently with oxoglutarate rescue assays (see relevant section below), oxoglutarate was added at the same time as polymyxin B after standardization of the samples to an OD_{600} = 0.5.

Metabolite Measurements

Pellets of approximately 10^8 cells were collected from PMB survival assays at each time-point. Glutamate, aspartate and coenzyme A levels were quantified using a colorimetric assay utilized from Glutamate-, Aspartate- and Coenzyme A Assay Kits (all kits obtained from Sigma Aldrich) utilizing the entire, undiluted sample (10^8 cells). Assays were performed according to manufacturer's instructions in at least 2 biological replicates per strain, per timepoint.

Polymyxin B Minimum Inhibitory Concentration (MIC) Determination

To determine the minimum inhibitory concentration of PMB in strains used in this study the broth microdilution method was used. Strains were grown at 37°C overnight with shaking, in cation-adjusted Mueller Hinton broth following clinical microbiology laboratory standard operating procedures (**CLSI**, 2018). Specifically, strains were sub-cultured at a starting OD_{600} of 0.05 and allowed to reach growth at an OD_{600} = 0.4 – 0.5. Cells were then normalized to and OD_{600} = 0.5 or roughly 10^5 cells. At this time, a 96 well polypropylene plate was prepared with a gradient of PMB concentrations (2-fold dilution from

64 μg/mL to 0.125 μg/mL) across the rows, plus a column with no PMB added as a growth control, and a media only column to serve as a negative control. Five microliters of the standardized culture were added to each well except those holding the media control. Plates were incubated statically at 37°C for 24 hours. At this time, the minimum inhibitory concertation was determined. Minimum inhibitory concentration was set as the concentration of polymyxin B in the well in which bacterial growth was diminished by greater than 95%. Each strain was tested with 3 technical replicates and 3 biological replicates.

Transcriptional Surge Experiments

To assess induction of *qseBC*, bacteria were grown in N-minimal media (Shin et al., 2006, Guckes et al., 2013b) at 37°C with shaking (220 rotations per minute). N-minimal media were inoculated with strains of interest at starting optical density at a wavelength of 600 nm (OD_{600}) of 0.05. Strains were allowed to reach mid-logarithmic growth phase (OD_{600} = 0.5). At this time, 4-milliliters of culture was withdrawn for processing (see below) and the remainder of the culture was split into two. To one of the two split cultures, ferric chloride (Fisher) was added at a final concentration of 100 μM, while the other culture served as the unstimulated control. Cultures were returned to 37°C with shaking. Four-milliliter samples were withdrawn from each culture at 15- and 60-minutes post stimulation for RNA processing, antibiotic susceptibility profiling and metabolomics as described above. All samples were centrifuged at 4000 x g for 10 minutes upon collection. The supernatant was decanted and the fraction containing the cell pellet was flash frozen in dry ice – ethanol and stored at -80°C until RNA extraction.

Mass spectrometry of lipid A species

200 mL cultures of each strain were grown at 37°C in N-minimal media supplemented with 10 µg/mL Niacin. At an OD_{600} of ~0.5, 100 µM of iron was added to the indicated strains and then all strains continued growing at 37°C for an additional hour. Cultures were harvested and lipid A was isolated from cells as previously described (Purcell et al., 2022, Henderson et al., 2013). Mass spectra of purified lipid A were acquired in the negative-ion linear mode using a matrix-assisted laser desorption-ionization time-of-flight (MALDI-TOF) mass spectrometer (Bruker Auto-flex speed). The matrix used was a saturated solution of 6-aza-2-thiothymine in 50% acetonitrile and 10% tribasic ammonium citrate (9:1, v/v). Sample and plate preparation were done as previously described (Henderson et al., 2013, Purcell et al., 2022).

Statistical Analyses

For antibiotic survival assays, the percent survival of strains in specific conditions were calculated (mean ± SEM, N =3) and were compared to a control strain using an unpaired T-test to performed using Prism software. For polymyxin B survival assays in which several strains were compared to UTI89 with ferric iron added, a one-way ANOVA was performed with multiple comparisons. For antibiotic survival assays in which several strains were compared one another a one-way ANOVA with multiple comparisons was used. For transcriptional surge experiments across time, no statistical test was used, but the mean ± SEM was displayed. For RNA sequencing data, q-value was calculated by the Rockhopper software when calculating for differential expression between two conditions. For metabolite measurements, no statistical test was used, a representative of three biological replicates was displayed.

Data and Code Availability

RNA sequencing data submission can be found on ArrayExpress at E-MTAB-9277. ChIP-on-chip is pending submission at ArrayExpress.

Results

QseB mediates resistance to positively charged antibiotics

In previous work we determined that the PmrAB two-component system interacts – via phosphotransfer events – with QseB, a transcription factor that forms a two-component system with the QseC membrane-bound receptor Figure 7B and (Kostakioti et al., 2009, Guckes et al., 2013a, Guckes et al., 2017)). Specifically, we discovered that activation of the PmrB receptor by one of its ligands – ferric iron – leads to phosphorylation of both the cognate PmrA and the non-cognate QseB and that both phosphorylation events are necessary for *E. coli* to mount resistance to polymyxin B (Guckes et al., 2017). Deletion of *pmrB* abolishes the ability of *E. coli* to survive polymyxin intoxication; deletion of either *pmrA* or *qseB* leads to a two- to ten-fold reduction in survival, with the double deletion mutant Δ*pmrA*Δ*qseB* phenocopying the *pmrB* deletion (Figure 8 and (Guckes et al., 2017)). While PmrA regulates the expression of LPS-modifying enzymes in both *Salmonella* and *E. coli* (Gunn et al., 1998, Gunn et al., 2000), the role of QseB in mediating resistance to polymyxin B in *E. coli* has been elusive. Intriguingly, studies have recently reported the presence of an additional *qseBC* locus within an *mcr*-containing plasmid in an isolate that is resistant to colistin, another polycationic antimicrobial, (Kieffer et al., 2019) further suggesting a role for the QseBC two-component system in LPS modification.

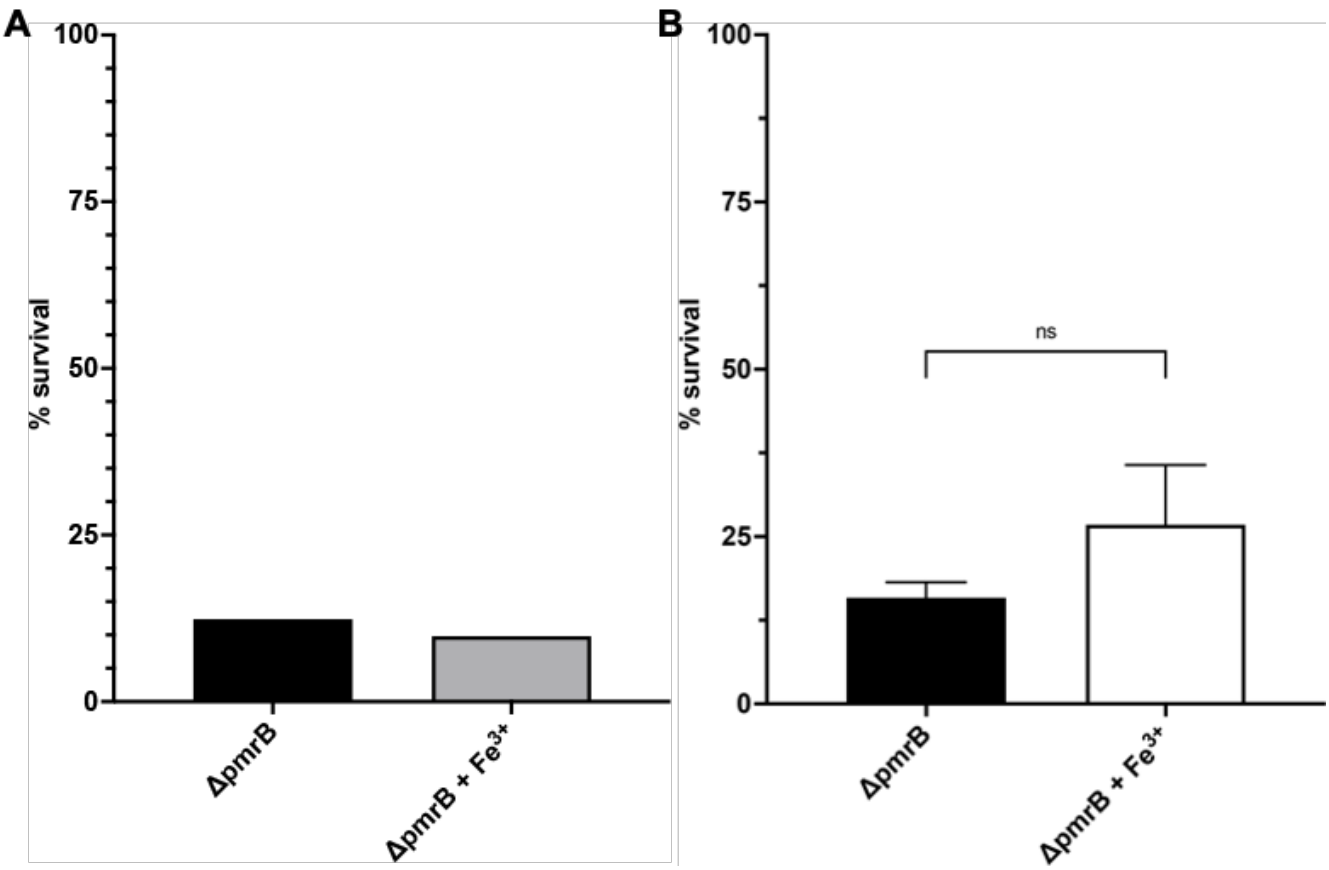

Figure 8: In the absence of *pmrB,* UPEC is unable to mount resistance to positively charge antibiotics
A-B) Graphs depict results of a polymyxin B survival assay for the UTI89Δ*pmrB* . Cells were allowed to reach mid logarithmic growth phase in the presence or absence of ferric iron and normalized. Cells were then exposed to amikacin (A) polymyxin B (B) for one hour. At this time cells were serially diluted and plated to determine colony forming units per milliliter. To determine percent survival, antibiotic-treated cells were compared to the untreated controls (mean ± SEM, n = 3 biological repeats for polymyxin B, n =1 for amikacin). To determine statistical significance, a one-way ANOVA was performed with multiple comparisons between the untreated-and treated samples of polymyxin B treated cells, ns, no statistical significance detected by test used.

If QseB-mediated control facilitates modification of the cell envelope to a less negatively charged state, one would predict that QseB activation would also lead to resistance to other positively charged antibiotics. To test this hypothesis, isogenic strains lacking QseB (UTI89Δ*qseB*), or carrying QseB in the native locus (UTI89) or extra-chromosomally (UTI89Δ*qseB* /pQseB), were tested for their ability to resist gentamicin and amikacin, aminoglycoside antibiotics that are positively charged. Nitrofurantoin, which is neutral, along with polymyxin B were used as negative and positive controls respectively (Figure 7C). Strains were tested for their ability to survive a concentration of antibiotic at up to 5 times the established minimum inhibitory concentration (MIC) after growth to mid-logarithmic growth phase in nutrient-limiting media as previously used to mimic the host environment and induce activation of the PmrAB two-component system (Groisman et al., 1997, Guckes et al., 2013b, Guckes et al., 2017). Bacterial survival was calculated during growth in media alone (black bars) or in media supplemented with 100mM ferric iron – the activating signal for the PmrB receptor (white bars), after 60 minutes.

Strains harboring QseB (wild-type strain or the Δ*qseB*/pQseB complemented strain) exhibited 75-95% survival in the presence of positively charged antibiotics when pre-conditioned with ferric iron (Figure 7C, top and bottom panels). However, the strain lacking *qseB* (Δ*qseB,* Figure 7C middle panel**)** exhibited a marked decline in survival regardless of the presence of ferric iron that was not significantly different from the survival of the un-stimulated strain. The uncharged antibiotic nitrofurantoin led to effective bacterial killing of all genetic backgrounds (Figure 7C). These data indicate that the QseB transcription factor mediates resistance to positively charged antibiotics.

Given the genomic plasticity associated with the species *E. coli* (Rasko et al., 2008), we next asked whether the QseB signaling drives antibiotic resistance to cationic antibiotics in isolates from three of

the most prevalent *E. coli* phylogenetic clades, B1, B2 and E. Using a representative panel of *E. coli* strains that lack plasmid-borne polymyxin B resistance determinants and are sensitive to polymyxin by standard clinical laboratory testing (Figure 9A), we saw a robust transcriptional surge, an increase in transcript abundance soon after activation, followed by a slow reset, of the *qseB* promoter in all tested strains in response to ferric iron (Figure 9C) that coincided with an elevated survival (77%-100%) in 2.5X the MIC of polymyxin B compared to untreated controls (Figure 9C). Deletion of *qseB* or *qseBC* in well-characterized enterohemorrhagic *E. coli* (EHEC) strains 86-24 and 87-14 led to a significant reduction in polymyxin B resistance compared to the wild-type parent (Figure 10), which was rescued upon extra-chromosomal complementation with a wild-type copy of *qseB*. Notably, strain Sakai that harbors a truncated, non-functional copy of QseC, exhibits intrinsic resistance to polymyxin B (Figure 10, consistent with the model that absence of functional QseC leads to uncontrolled PmrB-to-QseB phosphotransfer and subsequent intrinsic resistance. Supporting this notion, deletion of *qseB* or the entire *qseBC* locus in this strain phenocopies the *qseB* deletion in the other EHEC isolates (Figure 10). Combined these results indicate that resistance to positively charged antibiotics is mediated by QseB in diverse *E. coli* clades. To further probe the mechanism by which QseB mediates antibiotic resistance we used the uropathogenic *E. coli* (UPEC) strain UTI89.

QseB and PmrB support some LPS modifications in the absence of PmrA.

We previously reported a synergistic effect of QseB and PmrA in mediating resistance to polymyxin B (Guckes et al., 2017), and our data here indicate a role for QseB in mediating resistance to other positively charged antibiotics. Together, these observations suggest that QseB is involved in mediating changes to the cell envelope charge. To determine whether QseB leads to LPS modification, we analyzed

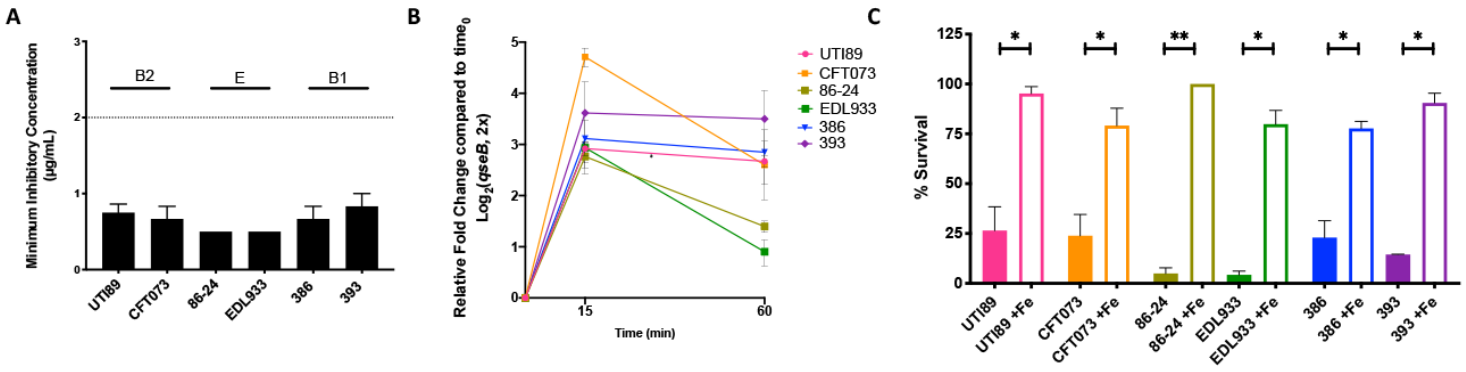

Figure 9: Representatives of different pathotypes of *E. coli* all mount resistance to polymyxin B
A) Graph depicts the polymyxin B minimum inhibitory concentration (MIC) determined for the strains of pathogenic *E. coli* used in our studies. These strains were selected so as to represent the most prevalent phylogenetic clades (mean ± SEM is shown, n = 3 biological repeats). (B) Graph depicts qPCR results tracking the activation of the *qse* operon following the addition of ferric iron to the media. Briefly, cells were allowed to reach exponential growth phase. Cells were then collected before and at 15-and 60 minutes post addition of ferric iron. RNA was extracted, DNAse treated, and reverse transcribed, as described in the methods section. The resulting cDNA was quantified, normalized for concentration and subjected to qPCR using TaqMan chemistry and a probe complementary to *qseB* was used (See Table 2). Graph depicts log2-fold change of *qseB* transcripts at each time point relative to the sample taken before stimulation (mean ± SEM, n = 3biological repeats). (C) Graph depicts polymyxin survival of representative *E. coli* strains. (mean ± SEM, n = 3biological repeats). To determine statistical significance, an unpaired t-test was performed between each strain treated with ferric iron and its untreated isogenic control.*, $p < 0.05$; **, $p < 0.01$.

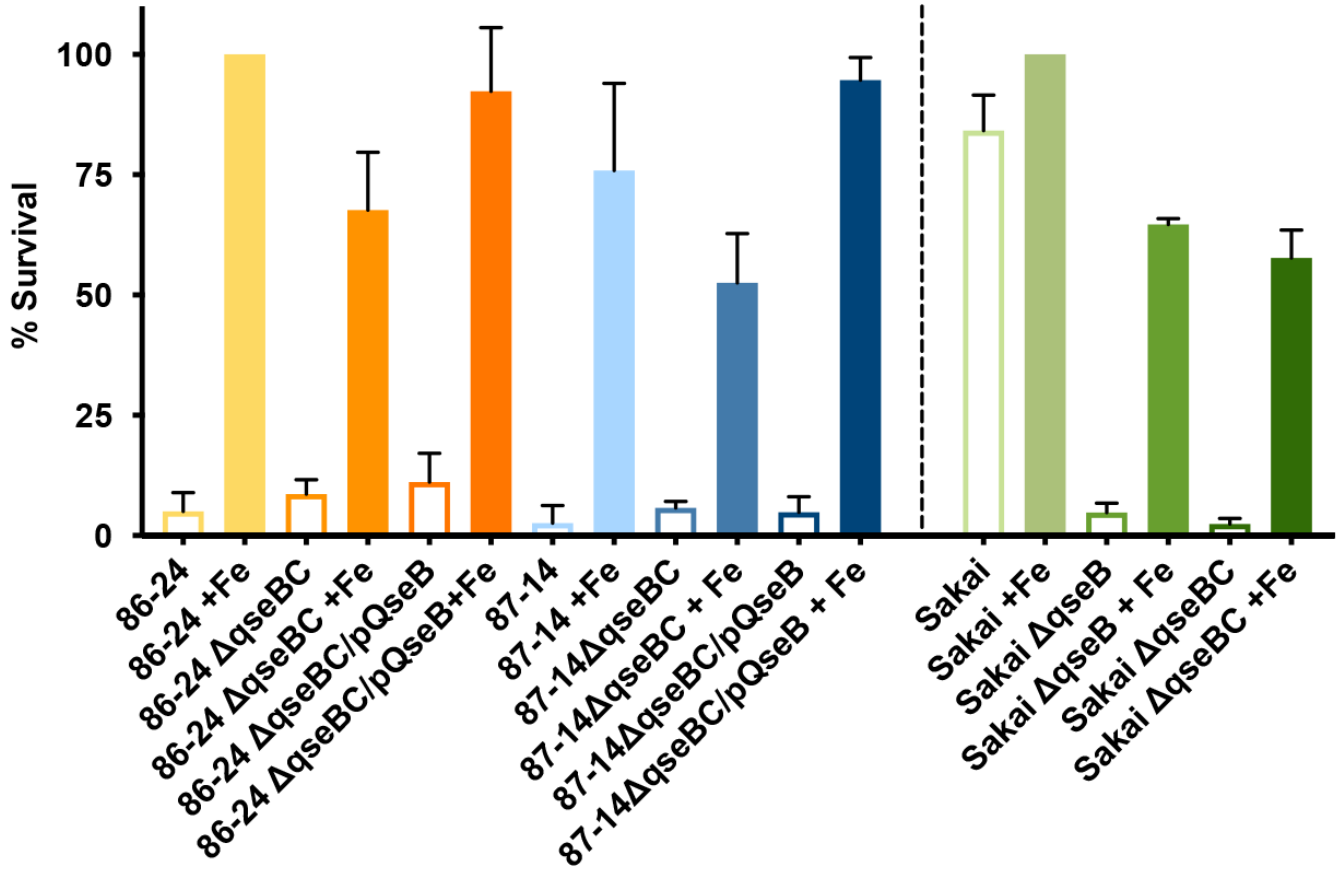

Figure 10: EHEC responds to ferric iron and mounts resistance to polymyxin B
Graph depicts results of polymyxin B survival assays completed for representative EHEC strains and isogenic mutants. Cells were allowed to reach mid logarithmic growth phase in the presence or absence of ferric iron and normalized. Cells were then exposed to polymyxin at 2.5 µg/mL for one hour. At this time cells were serially diluted and plated to determine colony forming units per mL. To determine percent survival, cells exposed to polymyxin were compared to isogenic untreated controls from the same culture. (mean ± SEM, n = 3biological repeats).

changes to the lipid A moiety of strain UTI89 and isogenic *qse* and *pmr* mutants with and without ferric iron stimulation. Analysis of lipid A from wild-type UTI89 produced molecular ions at 1796.0 and 1919.2 *m/z* corresponding to unmodified lipid A and the addition of a single pEtN, respectively (Figure 11A). With the addition of Fe^{3+} to the growth media, additional modifications were apparent including lipid A with two pEtN residues (2042.3 *m/z*) and a species modified with both L-Ara4N and pEtN (2049.4 *m/z*) indicating increased levels of lipid A modification. Deletion of *qseB* in wild-type UTI89 had no impact on lipid A structure and similar molecular ions were detected in the presence (*m/z* 1919.6, 2042.6, 2050.6) or absence (*m/z* 1796.3, 1919.2) of iron (Figure 11A). The additional species at *m/z* 1839.5 in the *qseB* mutant with Fe^{3+} arises from the loss of the 1-phosphate that is easily hydrolyzed during mass spectrometry from the $[pEtN]_2$-lipid A species (Rubin et al., 2015, Herrera et al., 2010, Zimmerman et al., 2020). This result indicates that QseB loss does not impair the covalent modification of lipid A.

The pEtN modification was lost in the UTI89Δ*pmrA*Δ*qseB* double mutant; only unmodified lipid A (*m/z* 1796.2) was present. Furthermore, addition of Fe^{3+} could not restore lipid A modifications in UTI89Δ*pmrA*Δ*qseB*. Given the current literature, this was expected since PmrA is necessary for transcription of genes encoding lipid A modification machinery. However, single and double modified species were easily detected in strain UTI89Δ*pmrA*Δ*qseC* (Figure 11), suggesting that QseB also regulates expression of *eptA (pmrC, yjdb) and arnT (pmrK).* Furthermore, the addition of Fe^{3+} was no longer required for production of doubly modified species in the UTI89Δ*pmrA*Δ*qseC* consistent with our previous report that in this strain PmrB constitutively activates QseB and results in a strain that shows intermediate levels of polymyxin resistance according to CLSI standards (Guckes et al., 2017). Together,

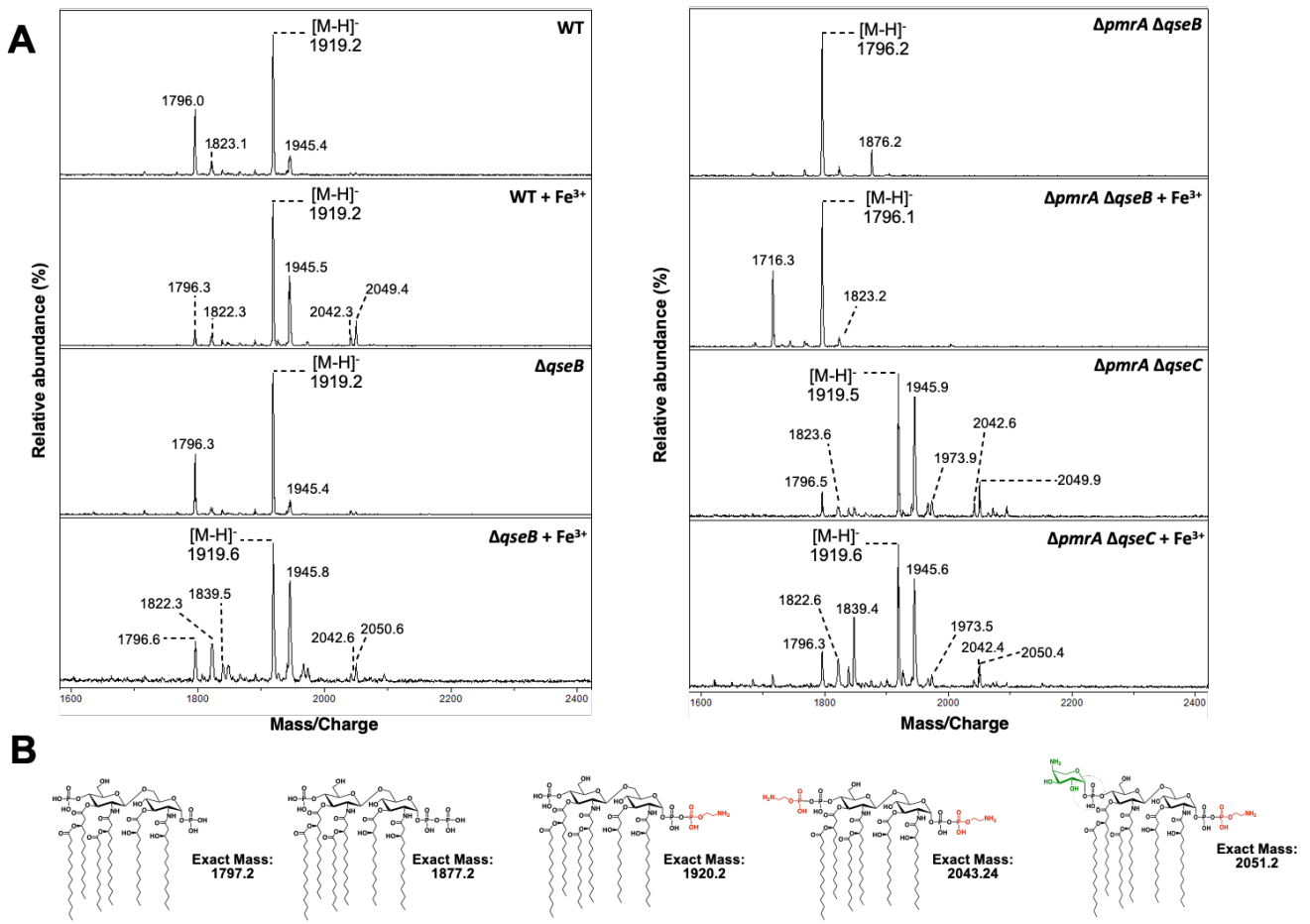

Figure 11: QseB promotes the modification of LPS in the absence of PmrA and QseC

A) Lipid A was isolated from the indicated strains grown in N-minimal media supplemented with 10 µg/mL of niacin and iron where indicated. Lipid A was analyzed using MALDI-TOF mass spectrometry in the negative-ion mode.InUTI89(left panel) there was unmodified (m/z1796.0) and pEtN modified (m/z1919.2) lipid A. For UTI89 + Fe^{3+}, additional peaks were observed at 2042.3 (2 pEtNs) and 2049.4 (pEtN, L-Ara4N) representing doubly modified species. Compared to wild-type UT189, loss of *qseB* (left panel) had no effect on lipid A structure, regardless of the addition of Fe^{3+}. Modification with pEtN and L-Ara4N was lost in Δ*pmrA*Δq*seB*(+/-Fe^{3+}) (right panel) with unmodified lipid A (m/z 1796.2) the major species. However, single and double modifications were easily detected in Δ*pmr*AΔ*qseC* (+/-Fe^{3+}). Description of minor peaks: Peaks at m/z of ~1822 and 1945 correspond to species detected at m/z of ~1796 and 1919 containing one acyl chain extended by two carbons, respectively. The minor peak at m/z 1839.5inΔ*qseB* (+Fe3+) contains a single pEtN, but lacks the 1-phosphate group that is easily hydrolyzed during mass spectrometry. Similarly, the peak at m/z 1716.3 in *pmrA*, *qseB* (+Fe^{3+}) is the loss of 1-phosphate from unmodified lipid A. The species at m/z 1876.2 represents a lipid A containing a 1-diphosphate moiety giving a tris-phosphorylated lipid A, a species detected in the absence of activated PmrA. Data is representative of three biological experiments. B) Proposed chemical structures and exact masses of relevant lipid A species.

these results indicate the ability of QseB to have transcriptional regulatory overlaps with PmrA. These data also suggest that QseB must play a distinct role in the modulation of antibiotic resistance

RNAseq profiling reveals regulatory redundancy between PmrA and QseB.

The lipid A profiling suggests that QseB regulates *eptA and arnT* expression since these are the enzymes responsible for the observed modifications in UTI89Δ*pmrA*Δ*qseC*. To decipher whether there are regulatory overlaps in transcription patterns between QseB and PmrA, steady-state transcript abundance across the activation surge were tracked over time via RNA sequencing (RNAseq). For these RNAseq experiments, the wild-type strain UTI89 and isogenic UTI89Δ*qseB*, UTI89Δ*pmrA*Δq*seB* or UTI89Δ*pmrA*Δq*seC* were grown under PmrB-activating conditions (100μM Ferric iron, Fe^{3+}) and samples were obtained for RNA sequencing immediately prior to (T=0), as well as 15 (T=15) and 60 (T=60) minutes post addition of ferric iron to the growth medium (Figure 12A). Output RNA sequencing data from three biological repeats per strain per timepoint were analyzed using Rockhopper software. Differential gene expression matrices within each strain were calculated to compare T = 0 to T =60 and T =15 minutes (Figure 12). An additional comparison of T=15 and T=60 was also made. Pairwise differences *across* strains were analyzed for each timepoint. Transcripts with a q value lower than 0.05 were considered significant. These analyses demonstrated that in the wild-type strain LPS modification gene expression surged over time, following stimulation with ferric iron (Figure 12B). However, the same clusters had no significant surge in the mutants lacking QseB (Figure 12B). Comparison of UTI89Δ*pmrA*Δ*qseC* to wild-type UPEC at t=0, t=15 and t=60 revealed that indeed in the UTI89Δ*pmrA*Δ*qseC* strain, both *arnT* and *eptA* (*yjdB*) are induced, along with other members of the *arn* operon. Together, these data indicate that QseB and PmrA share regulatory redundancy in mediating transcription of LPS modification genes.

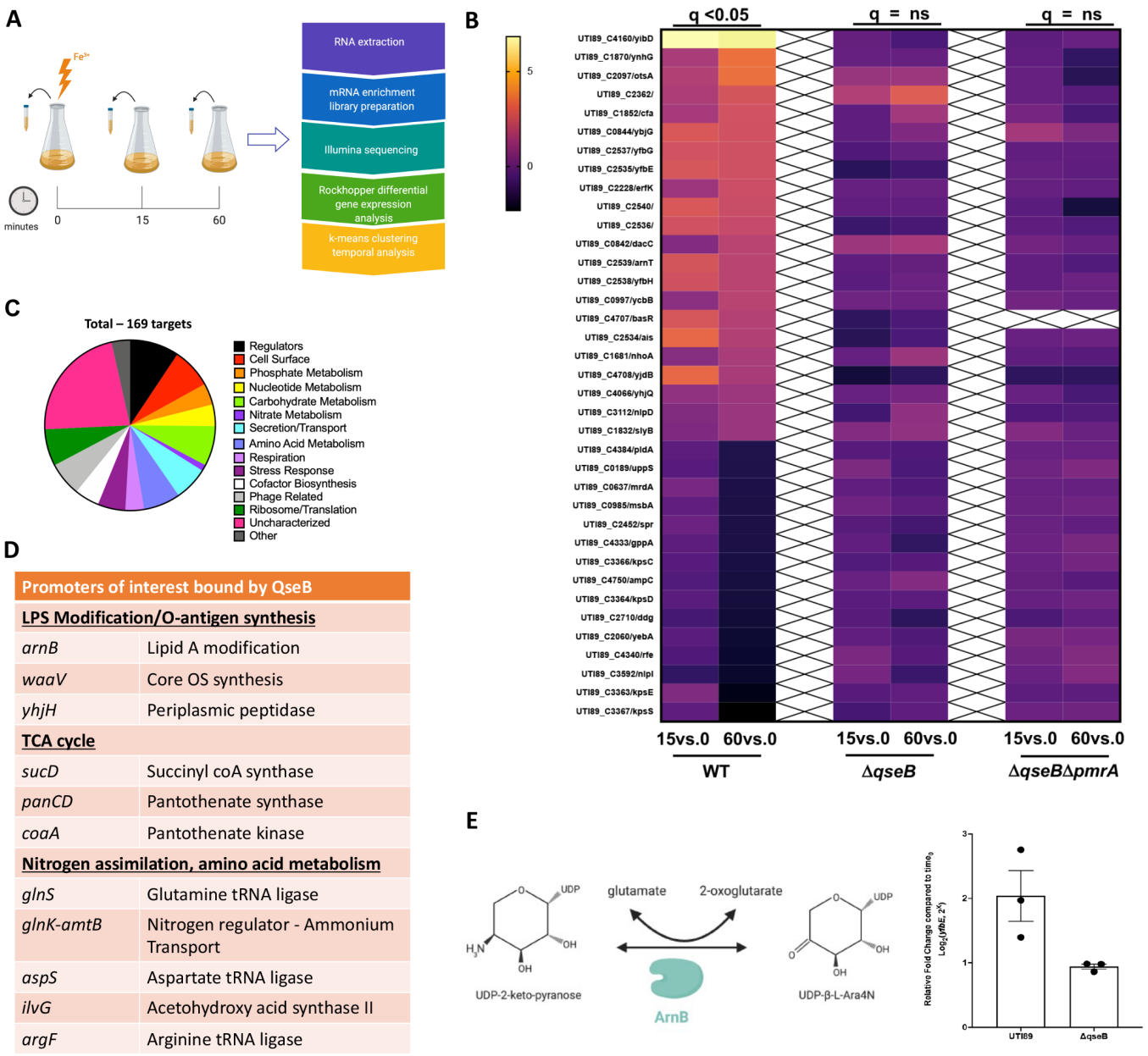

Promoters of interest bound by QseB	
LPS Modification/O-antigen synthesis	
arnB	Lipid A modification
waaV	Core OS synthesis
yhjH	Periplasmic peptidase
TCA cycle	
sucD	Succinyl coA synthase
panCD	Pantothenate synthase
coaA	Pantothenate kinase
Nitrogen assimilation, amino acid metabolism	
glnS	Glutamine tRNA ligase
glnK-amtB	Nitrogen regulator - Ammonium Transport
aspS	Aspartate tRNA ligase
ilvG	Acetohydroxy acid synthase II
argF	Arginine tRNA ligase

Figure 12: QseB and PmrA have regulatory overlaps.A) The schematic shows the pipeline for sample collection and data processing in the presented RNAseq study. B) Heatmaps indicate log2relative fold change of wild-type (WT) UTI89 and the isogenic ΔqseB, andΔqseBΔpmrA strains, for genes involved in metabolism after stimulation with ferric iron at 15-and 60-minutes post-stimulation. These genes were significantly (q<0.05) changed at 60 minutes compared to pre-stimulation (T=0) in wild-type UTI89, but showed no statistically significant change in the absence of *qseB* alone or in the absence of both *qseB* and *pmrA*. C-D)Direct targets of QseB identified in chIP-on-chip analyses. C) Pie chart indicates the

distribution of 169 unique DNA promoter sequences bound by QseB in pull-down experiments using tagged QseB and cross-linking, followed by immunoprecipitation, reversal of the crosslinks and hybridization of eluted DNA onto Affymetrix UTI89-specific chips. The data are from three independent biological experiments and exclude non-specific targets isolated through immunoprecipitation with vector control. (D)Subset of the direct targets of QseB. E) Cartoon depicts the conversion of UDP 2-keto pyranose to UDP-b-L-Ara4N by ArnB, in a reaction that consumes a glutamate molecule and produces an oxoglutarate molecule in the process. The graph depicts the expression of yfbE(arnB) at 60 minutes post stimulation with ferric iron in UTI89 and UTI89ΔqseB. Briefly, cells were grown tomid-log growth phase. Cells were collected before stimulationand at 60 minutes post-stimulation with ferric iron for RNA extraction and reverse transcription. Resulting cDNA was subjected to qPCR with a probe complementary to the yfbE region (See Table 2 for corresponding primers and probe). Graph depicts log2-fold change ofyfbE transcripts at each time point relative to the sample taken before stimulation (mean ± SEM, n = 3biological repeats, depicted as dots in the graph).

To further validate RNAseq experiments and to identify promoters bound by QseB, we performed a chiP-on-chip experiment, using the UTI89Δ*qseB* strain that harbors a construct expressing Myc-His-tagged QseB under an arabinose-inducible promoter (Kostakioti et al., 2009, Guckes et al., 2013b, Guckes et al., 2017). An isogenic strain harboring the pBAD-MycHis A vector was used as a negative control. Pull-downs using an anti-Myc antibody were performed on six separate reactions, three for the experimental and three for the control strain. Analyses of the pull-down DNA revealed a total of 169 unique promoters bound by QseB and absent in the negative control (Figure 12C-D). Among the promoters identified was the promoter of *qseBC* – consistent with QseB's ability to regulate its own transcription (Kostakioti et al., 2009, Hadjifrangiskou et al., 2011, Clarke and Sperandio, 2005), as well as *yibD*, which we have previously validated as a QseB binding target (Guckes et al., 2013b, Guckes et al., 2017). Another promoter identified was indeed the *arnBCADTEF* promoter region, with portion of the *arnB* gene, which is the first gene in the operon, also pulled down the analyses (Figure 12D). Accordingly, qPCR analysis determined *arnB* transcript levels were 2.16 times lower in the *qseB* deletion mutant compared to the wild-type control (Figure 12E), validating that QseB transcriptionally regulates the *arn* operon

QseB controls central metabolism genes.

Our RNAseq and ChIP-on-chip profiling revealed that in addition to LPS-modification, QseB controls several genes that code for central metabolism enzymes. (Figure 13A). Among the most highly upregulated genes in the RNAseq profiling were genes involved in arginine and isoleucine biosynthesis, as well as genes encoding TCA cycle enzymes (Figure 13A). However, the same clusters had no significant surge in the mutants lacking QseB (Figure 13A). The chIP-on-chip analyses revealed *ilvG* and *argF* as QseB direct targets (Figure 12D) as, well as another set of metabolic targets including *glnK, glnS* and *aspS* that are involved in glutamine-glutamate and aspartate-glutamate interconversions respectively (Figure

13D). In media with low ammonia, glutamate can be synthesized via the combined action of glutamine- and glutamate synthases, encoded by *glnA* and *gltBD* respectively (Kumar and Shimizu, 2010). This occurs via the condensation of glutamate with ammonia by GlnA, followed by reductive transamination of the produced glutamine with oxoglutarate by GltBD. Under high nitrogen/ammonia conditions, glutamate is synthesized by glutamate dehydrogenase encoded by *gdhA* (Kumar and Shimizu, 2010). In the growth conditions used in our studies, ammonia was limiting, but the overall nitrogen concentration was 7.5mM. The *glnA* and *gdhA* loci were not part of the upregulated genes, but *ybaS* – which also converts glutamine to glutamate (Djoko et al., 2017) – and *gltA, gltB* and *gltD* were among the most highly upregulated genes, the surge of which depended on QseB (Figure 13). Consistent with previous studies demonstrating a high ATP and NADPH requirement for nitrogen assimilation/glutamate production (Reitzer, 2003, Yan, 2007), genes involved in aspartate, beta alanine oxaloacetate conversions, as well as a possible glutamate-fumarate shunt were identified as key QseB regulated target (Figure 13A-B) The genes involved in glutamate metabolism are particularly intriguing, given that the *arnB* gene product catalyzes transamination of undecaprenyl-4-keto-pyranose to undecaprenyl 4-amino-4-deoxy-L-arabinose (Figure 12E), which consumes glutamate, releasing oxoglutarate in the process. Previous work by the Raetz group indicated that this reaction is not energetically favored (Breazeale et al., 2003). We thus asked whether QseB regulates glutamate-oxoglutarate homeostasis during *E. coli's* response to positively charged antibiotics.

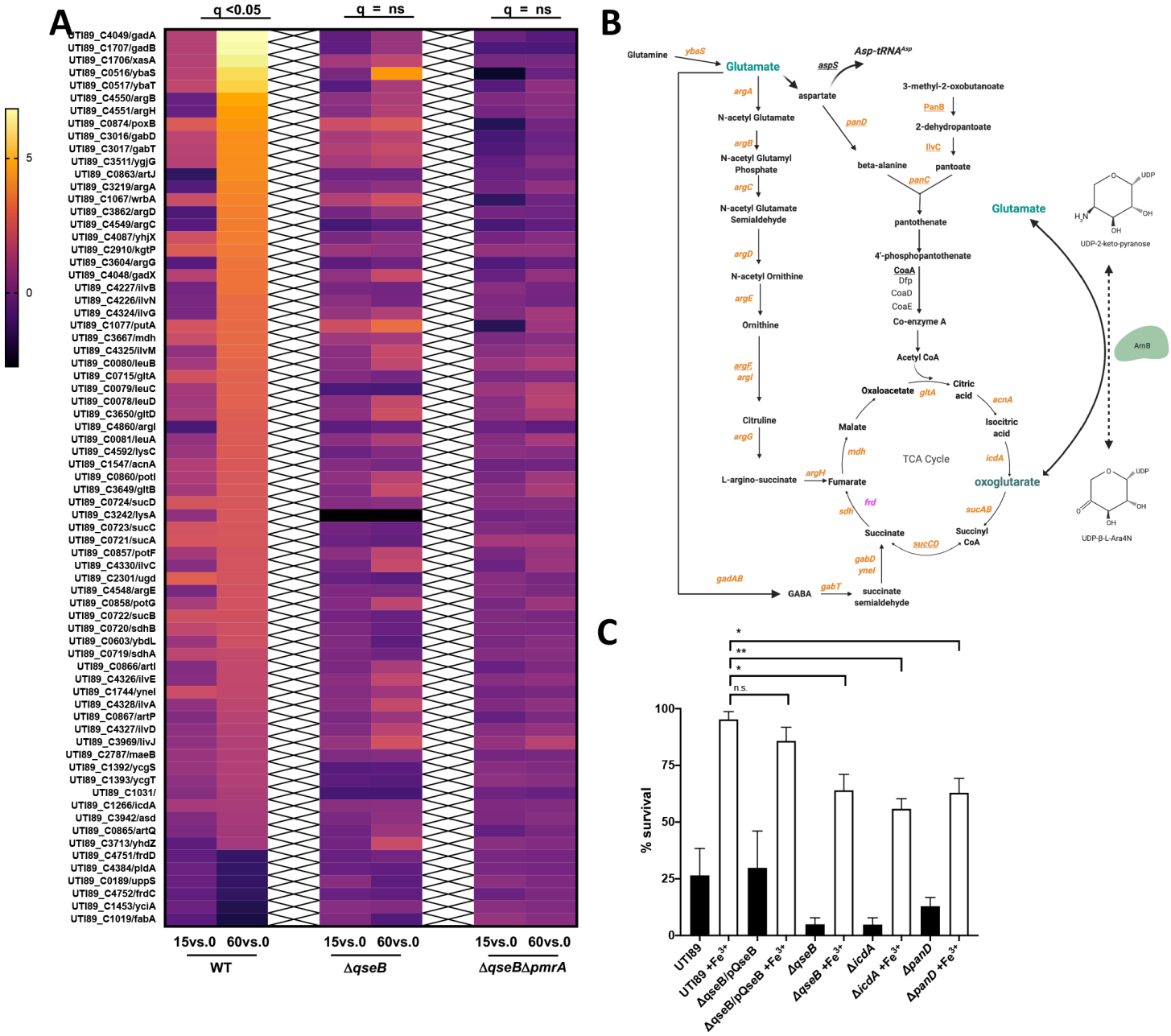

Figure 13: RNAseq profiling across time reveals a metabolic circuit controlled by QseB

Heatmaps indicate log_2 relative fold change of wild-type (WT) UTI89 and the isogenic Δ*qseB*, and Δ*qseB*Δ*pmrA* strains, for genes involved in metabolism after stimulation with ferric iron at 15-and 60-minutes post stimulation. These genes were significantly (q<0.05) changed at 60 minutes compared to pre-stimulation (T=0) in wild-type UTI89, but showed no statistically significant change in the absence of *qseB* alone or in the absence of both *qseB* and *pmrA*. B) Schematic outlines the metabolic pathways regulated by QseB. Genes in orange are upregulated at 60 minutes post-stimulation with ferric iron as indicated by RNA sequencing data. Genes in pink are downregulated at 60 minutes post-stimulation with ferric iron. Genes underlined are direct targets of QseB as indicated by ChIP-on-chip data.C) Graph depicts polymyxin B survival assays for wild-type *E. coli* and isogenic mutants deleted for *qseB*, *icdA*, or *panD*. Cells were allowed to reach mid-logarithmic growth phase in the presence or absence of ferric

iron and normalized. Cells were then either exposed to polymyxin at 2.5 μg/mL or without addition for one hour. To determine percent survival, cells exposed to polymyxin B were compared to those that were not (mean ± SEM, n = 3). To determine statistical significance, a one-way ANOVA with multiple comparisons was performed between strains treated with ferric iron and UTI89 wild-type treated with ferric iron. *, $p < 0.05$. N.S. denotes a comparison that did not result in statistical significance.

Glutamate – oxoglutarate homeostasis, regulated by QseB, is necessary for mounting antibiotic resistance.

To determine how the QseB-regulated metabolism genes would influence antibiotic resistance in a strain that contains both ArnB and QseB, we turned to a combination of metabolomics and mutagenesis. First, we created deletions in *panD* and *icdA*. PanD codes for an aspartate decarboxylase that converts aspartate into beta-alanine, which then feeds into the pantothenate pathway eventually resulting in coenzyme A production (Figure 13B) The *pan* gene operon is under the direct control of QseB, as the operon's promoter was bound by QseB (Figure 12D). We reasoned that if the identified QseB regulon is active during LPS modification, then we would detect changes in coenzyme A production and that deletion of *panD*, which is centrally placed in the identified pathway (Figure 13B) should impair antibiotic resistance. In parallel, we created a control *icdA* deletion mutant, disrupting the conversion of isocitrate to oxoglutarate (Figure 13B), thereby limiting oxoglutarate production, which we reasoned would be needed for GltAB activity. Obtained mutants were tested in polymyxin B survival assays alongside the wild-type parental strain and the isogenic *qseB* deletion mutant, as well as the *qseB* deletion mutant complemented with *qseB*. Strains were tested for their ability to survive a concentration of PMB at five times the established MIC. While the wild-type and the Δ*qseB*/pQseB complemented strains exhibited 85-95% survival in 5X the PMB MIC when pre-conditioned with ferric iron, the *qseB, panD* and *icdA* deletion mutants reproducibly exhibited a 50% reduction in survival (Figure 12C). Metabolite measurements of aspartate and coenzyme A, which are the first and last metabolites in the identified PanD pathway (Figure 13C), revealed altered aspartate and coenzyme A abundance in

cells devoid of QseB compared to wild-type samples (Figure 14), indicating, that QseB indeed influences production of these intermediates.

To determine how deletion of *qseB* influences glutamate levels during an antibiotic stress response, we quantified glutamate in wild-type UPEC, the Δ*qseB* strain and the Δ*qseB/*pQseB complemented control. For metabolomics measurements, samples were taken from wild-type UTI89, UTI89Δ*qseB* and the complemented strain UTI89Δ*qseB/*pQseB grown in the presence of ferric iron (PmrB activating signal) (Figure 15, red lines), polymyxin B (PMB) alone (Figure 15, blue lines), or in the presence of ferric iron and PMB (Figure 15, pink lines). Control cultures in which no additives were included (Figure 15, black lines) were also included. In the wild-type background, addition of polymyxin B, or polymyxin B/ferric iron, resulted in a rapid decrease in glutamate levels compared to cells exposed to ferric iron alone or no additives (Figure 15A) However, in the Δ*qseB* deletion strain there was no change in glutamate levels in the different growth conditions (Figure 15B). Complementation of Δ*qseB* with pQseB, which restores extrachromosomal expression of QseB from a high-copy plasm, results in a drop in glutamate levels shortly after addition of ferric iron, polymyxin B, or both (Figure 15C). These data indicate that glutamate levels change during the antibiotic response, in a manner that depends upon QseB.

If our transcriptional, metabolic and antibiotic resistance results point towards a central glutamate production circuit that is controlled by QseB and requires oxoglutarate, we next asked whether the susceptibility of the *qseB* deletion mutant to positively charged antibiotics could be rescued via the addition of exogenous oxoglutarate or glutamate. Addition of oxoglutarate to polymyxin B-treated samples of Δ*qseB* restored survival in 5X the antibiotic MIC (Figure 16). Addition of glutamate did not have the same effect (Figure 16). These data indicate that sufficient uptake of glutamate is not

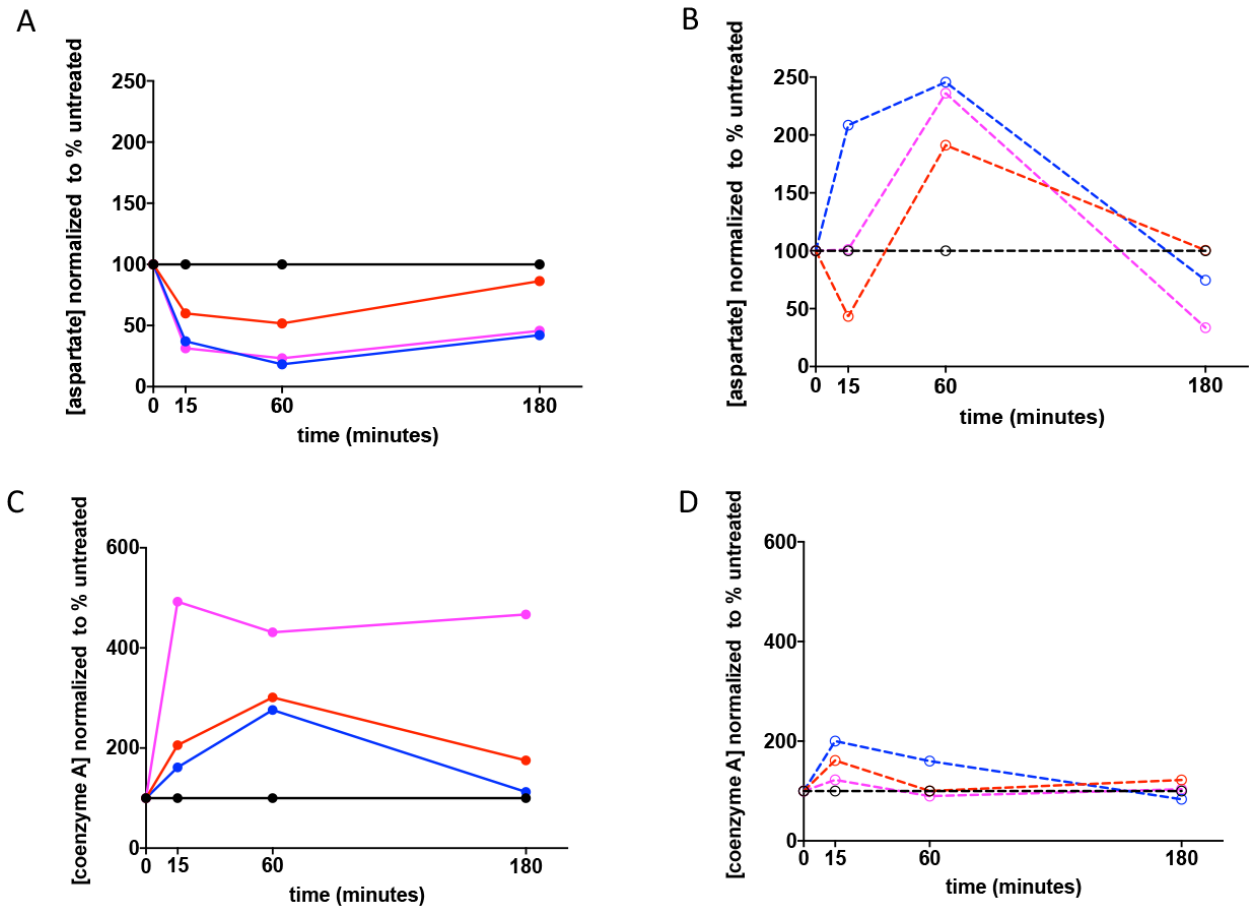

Figure 14: Coenzyme A and aspartate levels are influenced by QseB: Graphs indicate metabolite abundance for aspartate and Co-enzyme A over time, in wild-type *E. coli* and isogenic mutants under different stimulation conditions. Measurements are normalized to a sample in which no additives or conditions were changed (black lines). Pink lines show measurements from samples in which ferric iron and polymyxin were added. Blue lines show measurements from samples in which only polymyxin was added. Red lines show measurements in which only ferric iron was added. **A-B)** Graphs depict glutamate measurements in wild-type UTI89 (A), or UTI89Δ*qseB* (B). **C-D)** Graphs depict aspartate measurements in wild-type UTI89 (C), or UTI89Δ*qseB* (D). Graphs are representative of at least three biological repeats.

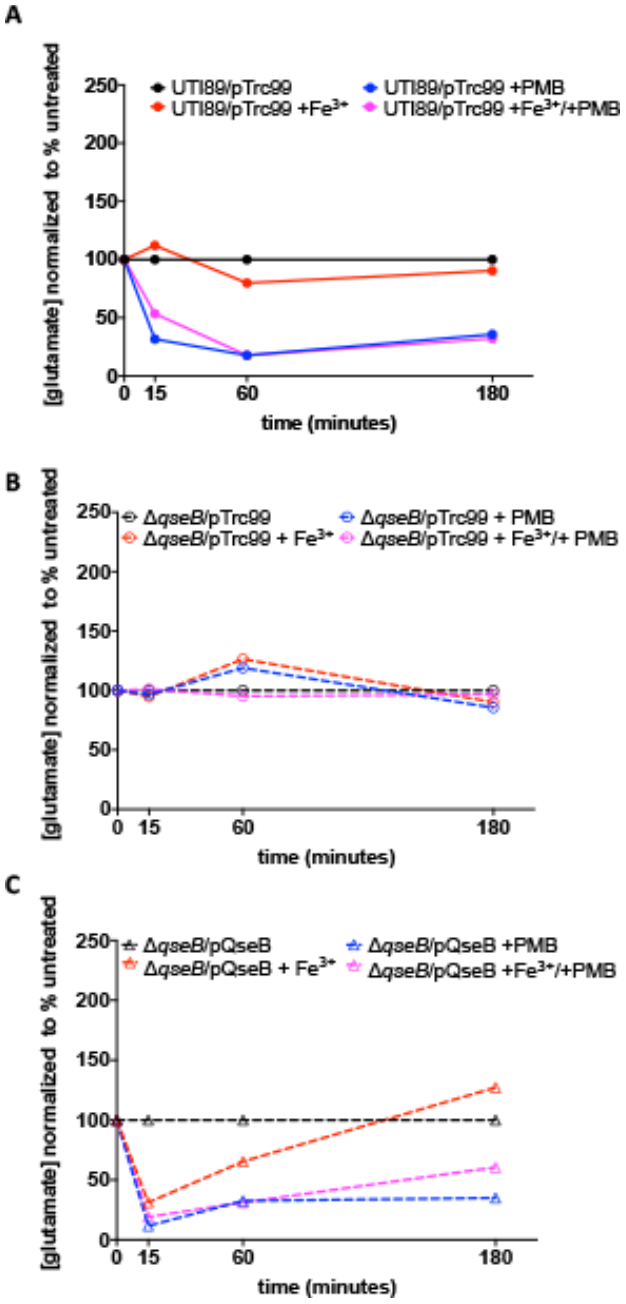

Figure 15: Glutamate metabolism is under the control of QseB.

A-C) Graphs depict glutamate abundance over time in wild-type *E. coli* and isogenic mutants under different stimulation conditions.Measurements are normalized to a sample in which no additives or conditions were changed (black lines). Pink lines show measurements from samples in which ferric iron and polymyxin were added. Blue lines show measurements from samples in which only polymyxin was added. Red lines show measurements in which only ferric iron was added.Glutamate was measured across time in wild-type UTI89 (A), UTI89ΔqseB/pTrc99 (B) and UTI89ΔqseB/pQseB(C).A representative of three biological replicates is depicted.

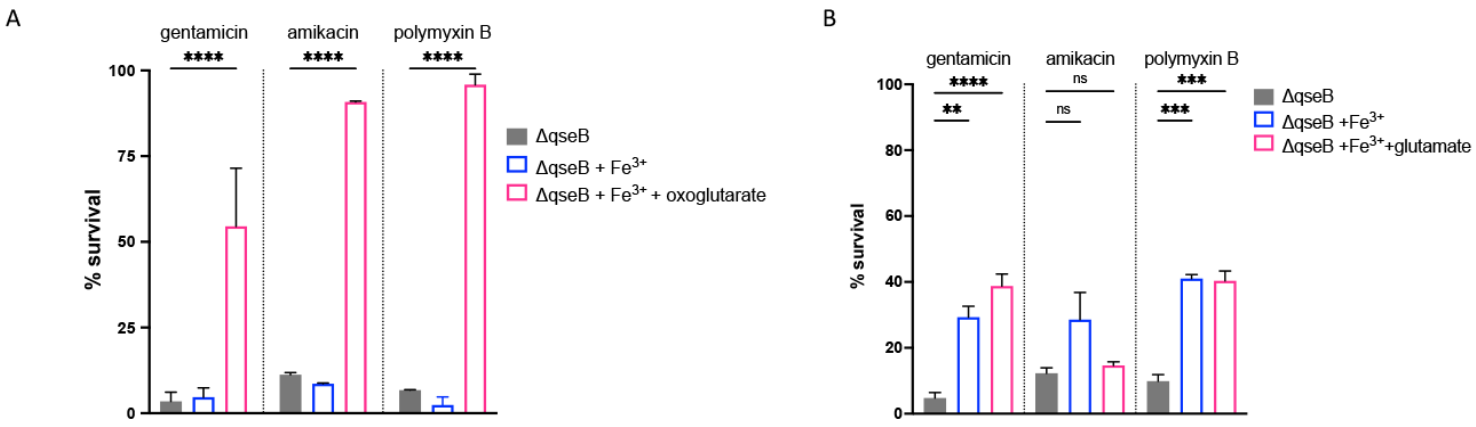

Figure 16: Addition of exogenous oxoglutarate rescues qseB deletion mutant

A-B) Graphs depict results of polymyxin B, gentamicin, and amikacin survival assays for the *qseB* deletion mutant in the presence or absence of exogenous oxoglutarate (A) or glutamate (B). Cells were allowed to reach mid logarithmic growth phase in the presence or absence of ferric iron and normalized. Cells were then exposed to antibiotic or to diluent alone (sterile water), for one hour. An additional subset of cells received both ferric iron and oxoglutarate (A) or glutamate (B). At this time cells were serially diluted and plated to determine colony forming units per milliliter. To determine percent survival, antibiotic-treated cells in which metabolite was added were compared to the antibiotic-treated controls that were not supplemented with oxoglutarate or glutamate (mean ± SEM, n = 3 biological repeats). To determine statistical significance, a one-way ANOVA was performed with multiple comparisons between the untreated-and treated samples. **, $p < 0.01$; ***, $p < 0.001$, N.S, no statistical significance detected by test used.

sufficiently occurring in the absence of QseB and that oxoglutarate-glutamate homeostasis controlled by QseB is necessary for mounting resistance to positively charged antibiotics.

Discussion

Bacteria can mount resistance to antibiotics through acquisition of mobile genetic elements, including plasmids that code for antibiotic resistance cassettes. However, in many pathogens, resistance to antimicrobial agents is encoded chromosomally. In *E. coli* and *Salmonella spp.*, resistance to positively charged antibiotics is intrinsically encoded in LPS modification genes. Yet, this intrinsic mechanism comes at a metabolic cost associated with diverting central metabolites to synthesize modified LPS. Our work builds upon this model and begins to unravel the complex metabolic consequences of antibiotic resistance While numerous studies have extensively described the various enzymes and pathways that contribute to antibiotic resistance, few have evaluated the metabolic impact of these chemical reactions on the cell. Moreover, the studies that do evaluate the metabolic impact of antibiotic resistance have primarily focused on global metrics such as population growth rate tradeoffs. More recently, several groups have begun to evaluate the influence of central metabolism on antibiotic susceptibility and are converging on a model whereby central metabolic activity – including respiratory rate and TCA cycle flux – plays a determining factor in antibiotic susceptibility (Amato et al., 2013, Hansen et al., 2008, Kohanski et al., 2010, Lopatkin et al., 2021, Lopatkin et al., 2019). Bactericidal antibiotics can exert toxic effects on the cell by elevating metabolic rate and promoting ROS production, and these effects can be mitigated by reducing metabolic activity. In addition to affecting the overall population growth and metabolic rates, antibiotic resistance mechanisms often consume central metabolites and accordingly exert a significant effect on cellular metabolism. In this work, we demonstrate that the generation of transiently

antibiotic resistant bacteria leads to a wholesale rewiring of central metabolism that may allow the cell to compensate for the consumption of metabolites during the reactions that generate antibiotic resistance.

We make two significant contributions to the field: 1) We demonstrate that in *E. coli*, QseB and PmrA share common targets in the genes that modify the LPS, but QseB plays a unique role in controlling central metabolism during LPS modification. 2) We demonstrate – through the requirement for oxoglutarate – that the anaplerotic routes identified in our analyses feed back into the TCA cycle to elevate metabolic rate and balance the glutamate necessary for mounting resistance to this class of antibiotics, without jeopardizing the cell's ability to assimilate nitrogen, a process that largely depends on glutamate (Kumar and Shimizu, 2010). By upregulating these pathways, the cell may compensate for the metabolic consequences of antibiotic resistance by regenerating and rebalancing the concentration of critical reaction intermediates.

QseB directly targets and controls several genes involved in fueling the TCA cycle during the response to positively charged antibiotics. Our data suggest that increased production of oxoglutarate by the modification of the lipid A domain of LPS may increase flux through the TCA cycle that is fueled – at least in part – by QseB-regulated pathways. Intriguingly, this process also requires the consumption of glutamate, which may be in part restored by the reversible reaction of ArnB. Our metabolomic data point towards the use of glutamate through the pantothenate pathway and co-enzyme A production, which can then enter the TCA cycle either as acetyl-CoA or succinyl-CoA (Figure 13). Likewise, conversion of glutamate to fumarate via the *arg* gene products would supply fumarate, while conversion of glutamate to GABA through the function of the *gab/gad* would re-introduce succinate into the TCA cycle.

This step would replenish succinate, bypassing the need to convert oxoglutarate to succinate via the *sucAB*- and *sucDC*-encoded complexes (Figure 13B). This could divert oxoglutarate for the production of glutamate via the activity of GdhA. Future work will focus on delineating the effects of QseB on GABA abundance and GdhA-mediated production of glutamate.

In studying emerging antibiotic resistance mechanisms, we tend to generally focus on understanding plasmid-encoded systems. Here, understanding a chromosomally encoded system may translate to emerging plasmid encoded systems, and pose a threat in the clinic, given that a new plasmid, *mcr*-9, encoding both a *mcr*-1 homologue and *qseBC*-like elements has been recently reported (Kieffer et al., 2019). This is especially concerning, because cationic antimicrobials, such as colistin are considered "antibiotics of last resort" and reserved for multi-drug resistant infections. The finding that *E. coli* and potentially other Enterobacteriaceae have the potential to mount an intrinsic resistance response to polymyxins and aminoglycosides raises the alarm for the need to better understand mechanisms that lead to heterogeneous induction of systems like QseBC in the bacterial pathogens. Lastly, this work demonstrates the need to understand how metabolic pathways can be exploited in pathogenic bacteria and may give new insights to potential therapeutic targets.

Work in this chapter elucidated a novel role for the response regulator, QseB. It also demonstrated that there is tight regulation between glutamate utilization and oxoglutarate production. This balance is likely needed to carefully control the amount of modified LPS intermediate produced by ArnB. This reaction is unfavorable in the forward direction, and requires excess amounts of glutamate. We found we could rescue a *qseB* deletion mutant by addition of oxoglutarate. Because oxoglutrate is important for mounting resistance to positively charge antibiotics, we predicted that another two-

component system, KguRS, that senses oxoglutarate could be involved in mounting resistance to positively charged antibiotics. KguRS will be further explored in Chapter 4.

CHAPTER IV

OXOGLUTARATE SENSING IS CRITICAL FOR THE INDUCTION OF POLYMYXIN B RESISTANCE IN UROPATHOGENIC *ESCHERICHIA COLI*

Portion of this work will be part of a manuscript intended for submission to the journal Microbiology. Additional contributors to this work are: Alexis Hollingsworth, Seth A. Reasoner, Dr. Kyle A. Floyd and Dr. Maria Hadjifrangiskou

Introduction

Two-component systems act as the eyes and ears of bacteria, allowing them to sense their environment. In bacteria that encounter a variety of environments, they are important for responding quickly to changes in their surroundings. Most two-component systems are comprised of a histidine kinase and a response regulator. The histidine kinase senses a specific ligand or set of ligands. It then autophosphorylates and passes the phosphoryl group onto the response regulator. The response regulator then goes on to enact some change in the cell, usually gene expression.

In the case of uropathogenic *E. coli* (UPEC), two-component systems are needed to sense a variety of niches from the gut to the urinary tract. Recently, Cai *et al.l* described in strain CFT073, a strain isolated from a pyelonephritis case, a novel two-component system that has only been found in uropathogenic *E. coli.* This two-component system, has been described as a 2-oxoglutarate sensor and named α-ketoglutarate utilization regulator/sensor (KguRS). In response to 2-oxoglutarate, KguR upregulates a target genomic island. Cai *et al* predicted that this genomic island encodes the components of a putative 2-oxoglutarate dehydrogenase and succinyl-CoA synthetase. Expression of the genes within

the genomic island after activation of KguRS was shown to be dependent upon oxygen tension. Expression of target genes is higher under anaerobiosis. Further, deletion of these target genes displayed a growth defect in anaerobic conditions. A *kguRS* mutant also had reduced fitness in a murine model of infection in both the kidneys and the bladder. These findings together suggest that KguRS may a key role in allowing the cell to adapt to changing oxygen tension during infection and to utilize 2-oxoglutarate, where abundant, as a primary carbon source(Cai et al., 2013).

Our work demonstrated that QseB controls metabolism genes centered on glutamate biosynthesis and 2-oxoglutarate – glutamate homeostasis as identified through RNA sequencing and ChiP-on-chip analyses. Deletion of *qseB* led to decreased antibiotic susceptibility but also perturbs glutamate levels in the cells. Further, addition of exogenous oxoglutarate but not glutamate rescue the *qseB* deletion mutant during an antibiotic challenge. This suggests that the cell requires *de novo* replacement of glutamate during a response to positively charged antibiotics. Control of oxoglutarate-glutamate homeostasis is crucial for UPEC's response to positively charged antibiotics. However, little is known about the role that oxoglutarate sensing plays during UPEC's response to positively charged antibiotics. Here we build upon the previous characterization of KguRS and describe its role during a response to positively charged antibiotics.

Methods

Strains and constructs

Experiments were performed in the characterized cystitis strain UTI89 and isogenic mutant. created previously, UTI89Δ*qseB* (Kostakioti et al., 2009), and for this study UTI89Δ*kguRS*. All overnight cultures were grown in LB, shaking at 37°C. Conditions for each assay are denoted below.

Growth assays

For aerobic growth assays, UTI89 and UTI89Δ*kguRS* were propagated overnight shaking at 37°C. The OD_{600} was measured seeded new cultures at an OD_{600} of 0.05. Isolates were propagated shaking at 37°C. Every hour the OD_{600} was obtained for 8 hours. For hypoxic growth assays, a new culture was started as above. The culture was placed in a 4% oxygen hypoxic incubator, shaking at 37°C. Every hour the OD_{600} was obtained for 8 hours.

Motility assays

Overnight cultures of UTI89, UTI89Δ*kguRS,* and UTI89Δ*qseB* were prepared. Using a straight metal rod, strains were stabbed into the middle of a well containing 0.25% LB agar supplemented with 2,3,5-triphenyltetrazolium chloride (TTC), to more easily visualize the growth. A second set of LB agar plates was additionally supplemented with nitrate. Agar plates were then placed in a 37 °C static incubator for 7 hours. In parallel, motility assays were prepared and incubated in an anaerobic chamber. After incubation, the diameter bacteria moved from the central stab was measured. To determine significance between strains of the same conditions, a one-way ANOVA with multiple comparisons was performed.

Biofilm setup

UTI89, UTI89*ΔkguRS,* and UTI89*ΔqseB* and were propagated overnight shaking at 37°C. Biofilms were seeded by spotting 10 μL of overnight culture onto a YESCA plate. Plates were incubated for 13

days aerobically and hypoxically. For hypoxic conditions, the Campy GasPak system was used. On days: 1, 3, 6, 8, 10, and 13 biofilm diameter was measured. No statistical test used to compare these diameters. The mean of 3 biofilms were displayed on the corresponding graph. For images of biofilms, a representative of the three was displayed.

Antibiotic Survival Assays

To assess the susceptibility of strains to polymyxin B and gentamicin, strains were grown in N-minimal media in the absence (unstimulated) and presence (stimulated) of ferric iron (at a final concentration of 100μM) as described in Chapter 2. When bacteria reached an OD_{600} of 0.5, they were normalized to an OD_{600} of 0.5 in 5ml of 1X phosphate buffered saline (PBS) and split into two groups: A) Nothing added – "Total CFU's control"; B) choice of antibiotic (ABX) added at a final concentration of (2.5 μg/mL) – "– ABX treated". The "stimulated (+Ferric iron) samples also received ferric iron at a final concentration 100μM. Samples were incubated for 60 minutes at 37 °C after which samples were serially diluted and plated on nutrient agar plates (Lysogeny Broth agar) to determine colony forming units per milliliter (CFU/mL). Percent survival as a function of ferric iron pre-stimulation was determined by using the formula below:

$$\frac{((\boldsymbol{ABX} + \boldsymbol{Fe^{3+}})\frac{\boldsymbol{CFU}}{\boldsymbol{mL}}) - (\boldsymbol{ABX}\frac{\boldsymbol{CFU}}{\boldsymbol{mL}})}{\left(\boldsymbol{Fe^{3+}}\frac{\boldsymbol{CFU}}{\boldsymbol{mL}}\right) - (\boldsymbol{unstimulated}\ \frac{\boldsymbol{CFU}}{\boldsymbol{mL}})}\ \boldsymbol{X\ 100} = \%\ \boldsymbol{survival}$$

To determine percent survival, antibiotic-treated cells were compared to the antibiotic-treated controls (mean ± SEM, n = 3 biological repeats). To determine statistical significance, a one-way ANOVA was performed with multiple comparisons between the untreated-and treated samples.

Results

KguRS is a two-component system unique to UPEC that senses 2-oxoglutarate. It is proposed that this system is responsive to oxygen tension and upregulates a genomic island that encodes the components of a putative 2-oxoglutarate dehydrogenase and succinyl-CoA synthetase. Because of previous work in Chapter 3, that uncovered that QseB is a regulator of metabolism, that depends upon a balance of oxoglutarate- glutamate metabolism we wanted to characterize KguRS in a well studied strain of UPEC, UTI89.

We first compared the growth rate of in lysogeny broth at 37 °C in atmospheric oxygen conditions. The mutant UTI89Δ*kguRS* did not have a defect in growth compared to wild-type UTI89. We then compared the growth rate of UTI89 and UTI89Δ*kguRS* in N-minimal media in 4% oxygen to mimic the nutrient and oxygen limiting conditions of the bladder (Figure 17A-B). The resulting growth kinetics did not significantly differ between wild-type UTI89 and UTI89Δ*kguRS* (Figure 17A-B).

Because KguRS signaling is different in response to varying oxygen tension, we asked if biofilm architecture or growth could be altered in the UTI89Δ*kguRS* mutant, given the presence of oxygen gradients in biofilms (Beebout et al., 2019). We seeded biofilms of wild-type UTI89, UTI89*ΔkguRS,* and UTI89*ΔqseB* on YESCA agar and allowed them to grow at room temperature for 13 days in both atmospheric and 4% oxygen conditions. The diameter of the biofilms was measured every day (Figure 18A-B). Images of the biofilms were also taken at day 13 to compare total architecture. We found that there was no significant differences in biofilm diameter or architecture between the wild-type UTI89 and the mutants (Figure 18A-B).

We then asked if there were differences in the motility of wild-type UTI89, UTI89Δ*kguRS,* and UTI89Δ*qseB.* We inoculated soft agar with overnight cultures of wild-type UTI89, UTI89Δ*kguRS,* and UTI89Δ*qseB* and incubated them at 37 °C statically in both atmospheric and anaerobic conditions with and without the presence of nitrate. After 7 hours, we measured the diameter in which the bacteria moved from the central inoculation. There was no significant difference between the distance that the mutants and wild-type UTI89 swam in aerobic conditions with and without nitrate (Figure 19A-B). Interestingly, the UTI89Δ*kguRS* anaerobic samples that had nitrate added swam significantly further than wild-type and UTI89Δ*qseB* matched samples (Figure 19 C-D). Previous work in this thesis (Chapter 3) elucidated a novel role for the response regulator QseB, that both targets lipid A modifying enzymes and acts as a regulator of metabolism during LPS modification. We found that glutamate-oxoglutarate metabolism was important during LPS modification and survival against positively charged antibiotics. Because KguS is a sensor of oxoglutarate, we asked if the system played a role in survival against positively charged antibiotics. To test this, we performed a survival assay with polymyxin B at 5X the MIC in the presence and absence of ferric iron, in UTI89*Δ*kguRS,* and used UTI89*Δ*qseB* and UTI89 wild-type as a control We found that UTI89*Δ*kguRS* was unable to mount resistance to polymyxin B in the presence or absence of ferric iron (Figure 20). We hypothesized that the inability to sense oxoglutarate may lead to downstream disruptions in the glutamate-oxoglutarate balance. We postulated that the addition of 2-oxoglutarate to the media during a challenge with polymyxin B may be able to bypass this defect. We tested this hypothesis and found that the addition of 2-oxoglutarate during a polymyxin B with ferric iron, restored UTI89*Δ*kguRS* mutant's ability to mount resistance to polymyxin B (Figure 20).

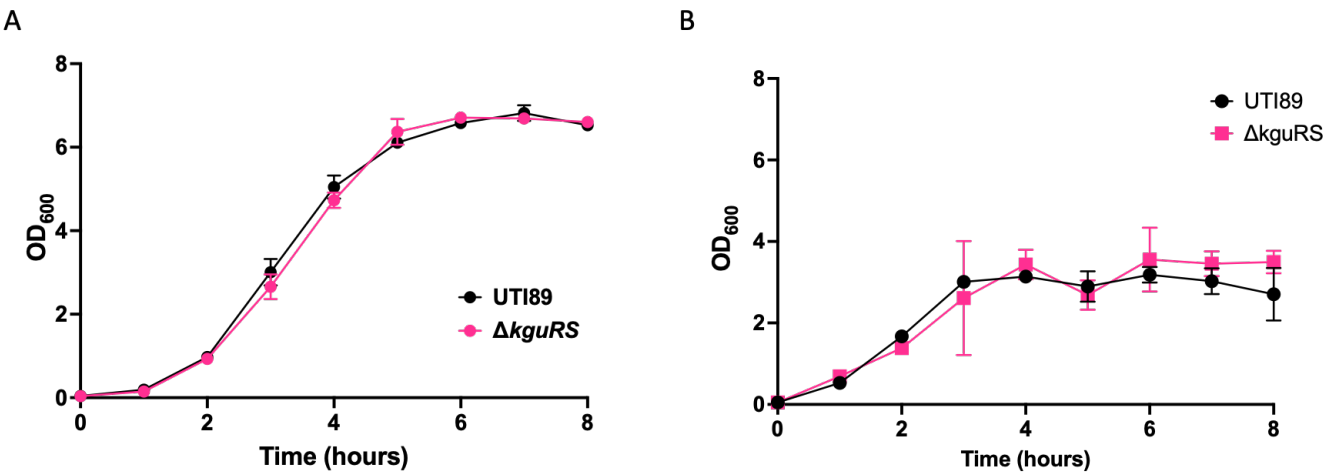

Figure 17: Growth kinetics are not significantly different between wild-type UTI89 and a *kguRS* deletion mutant

A) The growth kinetics of UTI89 and UTI89ΔkguRS were measured in aerobic conditions shaking at 37°C. Optical density was measured every hour. B) The growth kinetics of UTI89 and UTI89ΔkguRS were measured in hypoxic conditions (4% oxygen) shaking at 37°C. Optical density was measured every hour.

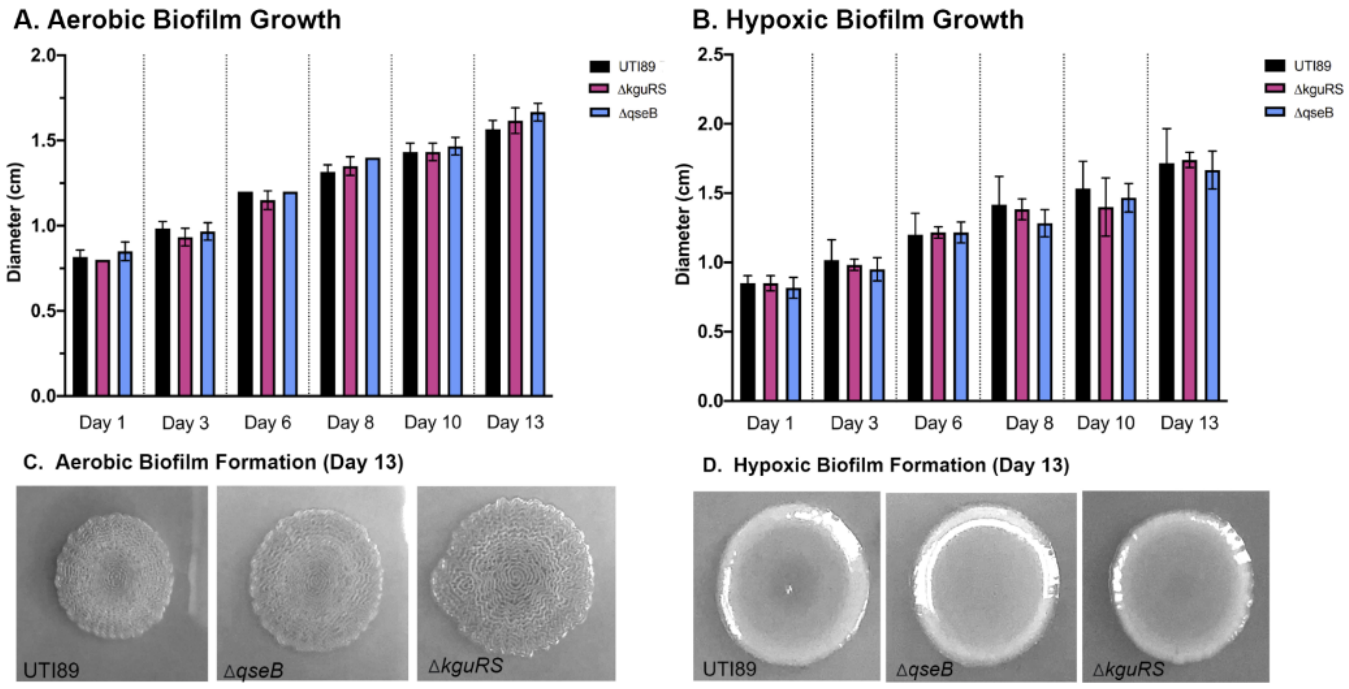

Figure 18: Biofilm morphology and growth dynamics are not altered in the *kguRS* deletion mutant Biofilm diameters were measured for UTI89, Δ*qseB*, and *ΔkguRS* for 13 days in aerobic conditions at room temperature. B) Biofilm diameters were measured for UTI89, Δ*qseB*, and *ΔkguRS* for 13 days in hypoxic conditions at room temperature. C) Day 13 aerobically grown biofilms were imaged and compared for gross architectural differences. D) Day 13 hypoxically grown biofilms were imaged and compared for gross architectural differences.

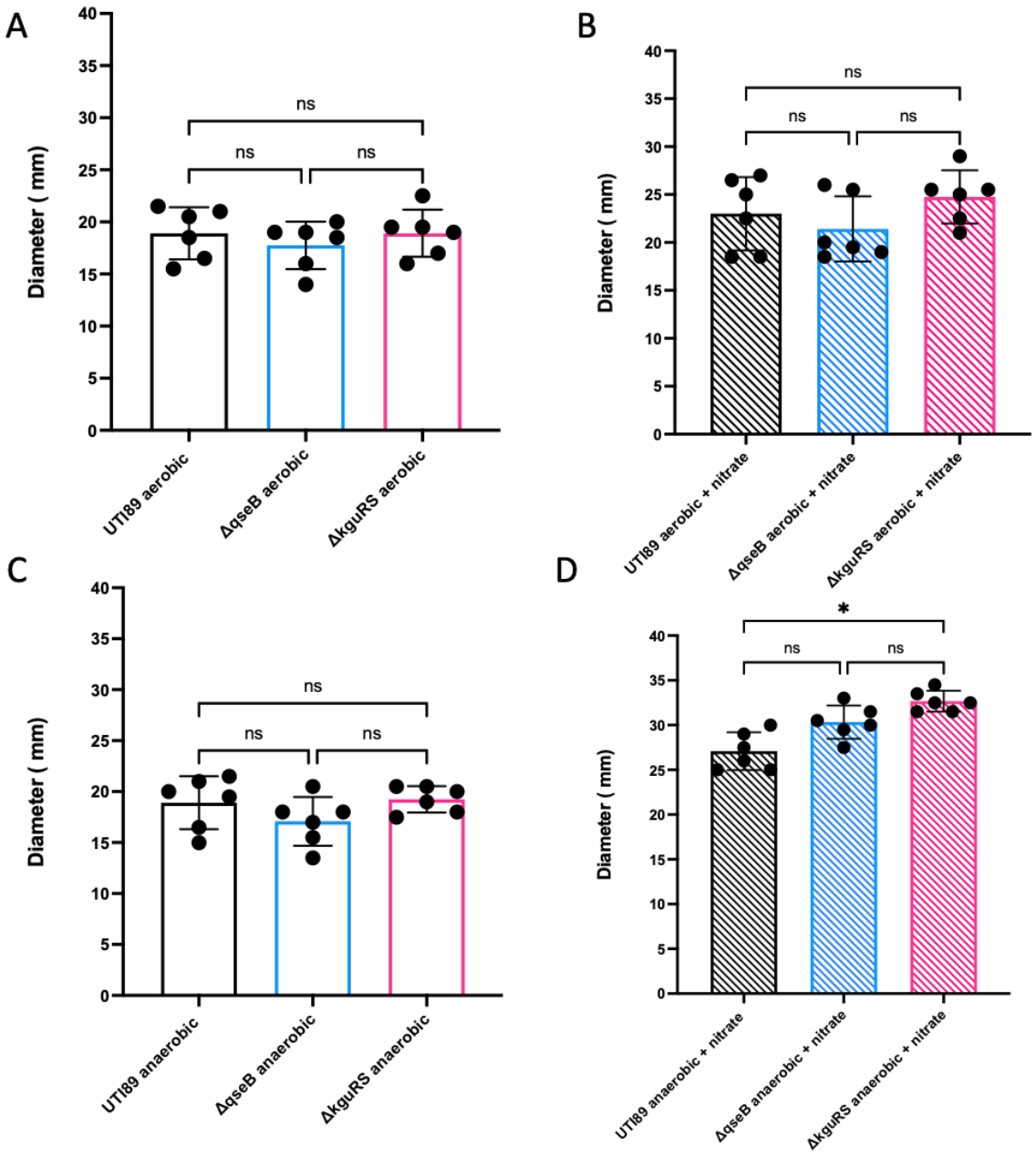

Figure 19: The *kguRS* mutant swims significantly further than wild-type in anaerobic conditions with nitrate as an alternative electron acceptor

Graphs showing diameters that UTI89, Δ*qseB*, and *ΔkguRS* traveled in 0.75% LB agar after 7 hours in A) aerobic conditions B) aerobic conditions supplemented with nitrate C) anaerobic conditions D) anaerobic conditions supplemented with nitrate. To determine significance between strains of the same conditions, a one-way ANOVA with multiple comparisons was performed. N =6, *, p <0.05, ns, no statistical significance detected by test.

Discussion

Cai *et al.* proposed that the KguRS system may be important in pathogenesis in the kidneys where 2- oxoglutarate is abundant. There UPEC may sense oxoglutarate and utilize it as a main carbon source. We found that a *kguRS* mutant did not have major differences in growth kinetics in planktonic culture or in biofilm growth, regardless of oxygen tension. This does not support Cai et al's finding that KguRS is under control of oxygen tension, although these results could be repeated in an anaerobic condition. Further, we found that motility was largely unaffected in the mutant, except in anaerobic conditions with nitrate as an alternative electron acceptor. The exact mechanism that allows the mutant to swim further in anaerobic conditions with nitrate supplementation remains elusive.

KguRS is only found in B2 clade *E. coli.* How it is intertwined into the metabolism of these *E. coli* is not yet understood. Extraintestinal *E. coli* (ExPEC), tend to have amplified genomes, so it may be useful to have additional metabolic regulators. Future work may involve further characterization of this strain during pathogenesis or transfer into a strain of *E. coli* that is not an UPEC.

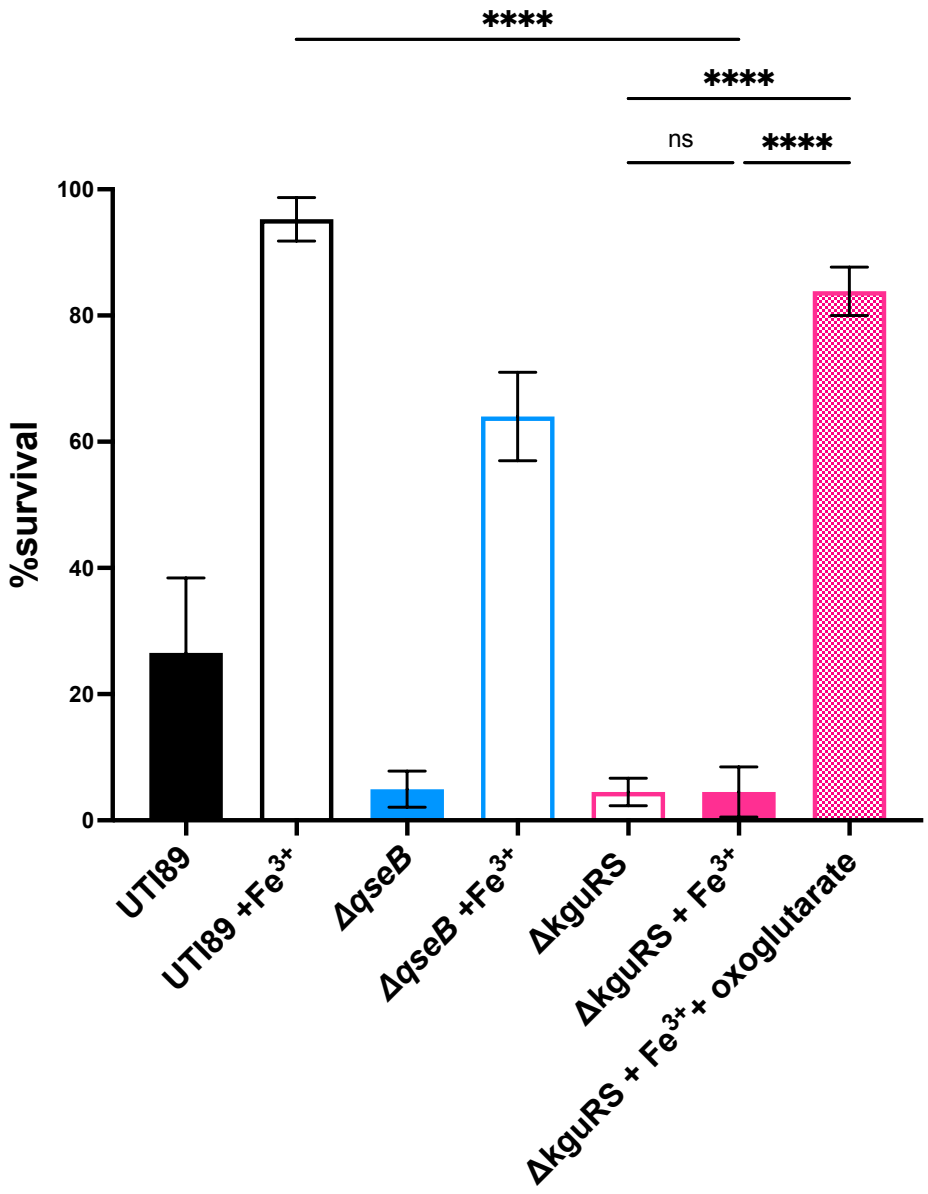

Figure 20: The *kguRS* mutant is rescued by the addition of oxoglutarate in a polymyxin B challenge
Graph depict results of a polymyxin B survival assay for the WT, Δ*qseB* , and Δ*kguRS.* Cells were allowed to reach mid logarithmic growth phase in the presence or absence of ferric iron and normalized. Cells were then exposed to polymyxin, for one hour. An additional subset of Δ*kguRS* cells received both ferric iron and oxoglutarate. At this time cells were serially diluted and plated to determine colony forming units per milliliter. To determine percent survival, antibiotic-treated cells were compared to the antibiotic-treated controls (mean ± SEM, n = 3 biological repeats). To determine statistical significance, a one-way ANOVA was performed with multiple comparisons between the untreated-and treated samples. ****, $p < 0.0001$, ns, no statistical significance detected by test used.

CHAPTER V

FUTURE DIRECTIONS

Introduction

Understanding how bacteria mount resistance is critically important to develop strategies to combat antibiotic resistance. Heteroresistance is a phenomenon in which only a subpopulation of bacteria are resistant to a given antibiotic and survive an antibiotic assault. Although two-component system manipulation has been implicated as a mechanism for heteroresistance before, we demonstrate how heterogeneously expressed chromosomally encoded two-component systems allow uropathogenic *Escherichia coli* to mount resistance to positively charged antibiotics (Chapter 2 and 3).

This resistance is largely accomplished through the PmrAB and QseBC systems. Where, the histidine kinase PmrB is activated by ferric iron, and phosphorylates both its cognate response regulator PmrA, and non-cognate response regulator QseB. QseC is important for acting as a reverse phosphotransferase to control the levels of activated QseB.

The response regulators PmrA and QseB act as transcription factors and together increase the expression of LPS modifying enzymes (Figure 12). Here, I have described a novel role for QseB (Chapter 3) as a regulator of metabolism during LPS modification. I also demonstrate that the 2-oxoglutarate sensing two-component system KguRS is also involved in the ability of UPEC to mount resistance to polymyxin B, likely through its ability to sense 2-oxoglutarate and enact changes in the cell that regulate 2-oxoglutarate levels. We showed that glutamate-oxoglutarate metabolism is crucial for the cell to

mount resistance to positively charged antibiotics (Chapter 3). Yet, questions about how these systems work together to mount resistance against positively charged antibiotics remain.

QseBC-PmrAB biochemical interactions

The mechanism by which the PmrAB and QseBC system interacts biochemically has not been fully elucidated. Work in this thesis and previous work by others demonstrated that QseB and PmrA have shared targets. How these response regulators act at these sites is unknown. Biochemical assays such as DNA footprinting and primer extension assays should be performed to determine which transcription product is prominent when QseB and PmrA are both present at the same target and to confirm the binding sequence of QseB. Previous work by our group showed that both QseB and PmrA cannot bind simultaneously at the same site, but may increase the binding efficiency of each other. To determine if QseB and PmrA directly interact, a yeast-two hybrid experiment could be used. Further, the ability for PmrB and QseB to cross interact has been well described. However, the interaction between QseC and PmrA has not been investigated. A radioactive phosphotransferase and phosphatase assay could be performed to determine if QseC can phosphorylate or dephosphorylate PmrA. It was reported in the early characterizations of the QseBC system, that QseC was a catecholamine sensor. However, work by our group and others has been unable to replicate this result (Guckes et al., 2013a, Breland et al., 2017b). Because QseBC interacts with PmrAB in *E. coli*, and when activated together protects the cell against cationic membrane stress, it may be plausible that QseC also senses cationic peptides or antibiotics. This could be tested via an autokinase assay using different cationic stressors such as polymyxin B and LL37 as candidate QseC ligands.

QseB's control over glutamate-oxoglutarate metabolism

Work in this thesis uncovered a critical role for the response regulator, QseB during LPS modification (Chapter 3). QseB targets and regulates several genes that code for metabolic enzymes connected to the tricarboxylic acid (TCA). cycle. My data suggests that there is an increased amount of oxoglutarate via the modification of the lipid A moiety of LPS. This increased amount of oxoglutarate is processed through the TCA cycle, which is partially under QseB control. Glutamate consumption appears to play a key role in mediating the response to positively charged antibiotics and is consumed through the pantothenate pathway and enters the TCA cycle as acetyl-CoA or succinyl-CoA. Glutamate could also be converted to fumarate via the *arg* gene products. Glutamate could also be shunted to GABA through the *gab/gad* gene products and enter the TCA cycle as succinate.

A recent metabolomics project was conducted to better understand how metabolites change during a challenge with polymyxin B. We performed a polymyxin B survival assay and collected samples at time points in parallel with collection for CFU enumeration. We performed this polymyxin B assay on wild-type UTI89, UTI89*ΔqseB* and UTI89*ΔqseB*/pQseB to determine the role that QseB plays in controlling metabolism during a polymyxin B challenge. We then utilized a targeted mass spectrometry approach to determine how citrulline, fumarate, and succinate change over the course of the polymyxin B challenge. Results show that in wild-type UTI89 treated with polymyxin B, there is a robust increase in targeted metabolites over time. This increase is not seen in UTI89*ΔqseB* or UTI89*ΔqseB*/pQseB (Figure 21). Interestingly, targeted metabolite levels are high in UTI89*ΔqseB* and UTI89*ΔqseB*/pQseB prior to the start of the assay, but are low in wild-type control samples. This supports previous findings that QseB is a regulator of metabolism. The metabolomics data also includes several untargeted molecules of varying verified identities that differ between the groups surveyed. Future work should focus on deciphering

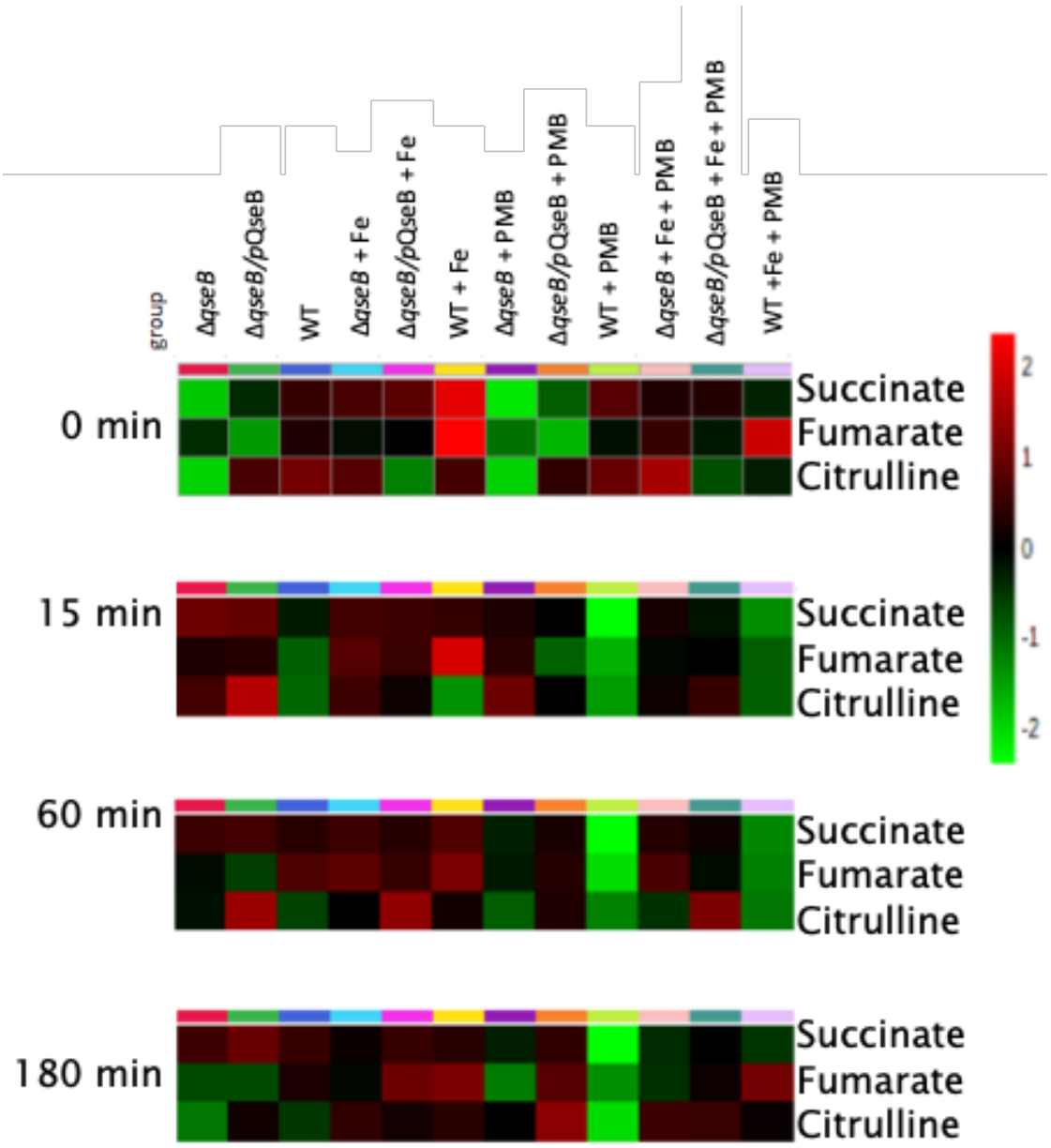

Figure 21: A metabolomics experiment reveals differences between a *qseB* deletion mutant and wild-type UTI89

A heatmap showing relative abundance of succinate, fumarate and citrulline across time for samples taken from a polymyxin B survival assay.

how the metabolic state controlled by QseB influences LPS modification kinetics, cellular turnover/replication rate and bacterial processes like production of virulence factors.

Further, work to understand how glutamate and oxoglutarate relationships to LPS modification is needed. As stated earlier, glutamate may enter the TCA cycle after conversion via *arg* and *gab/gab* gene products. The creation of deletion mutants of these genes could test their necessity in polymyxin B survival. A metabolic flux experiment with radiolabeled glutamate or oxoglutarate may show the fate of these molecules during LPS modification.

QseBC-PmrAB heterogeneity *in vivo*

PmrAB and QseBC have been demonstrated to be in important for mediating the resistance to cationic antibiotics. However, where these systems may be utilized in the host remains unclear. I hypothesize that these systems are activated heterogeneously to enable a portion of the population to survive an attack by neutrophils in the host, where they may encounter cationic peptides. To test this, bacteria labeled with both a fluorescent marker and the Pqse::GFP plasmid would utilized in a murine model of infection. After mice are sacrificed, flow cytometry could be used to determine the portion of the population signaling *qse* at different anatomical sites.

KguRS's role in mediating resistance to positively charged antibiotics

KguRS is an oxoglutarate sensing two-component system first characterized by Cai *et al* (REF). In this dissertation, I demonstrate that KguRS is involved in UPEC's ability to mount resistance to polymyxin B. Yet, more details about the system need to be elucidated. To better understand KguRS's role in pathogenesis and cross–interaction with QseBC-PmrAB an experiment could be performed utilizing a

murine model of infection. Deletion mutants of QseBC, PmrAB, and KguRS alone and together in combinations, could confirm previous work showing KguRS's defect in bladder and kidney, as well as any interactions that QseBC and PmrAB have during infection. Further, mice that have mutations in their ability to sense oxoglutarate could be utilized. Because these mice may have oxoglutarate in locations that they typically would not, a *kguRS* deletion mutant would likely be outcompeted by a strain with an intact KguRS system.

In addition to KguRS's role in mediating resistance to positively charged antibiotics the biochemical properties of the system remain largely unknown. To begin to understand this, a radiolabeled phosphotransfer assay could be performed. Although, Cai *et al.* showed that 2-oxoglutarate was a signal for KguS, this needs to be confirmed with a direct biochemical assay against other intermediates of the TCA cycle.

SUMMARY

In this dissertation I have shown how three, two-component systems may work together to confer resistance to positively charge antibiotics. I first show how PmrAB and QseBC two-component systems are heterogeneously expressed and lead to heteroresistance in urinary tract isolates. I then elucidate a novel role for the response regulator, QseB, as a regulator of metabolism during LPS modification. Finally, I show that the two-component system KguRS, which senses oxoglutarate, is necessary to mount resistance to positively charged antibiotics. Future work centers on uncovering the mechanism of how these systems work together to mount resistance to positively charged antibiotic

REFERENCES

ACKERMANN, M. 2015. A functional perspective on phenotypic heterogeneity in microorganisms. *Nat Rev Microbiol,* 13**,** 497-508.

AL-HASAN, M. N., ECKEL-PASSOW, J. E. & BADDOUR, L. M. 2010. Bacteremia complicating gram-negative urinary tract infections: a population-based study. *J Infect,* 60**,** 278-85.

ALEBOUYEH, M., YADEGAR, A., FARZI, N., MIRI, M., ZOJAJI, H., GHARIBI, S., FAZELI, Z., EBRAHIMI DARYANI, N., ASADZADEH AGHDAEI, H. & ZALI, M. R. 2015. Impacts of H. pylori mixed-infection and heteroresistance on clinical outcomes. *Gastroenterol Hepatol Bed Bench,* 8**,** S1-5.

ALEXANDER, H. E. 1948. Mode of action of streptomycin on type B Hemophilus influenzae. *Am J Dis Child,* 75**,** 428-30.

AMATO, S. M., ORMAN, M. A. & BRYNILDSEN, M. P. 2013. Metabolic control of persister formation in Escherichia coli. *Mol Cell,* 50**,** 475-87.

AMINOV, R. I. 2011. Horizontal gene exchange in environmental microbiota. *Front Microbiol,* 2**,** 158.

ANDERSON, P. & ROTH, J. 1981. Spontaneous tandem genetic duplications in Salmonella typhimurium arise by unequal recombination between rRNA (rrn) cistrons. *Proc Natl Acad Sci U S A,* 78**,** 3113-7.

ANDERSSON, D. I., NICOLOFF, H. & HJORT, K. 2019. Mechanisms and clinical relevance of bacterial heteroresistance. *Nat Rev Microbiol,* 17**,** 479-496.

ARNOLDINI, M., VIZCARRA, I. A., PEÑA-MILLER, R., STOCKER, N., DIARD, M., VOGEL, V., BEARDMORE, R. E., HARDT, W. D. & ACKERMANN, M. 2014. Bistable expression of virulence genes in salmonella leads to the formation of an antibiotic-tolerant subpopulation. *PLoS Biol,* 12**,** e1001928.

BALABAN, N. Q., MERRIN, J., CHAIT, R., KOWALIK, L. & LEIBLER, S. 2004. Bacterial persistence as a phenotypic switch. *Science,* 305**,** 1622-5.

BAND, V. I., CRISPELL, E. K., NAPIER, B. A., HERRERA, C. M., THARP, G. K., VAVIKOLANU, K., POHL, J., READ, T. D., BOSINGER, S. E., TRENT, M. S., BURD, E. M. & WEISS, D. S. 2016. Antibiotic failure mediated by a resistant subpopulation in Enterobacter cloacae. *Nat Microbiol,* 1**,** 16053.

BAND, V. I. & WEISS, D. S. 2019. Heteroresistance: A cause of unexplained antibiotic treatment failure? *PLoS Pathog,* 15**,** e1007726.

BARIN, J., MARTINS, A. F., HEINECK, B. L., BARTH, A. L. & ZAVASCKI, A. P. 2013. Hetero- and adaptive resistance to polymyxin B in OXA-23-producing carbapenem-resistant Acinetobacter baumannii isolates. *Ann Clin Microbiol Antimicrob,* 12**,** 15.

BASSETT, E. J., KEITH, M. S., ARMELAGOS, G. J., MARTIN, D. L. & VILLANUEVA, A. R. 1980. Tetracycline-labeled human bone from ancient Sudanese Nubia (A.D. 350). *Science,* 209**,** 1532-4.

BAYLISS, C. D. 2009. Determinants of phase variation rate and the fitness implications of differing rates for bacterial pathogens and commensals. *FEMS Microbiol Rev,* 33**,** 504-20.

BEEBOUT, C. J., EBERLY, A. R., WERBY, S. H., REASONER, S. A., BRANNON, J. R., DE, S., FITZGERALD, M. J., HUGGINS, M. M., CLAYTON, D. B., CEGELSKI, L. & HADJIFRANGISKOU, M. 2019. Respiratory Heterogeneity Shapes Biofilm Formation and Host Colonization in Uropathogenic Escherichia coli. *MBio,* 10.

BENNETT, B. D., KIMBALL, E. H., GAO, M., OSTERHOUT, R., VAN DIEN, S. J. & RABINOWITZ, J. D. 2009. Absolute metabolite concentrations and implied enzyme active site occupancy in Escherichia coli. *Nat Chem Biol,* 5**,** 593-9.

BOURRET, R. B., HESS, J. F., BORKOVICH, K. A., PAKULA, A. A. & SIMON, M. I. 1989. Protein phosphorylation in chemotaxis and two-component regulatory systems of bacteria. *J Biol Chem,* 264**,** 7085-8.

BRANNON, J. R., DUNIGAN, T. L., BEEBOUT, C. J., ROSS, T., WIEBE, M. A., REYNOLDS, W. S. & HADJIFRANGISKOU, M. 2020. Invasion of vaginal epithelial cells by uropathogenic Escherichia coli. *Nat Commun,* 11**,** 2803.

BREAZEALE, S. D., RIBEIRO, A. A. & RAETZ, C. R. 2003. Origin of lipid A species modified with 4-amino-4-deoxy-L-arabinose in polymyxin-resistant mutants of Escherichia coli. An aminotransferase (ArnB) that generates UDP-4-deoxyl-L-arabinose. *J Biol Chem,* 278**,** 24731-9.

BRELAND, E. J., EBERLY, A. R. & HADJIFRANGISKOU, M. 2017a. An Overview of Two-Component Signal Transduction Systems Implicated in Extra-Intestinal Pathogenic E. coli Infections. *Front Cell Infect Microbiol,* 7**,** 162.

BRELAND, E. J., ZHANG, E. W., BERMUDEZ, T., MARTINEZ, C. R. & HADJIFRANGISKOU, M. 2017b. The histidine residue of QseC is required for canonical signaling between QseB and PmrB in uropathogenic Escherichia coli. *J Bacteriol*.

BRENNAN, D., O'MORAIN, C., MCNAMARA, D. & SMITH, S. M. 2021. Molecular Detection of Antibiotic-Resistant Helicobacter pylori. *Methods Mol Biol,* 2283**,** 29-36.

CAI, W., WANNEMUEHLER, Y., DELL'ANNA, G., NICHOLSON, B., BARBIERI, N. L., KARIYAWASAM, S., FENG, Y., LOGUE, C. M., NOLAN, L. K. & LI, G. 2013. A novel two-component signaling system facilitates uropathogenic Escherichia coli's ability to exploit abundant host metabolites. *PLoS Pathog,* 9**,** e1003428.

CANNATELLI, A., DI PILATO, V., GIANI, T., ARENA, F., AMBRETTI, S., GAIBANI, P., D'ANDREA, M. M. & ROSSOLINI, G. M. 2014. In vivo evolution to colistin resistance by PmrB sensor kinase mutation in KPC-producing Klebsiella pneumoniae is associated with low-dosage colistin treatment. *Antimicrob Agents Chemother,* 58**,** 4399-403.

CHAIN, E., FLOREY, H. W., ADELAIDE, M. B., GARDNER, A. D., HEATLEY, N. G., JENNINGS, M. A., ORR-EWING, J. & SANDERS, A. G. 1993. Penicillin as a chemotherapeutic agent. 1940. *Clin Orthop Relat Res***,** 3-7.

CLARKE, M. B., HUGHES, D. T., ZHU, C., BOEDEKER, E. C. & SPERANDIO, V. 2006. The QseC sensor kinase: a bacterial adrenergic receptor. *Proc Natl Acad Sci U S A,* 103**,** 10420-5.

CLARKE, M. B. & SPERANDIO, V. 2005. Transcriptional autoregulation by quorum sensing Escherichia coli regulators B and C (QseBC) in enterohaemorrhagic E. coli (EHEC). *Mol Microbiol,* 58**,** 441-55.

CLSI 2018. *Methods for Dilution Antimicrobial Susceptibility Tests for Bacteria That Grow Aerobically—Eleventh Edition: M07,* Wayne, PA, USA, National Committee for Clinical Laboratory Standards.

COLLABORATORS, A. R. 2022. Global burden of bacterial antimicrobial resistance in 2019: a systematic analysis. *Lancet,* 399**,** 629-655.

CONNELL, I., AGACE, W., KLEMM, P., SCHEMBRI, M., MARILD, S. & SVANBORG, C. 1996. Type 1 fimbrial expression enhances Escherichia coli virulence for the urinary tract. *Proc Natl Acad Sci U S A,* 93**,** 9827-32.

D'COSTA, V. M., KING, C. E., KALAN, L., MORAR, M., SUNG, W. W., SCHWARZ, C., FROESE, D., ZAZULA, G., CALMELS, F., DEBRUYNE, R., GOLDING, G. B., POINAR, H. N. & WRIGHT, G. D. 2011. Antibiotic resistance is ancient. *Nature,* 477**,** 457-61.

DA SILVA, A. E. B., MARTINS, A. F., NODARI, C. S., MAGAGNIN, C. M. & BARTH, A. L. 2018. Carbapenem-heteroresistance among isolates of the Enterobacter cloacae complex: is it a real concern? *Eur J Clin Microbiol Infect Dis,* 37**,** 185-186.

DE JONG, L. A. W., VAN DER LINDEN, P. D., ROUKENS, M. M. B., VAN DE GARDE, E. M. W., VAN DER VELDEN, A. W., NATSCH, S. & USE, S. S. W. G. O. S. O. A. 2019. Consecutive antibiotic use in the outpatient setting: an extensive, longitudinal descriptive analysis of antibiotic dispensing data in the Netherlands. *BMC Infect Dis,* 19**,** 84.

DEWACHTER, L., FAUVART, M. & MICHIELS, J. 2019. Bacterial Heterogeneity and Antibiotic Survival: Understanding and Combatting Persistence and Heteroresistance. *Mol Cell,* 76**,** 255-267.

DJOKO, K. Y., PHAN, M. D., PETERS, K. M., WALKER, M. J., SCHEMBRI, M. A. & MCEWAN, A. G. 2017. Interplay between tolerance mechanisms to copper and acid stress in. *Proc Natl Acad Sci U S A,* 114**,** 6818-6823.

DURAND, G. A., RAOULT, D. & DUBOURG, G. 2019. Antibiotic discovery: history, methods and perspectives. *Int J Antimicrob Agents,* 53**,** 371-382.

EL-HALFAWY, O. M. & VALVANO, M. A. 2013. Chemical communication of antibiotic resistance by a highly resistant subpopulation of bacterial cells. *PLoS One,* 8**,** e68874.

ELOWITZ, M. B., LEVINE, A. J., SIGGIA, E. D. & SWAIN, P. S. 2002. Stochastic gene expression in a single cell. *Science,* 297**,** 1183-6.

EUCAST 2022. Breakpoint tables for interpretation of MICs and zone diameters. *In:* V_12.0_BREAKPOINT_TABLES (ed.) *Excel.* 12.0 ed. www.eucast.org.

FLEMING, A. 2001. On the antibacterial action of cultures of a penicillium, with special reference to their use in the isolation of B. influenzae. 1929. *Bull World Health Organ,* 79**,** 780-90.

FLOYD, K. A., MITCHELL, C. A., EBERLY, A. R., COLLING, S. J., ZHANG, E. W., DEPAS, W., CHAPMAN, M. R., CONOVER, M., ROGERS, B. R., HULTGREN, S. J. & HADJIFRANGISKOU, M. 2016. The UbiI (VisC) Aerobic Ubiquinone Synthase Is Required for Expression of Type 1 Pili, Biofilm Formation, and Pathogenesis in Uropathogenic Escherichia coli. *J Bacteriol,* 198**,** 2662-72.

FOXMAN, B. 2014. Urinary tract infection syndromes: occurrence, recurrence, bacteriology, risk factors, and disease burden. *Infect Dis Clin North Am,* 28**,** 1-13.

FREIRE-MORAN, L., ARONSSON, B., MANZ, C., GYSSENS, I. C., SO, A. D., MONNET, D. L., CARS, O. & GROUP, E.-E. W. 2011. Critical shortage of new antibiotics in development against multidrug-resistant bacteria-Time to react is now. *Drug Resist Updat,* 14**,** 118-24.

GERSON, S., BETTS, J. W., LUCAßEN, K., NODARI, C. S., WILLE, J., JOSTEN, M., GÖTTIG, S., NOWAK, J., STEFANIK, D., ROCA, I., VILA, J., CISNEROS, J. M., LA RAGIONE, R. M., SEIFERT, H. & HIGGINS, P. G. 2019. Investigation of Novel. *Antimicrob Agents Chemother,* 63.

GOULIAN, M. 2010. Two-component signaling circuit structure and properties. *Curr Opin Microbiol,* 13**,** 184-9.

GROISMAN, E. A., KAYSER, J. & SONCINI, F. C. 1997. Regulation of polymyxin resistance and adaptation to low-Mg2+ environments. *J Bacteriol,* 179**,** 7040-5.

GUCKES, K. R., BRELAND, E. J., ZHANG, E. W., HANKS, S. C., GILL, N. K., ALGOOD, H. M., SCHMITZ, J. E., STRATTON, C. W. & HADJIFRANGISKOU, M. 2017. Signaling by two-component system

noncognate partners promotes intrinsic tolerance to polymyxin B in uropathogenic Escherichia coli. *Sci Signal,* 10.

GUCKES, K. R., KOSTAKIOTI, M., BRELAND, E. J., GU, A. P., SHAFFER, C. L., MARTINEZ, C. R., 3RD, HULTGREN, S. J. & HADJIFRANGISKOU, M. 2013a. Strong cross-system interactions drive the activation of the QseB response regulator in the absence of its cognate sensor. *Proc Natl Acad Sci U S A*.

GUCKES, K. R., KOSTAKIOTI, M., BRELAND, E. J., GU, A. P., SHAFFER, C. L., MARTINEZ, C. R., HULTGREN, S. J. & HADJIFRANGISKOU, M. 2013b. Strong cross-system interactions drive the activation of the QseB response regulator in the absence of its cognate sensor. *Proc Natl Acad Sci U S A,* 110**,** 16592-7.

GUNN, J. S., LIM, K. B., KRUEGER, J., KIM, K., GUO, L., HACKETT, M. & MILLER, S. I. 1998. PmrA-PmrB-regulated genes necessary for 4-aminoarabinose lipid A modification and polymyxin resistance. *Mol Microbiol,* 27**,** 1171-82.

GUNN, J. S., RYAN, S. S., VAN VELKINBURGH, J. C., ERNST, R. K. & MILLER, S. I. 2000. Genetic and functional analysis of a PmrA-PmrB-regulated locus necessary for lipopolysaccharide modification, antimicrobial peptide resistance, and oral virulence of Salmonella enterica serovar typhimurium. *Infect Immun,* 68**,** 6139-46.

HADJIFRANGISKOU, M., KOSTAKIOTI, M., CHEN, S. L., HENDERSON, J. P., GREENE, S. E. & HULTGREN, S. J. 2011. A central metabolic circuit controlled by QseC in pathogenic Escherichia coli. *Mol Microbiol,* 80**,** 1516-29.

HANCOCK, R. E. W. 1999. Hancock Laboratory Methods: Modified MIC Method for Cationic Antimicrobial Peptides. 03/01/2022 13:43 ed. University of British Columbia, British Columbia.

HANSEN, S., LEWIS, K. & VULIĆ, M. 2008. Role of global regulators and nucleotide metabolism in antibiotic tolerance in Escherichia coli. *Antimicrob Agents Chemother,* 52**,** 2718-26.

HENDERSON, J. C., O'BRIEN, J. P., BRODBELT, J. S. & TRENT, M. S. 2013. Isolation and chemical characterization of lipid A from gram-negative bacteria. *J Vis Exp***,** e50623.

HERMES, D. M., PORMANN PITT, C., LUTZ, L., TEIXEIRA, A. B., RIBEIRO, V. B., NETTO, B., MARTINS, A. F., ZAVASCKI, A. P. & BARTH, A. L. 2013. Evaluation of heteroresistance to polymyxin B among carbapenem-susceptible and -resistant Pseudomonas aeruginosa. *J Med Microbiol,* 62**,** 1184-1189.

HERNDAY, A., KRABBE, M., BRAATEN, B. & LOW, D. 2002. Self-perpetuating epigenetic pili switches in bacteria. *Proc Natl Acad Sci U S A,* 99 Suppl 4**,** 16470-6.

HERRERA, C. M., HANKINS, J. V. & TRENT, M. S. 2010. Activation of PmrA inhibits LpxT-dependent phosphorylation of lipid A promoting resistance to antimicrobial peptides. *Mol Microbiol,* 76**,** 1444-60.

HIRAMATSU, K., ARITAKA, N., HANAKI, H., KAWASAKI, S., HOSODA, Y., HORI, S., FUKUCHI, Y. & KOBAYASHI, I. 1997. Dissemination in Japanese hospitals of strains of Staphylococcus aureus heterogeneously resistant to vancomycin. *Lancet,* 350**,** 1670-3.

HJORT, K., NICOLOFF, H. & ANDERSSON, D. I. 2016. Unstable tandem gene amplification generates heteroresistance (variation in resistance within a population) to colistin in Salmonella enterica. *Mol Microbiol,* 102**,** 274-289.

HUGHES, D. T., CLARKE, M. B., YAMAMOTO, K., RASKO, D. A. & SPERANDIO, V. 2009. The QseC adrenergic signaling cascade in Enterohemorrhagic E. coli (EHEC). *PLoS Pathog,* 5**,** e1000553.

HUH, D. & PAULSSON, J. 2011. Random partitioning of molecules at cell division. *Proc Natl Acad Sci U S A,* 108**,** 15004-9.

JOHNSON, J. R., NICOLAS-CHANOINE, M. H., DEBROY, C., CASTANHEIRA, M., ROBICSEK, A., HANSEN, G., WEISSMAN, S., URBAN, C., PLATELL, J., TROTT, D., ZHANEL, G., CLABOTS, C., JOHNSTON, B. D. & KUSKOWSKI, M. A. 2012. Comparison of Escherichia coli ST131 pulsotypes, by epidemiologic traits, 1967-2009. *Emerg Infect Dis,* 18**,** 598-607.

JUNG, K., BRAMEYER, S., FABIANI, F., GASPEROTTI, A. & HOYER, E. 2019. Phenotypic Heterogeneity Generated by Histidine Kinase-Based Signaling Networks. *J Mol Biol,* 431**,** 4547-4558.

KARVE, S., RYAN, K., PEETERS, P., BAELEN, E., ROJAS-FARRERAS, S., POTTER, D. & RODRÍGUEZ-BAÑO, J. 2018. The impact of initial antibiotic treatment failure: Real-world insights in patients with complicated urinary tract infection. *J Infect,* 76**,** 121-131.

KHANDIGE, S. & MØLLER-JENSEN, J. 2016. Fimbrial phase variation: stochastic or cooperative? *Curr Genet,* 62**,** 237-41.

KHATIB, R., JOSE, J., MUSTA, A., SHARMA, M., FAKIH, M. G., JOHNSON, L. B., RIEDERER, K. & SHEMES, S. 2011. Relevance of vancomycin-intermediate susceptibility and heteroresistance in methicillin-resistant Staphylococcus aureus bacteraemia. *J Antimicrob Chemother,* 66**,** 1594-9.

KIEFFER, N., ROYER, G., DECOUSSER, J. W., BOURREL, A. S., PALMIERI, M., ORTIZ DE LA ROSA, J. M., JACQUIER, H., DENAMUR, E., NORDMANN, P. & POIREL, L. 2019. , an Inducible Gene Encoding an Acquired Phosphoethanolamine Transferase in Escherichia coli, and Its Origin. *Antimicrob Agents Chemother,* 63.

KIM, J. J., KIM, J. G. & KWON, D. H. 2003. Mixed-infection of antibiotic susceptible and resistant Helicobacter pylori isolates in a single patient and underestimation of antimicrobial susceptibility testing. *Helicobacter,* 8**,** 202-6.

KOHANSKI, M. A., DWYER, D. J. & COLLINS, J. J. 2010. How antibiotics kill bacteria: from targets to networks. *Nat Rev Microbiol,* 8**,** 423-35.

KOSTAKIOTI, M., HADJIFRANGISKOU, M., PINKNER, J. S. & HULTGREN, S. J. 2009. QseC-mediated dephosphorylation of QseB is required for expression of genes associated with virulence in uropathogenic Escherichia coli. *Mol Microbiol,* 73**,** 1020-31.

KUMAR, R. & SHIMIZU, K. 2010. Metabolic regulation of Escherichia coli and its gdhA, glnL, gltB, D mutants under different carbon and nitrogen limitations in the continuous culture. *Microb Cell Fact,* 9**,** 8.

LEE, H., HSU, F. F., TURK, J. & GROISMAN, E. A. 2004. The PmrA-regulated pmrC gene mediates phosphoethanolamine modification of lipid A and polymyxin resistance in Salmonella enterica. *J Bacteriol,* 186**,** 4124-33.

LEHNER, B. 2008. Selection to minimise noise in living systems and its implications for the evolution of gene expression. *Mol Syst Biol,* 4**,** 170.

LESHO, E., YOON, E. J., MCGANN, P., SNESRUD, E., KWAK, Y., MILILLO, M., ONMUS-LEONE, F., PRESTON, L., ST CLAIR, K., NIKOLICH, M., VISCOUNT, H., WORTMANN, G., ZAPOR, M., GRILLOT-COURVALIN, C., COURVALIN, P., CLIFFORD, R. & WATERMAN, P. E. 2013. Emergence of colistin-resistance in extremely drug-resistant Acinetobacter baumannii containing a novel pmrCAB operon during colistin therapy of wound infections. *J Infect Dis,* 208**,** 1142-51.

LEWIS, K. 2020. The Science of Antibiotic Discovery. *Cell,* 181**,** 29-45.

LOPATKIN, A. J., BENING, S. C., MANSON, A. L., STOKES, J. M., KOHANSKI, M. A., BADRAN, A. H., EARL, A. M., CHENEY, N. J., YANG, J. H. & COLLINS, J. J. 2021. Clinically relevant mutations in core metabolic genes confer antibiotic resistance. *Science,* 371.

LOPATKIN, A. J., STOKES, J. M., ZHENG, E. J., YANG, J. H., TAKAHASHI, M. K., YOU, L. & COLLINS, J. J. 2019. Bacterial metabolic state more accurately predicts antibiotic lethality than growth rate. *Nat Microbiol,* 4**,** 2109-2117.

LÁZÁR, V. & KISHONY, R. 2019. Transient antibiotic resistance calls for attention. *Nat Microbiol,* 4**,** 1606-1607.

MASCELLINO, M. T., POROWSKA, B., DE ANGELIS, M. & OLIVA, A. 2017. Antibiotic susceptibility, heteroresistance, and updated treatment strategies in. *Drug Des Devel Ther,* 11**,** 2209-2220.

MERIGHI, M., SEPTER, A. N., CARROLL-PORTILLO, A., BHATIYA, A., PORWOLLIK, S., MCCLELLAND, M. & GUNN, J. S. 2009. Genome-wide analysis of the PreA/PreB (QseB/QseC) regulon of Salmonella enterica serovar Typhimurium. *BMC Microbiol,* 9**,** 42.

MIZUNO, T. 1997. Compilation of all genes encoding two-component phosphotransfer signal transducers in the genome of Escherichia coli. *DNA Res,* 4**,** 161-8.

MOONEY, R. A., DAVIS, S. E., PETERS, J. M., ROWLAND, J. L., ANSARI, A. Z. & LANDICK, R. 2009. Regulator trafficking on bacterial transcription units in vivo. *Mol Cell,* 33**,** 97-108.

MULVEY, M. A., LOPEZ-BOADO, Y. S., WILSON, C. L., ROTH, R., PARKS, W. C., HEUSER, J. & HULTGREN, S. J. 1998. Induction and evasion of host defenses by type 1-piliated uropathogenic Escherichia coli. *Science,* 282**,** 1494-7.

NELSON, M. L., DINARDO, A., HOCHBERG, J. & ARMELAGOS, G. J. 2010. Brief communication: Mass spectroscopic characterization of tetracycline in the skeletal remains of an ancient population from Sudanese Nubia 350-550 CE. *Am J Phys Anthropol,* 143**,** 151-4.

NEWMAN, J. R., GHAEMMAGHAMI, S., IHMELS, J., BRESLOW, D. K., NOBLE, M., DERISI, J. L. & WEISSMAN, J. S. 2006. Single-cell proteomic analysis of S. cerevisiae reveals the architecture of biological noise. *Nature,* 441**,** 840-6.

NICOLOFF, H., HJORT, K., LEVIN, B. R. & ANDERSSON, D. I. 2019. The high prevalence of antibiotic heteroresistance in pathogenic bacteria is mainly caused by gene amplification. *Nat Microbiol,* 4**,** 504-514.

NORMARK, S., EDLUND, T., GRUNDSTRÖM, T., BERGSTRÖM, S. & WOLF-WATZ, H. 1977. Escherichia coli K-12 mutants hyperproducing chromosomal beta-lactamase by gene repetitions. *J Bacteriol,* 132**,** 912-22.

OIKONOMOU, O., PANOPOULOU, M. & IKONOMIDIS, A. 2011. Investigation of carbapenem heteroresistance among different sequence types of Pseudomonas aeruginosa clinical isolates reveals further diversity. *J Med Microbiol,* 60**,** 1556-1558.

PATERSON, D. L. 2000. Recommendation for treatment of severe infections caused by Enterobacteriaceae producing extended-spectrum beta-lactamases (ESBLs). *Clin Microbiol Infect,* 6**,** 460-3.

PETTERSSON, M. E., SUN, S., ANDERSSON, D. I. & BERG, O. G. 2009. Evolution of new gene functions: simulation and analysis of the amplification model. *Genetica,* 135**,** 309-24.

PLENER, L., LORENZ, N., REIGER, M., RAMALHO, T., GERLAND, U. & JUNG, K. 2015. The phosphorylation flow of the Vibrio harveyi quorum-sensing cascade determines levels of phenotypic heterogeneity in the population. *J Bacteriol,* 197**,** 1747-56.

PLIPAT, N., LIVNI, G., BERTRAM, H. & THOMSON, R. B. 2005. Unstable vancomycin heteroresistance is common among clinical isolates of methiciliin-resistant Staphylococcus aureus. *J Clin Microbiol,* 43**,** 2494-6.

PURCELL, A. B., VOSS, B. J. & TRENT, M. S. 2022. Diacylglycerol Kinase A Is Essential for Polymyxin Resistance Provided by EptA, MCR-1, and Other Lipid A Phosphoethanolamine Transferases. *J Bacteriol,* 204**,** e0049821.

RAM, S. & GOULIAN, M. 2013. The architecture of a prototypical bacterial signaling circuit enables a single point mutation to confer novel network properties. *PLoS Genet,* 9**,** e1003706.

RASKO, D. A., ROSOVITZ, M. J., MYERS, G. S., MONGODIN, E. F., FRICKE, W. F., GAJER, P., CRABTREE, J., SEBAIHIA, M., THOMSON, N. R., CHAUDHURI, R., HENDERSON, I. R., SPERANDIO, V. & RAVEL, J. 2008. The pangenome structure of Escherichia coli: comparative genomic analysis of E. coli commensal and pathogenic isolates. *J Bacteriol,* 190**,** 6881-93.

REITZER, L. 2003. Nitrogen assimilation and global regulation in Escherichia coli. *Annu Rev Microbiol,* 57**,** 155-76.

REUVEN, P. & ELDAR, A. 2011. Macromotives and microbehaviors: the social dimension of bacterial phenotypic variability. *Curr Opin Genet Dev,* 21**,** 759-67.

RINDER, H., MIESKES, K. T. & LÖSCHER, T. 2001. Heteroresistance in Mycobacterium tuberculosis. *Int J Tuberc Lung Dis,* 5**,** 339-45.

RUBIN, E. J., HERRERA, C. M., CROFTS, A. A. & TRENT, M. S. 2015. PmrD is required for modifications to escherichia coli endotoxin that promote antimicrobial resistance. *Antimicrob Agents Chemother,* 59**,** 2051-61.

SANDEGREN, L. & ANDERSSON, D. I. 2009. Bacterial gene amplification: implications for the evolution of antibiotic resistance. *Nat Rev Microbiol,* 7**,** 578-88.

SATOLA, S. W., FARLEY, M. M., ANDERSON, K. F. & PATEL, J. B. 2011. Comparison of detection methods for heteroresistant vancomycin-intermediate Staphylococcus aureus, with the population analysis profile method as the reference method. *J Clin Microbiol,* 49**,** 177-83.

SCHATZ, A., BUGIE, E. & WAKSMAN, S. A. 2005. Streptomycin, a substance exhibiting antibiotic activity against gram-positive and gram-negative bacteria. 1944. *Clin Orthop Relat Res***,** 3-6.

SCHWAN, W. R. 2011. Regulation of genes in uropathogenic Escherichia coli. *World J Clin Infect Dis,* 1**,** 17-25.

SHIN, D., LEE, E. J., HUANG, H. & GROISMAN, E. A. 2006. A positive feedback loop promotes transcription surge that jump-starts Salmonella virulence circuit. *Science,* 314**,** 1607-9.

SIMPSON, B. W. & TRENT, M. S. 2019. Pushing the envelope: LPS modifications and their consequences. *Nat Rev Microbiol,* 17**,** 403-416.

SMITS, W. K., KUIPERS, O. P. & VEENING, J. W. 2006. Phenotypic variation in bacteria: the role of feedback regulation. *Nat Rev Microbiol,* 4**,** 259-71.

STOCK, A. M., ROBINSON, V. L. & GOUDREAU, P. N. 2000. Two-component signal transduction. *Annu Rev Biochem,* 69**,** 183-215.

STOCK, J. B., NINFA, A. J. & STOCK, A. M. 1989. Protein phosphorylation and regulation of adaptive responses in bacteria. *Microbiol Rev,* 53**,** 450-90.

STÆRK, K., KHANDIGE, S., KOLMOS, H. J., MØLLER-JENSEN, J. & ANDERSEN, T. E. 2016. Uropathogenic Escherichia coli Express Type 1 Fimbriae Only in Surface Adherent Populations Under Physiological Growth Conditions. *J Infect Dis,* 213**,** 386-94.

SUBASHCHANDRABOSE, S. & MOBLEY, H. L. T. 2015. Virulence and Fitness Determinants of Uropathogenic Escherichia coli. *Microbiol Spectr,* 3.

SUGINO, Y. & HIROTA, Y. 1962. Conjugal fertility associated with resistance factor R in Escherichia coli. *J Bacteriol,* 84**,** 902-10.

SUTHERLAND, R. & ROLINSON, G. N. 1964. ACTIVITY OF AMPICILLIN IN VITRO COMPARED WITH OTHER ANTIBIOTICS. *J Clin Pathol,* 17**,** 461-5.

TABER, H. W., MUELLER, J. P., MILLER, P. F. & ARROW, A. S. 1987. Bacterial uptake of aminoglycoside antibiotics. *Microbiol Rev,* 51**,** 439-57.

TALLY, F. P. & DEBRUIN, M. F. 2000. Development of daptomycin for gram-positive infections. *J Antimicrob Chemother,* 46**,** 523-6.

TEUBER, M. & BADER, J. 1976. Action of polymyxin B on bacterial membranes. Binding capacities for polymyxin B of inner and outer membranes isolated from Salmonella typhimurium G30. *Arch Microbiol,* 109**,** 51-8.

THATTAI, M. & VAN OUDENAARDEN, A. 2004. Stochastic gene expression in fluctuating environments. *Genetics,* 167**,** 523-30.

VAARA, M., VAARA, T., JENSEN, M., HELANDER, I., NURMINEN, M., RIETSCHEL, E. T. & MÄKELÄ, P. H. 1981. Characterization of the lipopolysaccharide from the polymyxin-resistant pmrA mutants of Salmonella typhimurium. *FEBS Lett,* 129**,** 145-9.

VAN HAL, S. J., JONES, M., GOSBELL, I. B. & PATERSON, D. L. 2011. Vancomycin heteroresistance is associated with reduced mortality in ST239 methicillin-resistant Staphylococcus aureus blood stream infections. *PLoS One,* 6**,** e21217.

VLAMAKIS, H., CHAI, Y., BEAUREGARD, P., LOSICK, R. & KOLTER, R. 2013. Sticking together: building a biofilm the Bacillus subtilis way. *Nat Rev Microbiol,* 11**,** 157-68.

WAKAMOTO, Y., DHAR, N., CHAIT, R., SCHNEIDER, K., SIGNORINO-GELO, F., LEIBLER, S. & MCKINNEY, J. D. 2013. Dynamic persistence of antibiotic-stressed mycobacteria. *Science,* 339**,** 91-5.

WOLF, D. M., VAZIRANI, V. V. & ARKIN, A. P. 2005. Diversity in times of adversity: probabilistic strategies in microbial survival games. *J Theor Biol,* 234**,** 227-53.

YAN, D. 2007. Protection of the glutamate pool concentration in enteric bacteria. *Proc Natl Acad Sci U S A,* 104**,** 9475-80.

ZHENG, C., LI, S., LUO, Z., PI, R., SUN, H., HE, Q., TANG, K., LUO, M., LI, Y., COUVIN, D., RASTOGI, N. & SUN, Q. 2015. Mixed Infections and Rifampin Heteroresistance among Mycobacterium tuberculosis Clinical Isolates. *J Clin Microbiol,* 53**,** 2138-47.

ZHOU, Z., RIBEIRO, A. A., LIN, S., COTTER, R. J., MILLER, S. I. & RAETZ, C. R. 2001. Lipid A modifications in polymyxin-resistant Salmonella typhimurium: PMRA-dependent 4-amino-4-deoxy-L-arabinose, and phosphoethanolamine incorporation. *J Biol Chem,* 276**,** 43111-21.

ZIMMERMAN, S. M., LAFONTAINE, A. J., HERRERA, C. M., MCLEAN, A. B. & TRENT, M. S. 2020. A Whole-Cell Screen Identifies Small Bioactives That Synergize with Polymyxin and Exhibit Antimicrobial Activities against Multidrug-Resistant Bacteria. *Antimicrob Agents Chemother,* 64.